Remarks

This paper is being filed in lieu of an appeal brief, and is in response to the Office Action mailed April 6, 2005. This paper is being filed within the designated response period, and no fee is believed due. The Commissioner is hereby authorized to charge any fees which may be due for filing of this paper to deposit account no. 50-2719.

By action of this amendment, claims 28 and 29 have been canceled without prejudice or disclaimer, and claims 11-13, 15 and 22 have been amended. No new matter has been added by these amendments. Claims 1, 11-15, 17-23, 26 and 27 are pending and under examination.

Based on the changes above and the following remarks, reconsideration of the claims is respectfully requested.

Response to Section 112, 2nd paragraph rejections

Claims 22 and 28 are rejected as being indefinite because the phrase "mammalian neuronal ASIC cationic channels" allegedly does not provide any structural limitation to the claim. Claim 28 has been canceled without prejudice or disclaimer, and therefore the rejection is moot as to this claim. Claim 22 has been amended to specify that the claimed ASIC channel has an amino acid sequence of SEQ ID NO: 2, SEQ ID NO: 4 or SEQ ID NO: 8. Without acquiescing to the propriety of the rejection, the Applicants submit that the amendment to claim 22 confers sufficient structure for one of ordinary skill in the art to determine the metes and bounds of the claim. The Applicants respectfully request that the indefiniteness rejection of claim 22 be withdrawn.

Claims 12, 13 and 15 are rejected as indefinite because it is allegedly not clear whether the recited nucleotides are contained in the specified SEQ ID NO or in some other sequence. As indicated in the previous response, the word "inclusive" was meant to indicate that the claimed nucleic acid sequence includes the nucleotides by which the sequence is bounded. Using claim 12 as an example, the claimed nucleic acid sequence therefore constitutes nucleotides 123 to 1700 of SEQ ID NO: 1 (and not nucleotides 124 to 1699) of SEQ ID NO: 1. Likewise, the nucleic acid sequence of claims 13 and 15 are nucleotides 109 to 1542 of SEQ ID NO: 3 and nucleotides 109 to 1785 of SEQ ID NO: 7, respectively. The word "inclusive" in claims 12, 13 and 15 has been set off by commas, to more clearly indicate its intended meaning. These claims

have also been amended to replace the phrase "bounded by" with the word "from," to further clarify that the nucleic acid sequences are inclusive of the recited nucleotides. Support for amended claims 12, 13 and 15 is found in the sequence listing filed on August 5, 1998. No new matter has been added by these amendments. The Applicants respectfully request that the indefiniteness rejection of claims 12, 13 and 15 be withdrawn.

Claims 23 and 29 are rejected as indefinite for depending upon an allegedly indefinite intermediate or base claim. Claim 29 has been canceled without prejudice or disclaimer, and therefore the rejection is moot as to this claim. As discussed above, claim 22 is believed to be definite. The indefiniteness rejection of claim 23, which depends from claim 22, should therefore be withdrawn.

Response to Section 112 (new matter) rejection

Claim 1 is rejected as allegedly containing new matter, for indicating that SEQ ID NOS. 2, 4 or 8 constituted "part or all" of the claimed ASIC channel. The Examiner's attention is drawn to page 4, lines 1-8 of the specification[1], which disclose that the claimed ASIC channels can be hybrids constituted by different proteins of the invention. The passage on page 4 reads:

> The invention also relates to a hybrid cationic channel constituted by the combination of a first protein constituting a proton-activated ionic channel according to the invention with a second protein constituting a proton-activated ionic channel. Advantageously, the second protein is also a protein constituting a proton-activated ionic channel according to the invention. As an example of such a combination, one can cite the combination of the protein of the ASIC1A or ASIC2A or DRASIC channel with the protein of the MDEG1 channel, enabling formation of a hybrid channel . . .

Thus, the specification as filed clearly discloses that the proteins of claim 1 can constitute part (as in a hybrid) or all of the recited ASIC channel. Claim 1 is thus fully described and supported by the specification, and the Applicants therefore respectfully request that the section 112 (new matter) rejection of claim 1 be withdrawn.

---

[1] All references to the specification in this Response are to the substitute specification filed November 7, 2002.

The passages on pages 15-20 of the Office Action appear to interpret the recitation of "part or all" in claim 1 to indicate that the claim covers mutants, variants, analogs, homologs or derivatives of SEQ ID NOS: 2, 4 and 8. However, the phrase "part or all" in claim 1 refers to the recited ASIC channel, and not to the claimed proteins of SEQ ID NOS: 2, 4 and 8. Without remarking on whether the specification contains adequate written description for mutants, variants, analogs, homologs or derivatives of the proteins recited in claim 1, the Applicants respectfully point out that claim 1 as written is not directed to such mutants, variants, etc. of SEQ ID NOS. 2, 4 or 8. Rather, claim 1 specifies that the ASIC channel can be partly or wholly constituted by the full amino acid sequences as set forth in SEQ ID NOS: 2, 4 or 8. Thus, as evidenced by the passage from page 4 quoted above, claim 1 is fully described and supported by the specification.

Response to Section 101 rejections

Claim 11 is rejected as allegedly not being drawn to statutory subject matter. Claim 11 has been amended to recited an "isolated and purified" nucleic acid, as suggested by the Examiner, and the Applicants request that the rejection of claim 11 be withdrawn.

Claims 1, 11-13, 15, 17-23 and 26-29 remain rejected under 35 USC section 101 for allegedly lacking utility. These claims are also rejected as non-enabled, because one skilled in the art would allegedly not know how to use the claimed invention if an appropriate utility has not been established. Claims 28 and 29 have been canceled without prejudice or disclaimer, and therefore the rejections are moot as to these claims. The utility and non-enablement rejections with respect to claims 1, 11-13, 15, 17-23 and 26-27 are addressed below.

A claimed invention meets the utility requirements of § 101 if one skilled in the art would appreciate why such invention is useful and if the utility is specific, substantial and credible. *Utility Examination Guidelines*, 66(4) F.R. 1092, 1098, January 5, 2001. Where the applicant has asserted that a claimed invention is useful for any particular practical purpose (*i.e.*, it has a "specific and substantial utility"), and the assertion would be considered credible by a person of ordinary skill in the art, then a rejection based on lack of utility should not be imposed. *Id.* As discussed in the previous response, the Applicants' specification asserts several specific, substantial and credible utilities.

The Office Action alleges that the specification does not establish a specific, substantial and credible utility for the claimed proteins constituting the recited ASIC channel. In particular, the Office Action alleges on pg. 12 that "[e]ven if the expression of Applicants individual polynucleotides/polypeptides are affected by a test compound in an array for drug screening, the specification does not disclose any specific and substantial interpretation for the result, and none is known in the art." The Applicants respectfully disagree.

The specification states on page 10, lines 1-4 that proteins constituting ASIC channels can be used for the fabrication of drugs for treatment and prevention of pathologies such as cerebral neuronal degeneration, which may occur following a stroke. Neuronal degeneration following ischemia (stroke) is caused by ASIC channel hyperactivity (excitotoxicity); see page 8, lines 7-13. The specification also discloses on page 8, lines 4-6 that the claimed ASIC proteins "enable the investigation of blockers that that can inhibit neurodegeneration induced by hyperexpression of these channels." The specification further discloses on page 17 that the claimed ASIC channels can be inhibited by compounds such as amiloride, ethylisopropylamiloride (EIPA) and benzamil. Thus, one skilled in the art would readily understand that drugs for treatment and prevention of cerebral neuronal degeneration would constitute ASIC channel inhibitors, such as those actually identified by screening with the claimed ASIC channel proteins. According to the specification at page 17, lines 3-5, "[a]s shown in Fig. 6 (d, e), the ASIC channel exhibits the same pharmacology and is blocked in a reversible manner (Kd = 10 uM) by amiloride and its derivatives benzamil and EIPA.

A disclosure of the *in vitro* pharmacological activity of any compound, such as discussed above for the ASIC proteins, constitutes a showing of practical utility because such knowledge is "beneficial to the public." Cross v. Iizuka, 753 F.2d 1040, 1046 (Fed. Cir. 1985), quoting Nelson v. Bowler, 626 F.2d 853, 856 (CCPA 1980). *In vitro* tests which demonstrate a particular pharmacological activity are generally predictive of *in vivo* results, as long as there is a "significant probability" that *in vivo* testing for the activity will be successful. Id. at 1050. According to the Cross v. Iizuka court, "were this not so, the testing procedures of the pharmaceutical industry would not be as they are." Id. at 1050.

Here, the specification clearly correlates the activity of ASIC channels to the neuronal damage caused by ischemic events, and shows an *in vitro* pharmacologic activity for the claimed

ASIC proteins; *i.e.*, that they can be antagonized by certain compounds. One skilled in the art would reasonably believe that such antagonists could be administered, for example, to stroke victims, where they would block ASIC channel activity in ischemic areas of the brain and lessen the neurodegeneration caused by hyperstimulation of endogenous ASIC channels. The incidence of neuronal cell death following stroke would consequently be reduced. *In vivo* confirmation of the disclosed *in vitro* pharmacologic activity is not required, where there is a contemporaneous teaching correlating the *in vitro* activity to an *in vivo* effect. Rasmusson v. SmithKline Beecham Corp. 413 F.3d 1318, 1324 (Fed. Cir. 2005). Moreover, the Federal Circuit has stated:

> We perceive no insurmountable difficulty . . . in finding that the first link in the screening chain, *in vitro* testing, may establish a practical utility for the compound in question. Successful *in vitro* testing will marshal resources and direct the expenditure of effort to further *in vivo* testing of the most potent compounds, thereby providing an immediate benefit to the public, analogous to the benefit provided by the showing of *in vivo* utility."
>
> In re Fisher, 04-1465, pg. 21 (Fed. Cir. 9/7/2005), quoting Cross v. Iizuka.

The credibility of the asserted utility discussed above was recently supported in several post-filing publications:

In the previous Response, the Applicants cited a post-filing study by Xiong et al. (*Cell*, 2004, 118: 687; submitted previously) that demonstrated the involvement of ASIC1 channel activity in neuronal death after ischemia. Several other post-filing publications also show that ASIC channels are expressed in brain neurons (see Baron et al., 2002, J Phys, 539.2: 485-494; Wemmie et al., 2003, J Neurosci 23(13): 5496-5502; and Allen and Attwell, 2002, J Phys 543.2: 521-529, copies enclosed). In particular, Baron et al. (2002) report the presence of functional ASIC channels in hippocampal neurons. The studies disclosed in Wemmie et al. (2003) involved an immunochemistry examination of the ASIC1 protein distribution in the brain, which revealed that ASIC1 levels differed between brain regions and was higher in those areas supporting rich synaptic connectivity. Allen and Attwell (2002) characterized the pH-dependent activation of ASIC channels in cerebellar Purkinje cells.

When ASIC1a channels are blocked with a specific toxin (*e.g.*, PcTx1, as disclosed in Baron et al. (2002)), or if the ASIC1 gene is knocked-out (*e.g.*, as in the ASIC1-null mice used in Wemmie et al. (2003)), neuronal death after brain ischemia is dramatically reduced. Thus, ASIC1a channel activity is a cause of neuronal loss after ischemia, and drugs that block ASIC1 channels (such as the ASIC1a antagonist PcTx1) help prevent neuronal loss. Comments on the Xiong et al. (2004) study were published in two other journals (Love, 2004, The Lancet Neurology, 3: 636; and Benveniste and Dingledine, 2005, N. Engl. J. Med., 2005, vol. 352:85-86; submitted with previous Response), which also suggested a potential use of ASIC channel blockers for the prevention of post ischemic neuronal loss.

The Office Action alleges on page 8 that "amiloride sensitivity cannot be used to infer a specific or well-established utility" (citing to Berediev et al., page 15034, col. 1). However, the Love, 2004 article cites to John Wood from University College in London, who states that "non-toxic molecules such as amiloride can be rapidly assessed for their utility as neuroprotectants," indicating that one skilled in the art would consider the further characterization of compounds such as ameloride is routine.

The Office Action also alleges on page 7 that the function of ASIC channels in the brain is "obscure" and that "the function of these channels in the glia remains a mystery," again citing to Berediev. Berediev examined brain glioma cell lines, not brain glia. As discussed in the previous Response, tumor cell lines are different from the parental non-transformed cells, and tumors are often associated with chromosomal rearrangements and changes in gene expression patterns. Thus the presence of an ASIC current in certain glioma cells does not imply or necessitate a role for these channels in untransformed brain glia. Indeed, expression of ASIC channels has never been described in glia, and the report by Berediev is the only one that describes ASIC channels in glioma and in glioma cell lines. Conversely, Chen et al. (1998, Proc. Nat. Acad. Sci. USA 95: 10240-10245; enclosed) show in Fig. 2 that neither ASIC1 nor ASIC3 is expressed in another glioma cell line (C6 glioma). Thus ASIC channels are only expressed in certain gliomas and there is no report of expression of ASIC channels in normal brain glia. Thus, the comments in the Office Action that the role of ASIC channels in glia is not known is disingenuous, since the current literature confirms an expression of ASIC channels in brain neurons and no expression in normal brain glia. However, there is ample information in the

literature and in the Applicants' specification regarding expression of functional ASIC channels in brain neurons, as discussed above.

Thus, based on the disclosed *in vitro* pharmacologic activity of the claimed ASIC proteins, one skilled in the art would find the asserted utility of using these proteins to identify drugs for the treatment of post-ischemic neuronal cell death to be credible. The Revised Interim Utility Guidelines Training Materials state that an asserted utility for treating a disease is specific and substantial. Moreover, as long as a claimed invention meets at least one stated utility, the utility requirement is satisfied. *Stiftung v. Renishaw PLC*, 20 USPQ2d 1094, 1100 (Fed. Cir. 1991). The Applicants therefore submit that the specification discloses at least one specific, substantial and credible utility for the ASIC proteins of claim 1, and respectfully request that the utility rejection of claims 1, 11-13, 15, 17-23 and 26-27 be withdrawn.

Response to the section 112, 1st paragraph rejection

Claims 1, 11-13, 15, 17-23 and 26-27 are rejected under 35 U.S.C. §112, first paragraph. This rejection follows from and is dependent upon the §101 rejection discussed above; stating, in essence, that one skilled in the art would not know how to use the claimed invention because an appropriate utility has allegedly not been established. For the reasons set forth above, the application does, in fact, set forth at least one sufficient, specific, substantial and credible utility for the claimed proteins constituting the ASIC channels. Thus, one skilled in the art would know how to make and use the claimed invention. The §112, 1st paragraph enablement rejection of claims 1, 11-13, 15, 17-23 and 26-27 should therefore be withdrawn.

Conclusion

Based on the foregoing, the Applicants respectfully submit that the Application is now in a condition for allowance, which is respectfully requested.

Respectfully submitted,

Paul Carango

Paul Carango
Reg. No. 42,386
Attorney for Applicants

PC:rb
(215) 656-3320

Journal of Physiology (2002), **539.2**, *pp.* 485–494
© The Physiological Society 2002

DOI: 10.1013/jphysiol.2001.014837
www.jphysiol.org

ASIC-like, proton-activated currents in rat hippocampal neurons

Anne Baron, Rainer Waldmann and Michel Lazdunski

Institut de Pharmacologie Moléculaire et Cellulaire, CNRS-UMR 6097, 660 route des Lucioles, Sophia Antipolis, 06560 Valbonne, France

The expression of mRNA for acid sensing ion channels (ASIC) subunits ASIC1a, ASIC2a and ASIC2b has been reported in hippocampal neurons, but the presence of functional hippocampal ASIC channels was never assessed. We report here the first characterization of ASIC-like currents in rat hippocampal neurons in primary culture. An extracellular pH drop induces a transient Na^+ current followed by a sustained non-selective cation current. This current is highly sensitive to pH with an activation threshold around pH 6.9 and a $pH_{0.5}$ of 6.2. About half of the total peak current is inhibited by the spider toxin PcTX1, which is specific for homomeric ASIC1a channels. The remaining PcTX1-resistant ASIC-like current is increased by 300 μM Zn^{2+} and, whereas not fully activated at pH 5, it shows a $pH_{0.5}$ of 6.0 between pH 7.4 and 5. We have previously shown that Zn^{2+} is a co-activator of ASIC2a-containing channels. Thus, the hippocampal transient ASIC-like current appears to be generated by a mixture of homomeric ASIC1a channels and ASIC2a-containing channels, probably heteromeric ASIC1a+2a channels. The sustained non-selective current suggests the involvement of ASIC2b-containing heteromeric channels. Activation of the hippocampal ASIC-like current by a pH drop to 6.9 or 6.6 induces a transient depolarization which itself triggers an initial action potential (AP) followed by a sustained depolarization and trains of APs. Zn^{2+} increases the acid sensitivity of ASIC channels, and consequently neuronal excitability. It is probably an important co-activator of ASIC channels in the central nervous system.

(Resubmitted 29 November 2001; accepted 6 December 2001)
Corresponding author M. Lazdunski: Institut de Pharmacologie Moléculaire et Cellulaire, CNRS-UMR 6097, 660, route des Lucioles, Sophia Antipolis, 06560 Valbonne, France. Email: ipmc@ipmc.cnrs.fr

H^+-gated cation channels are present in sensory neurons and in neurons of the central nervous system (CNS). Several H^+-gated cation channel subunits (ASIC, acid sensing ionic channels) have been cloned and functionally expressed so far: ASIC1a (Waldmann *et al.* 1997*b*), ASIC1b (Chen *et al.* 1998), ASIC2a (Price *et al.* 1996; Waldmann *et al.* 1996), ASIC2b (Lingueglia *et al.* 1997), ASIC3 (Waldmann *et al.* 1997*a*; de Weille *et al.* 1998; Babinski *et al.* 1999). Very recently, another putative ASIC subunit (ASIC4) was identified which seems not to be activated by acidic pH (Akopian *et al.* 2000; Grunder *et al.* 2000).

Functional ASIC channels are thought to be tetrameric assemblies of ASIC subunits (Coscoy *et al.* 1998; Waldmann *et al.* 1999). Both homomeric and heteromeric ASIC channels can be formed (Bassilana *et al.* 1997; Waldmann & Lazdunski, 1998; Waldmann *et al.* 1999; Babinski *et al.* 2000), thus contributing to the functional diversity of neuronal ASIC-like channels (Grantyn & Lux, 1988; Ueno *et al.* 1992; Varming, 1999; Escoubas *et al.* 2000; Sutherland *et al.* 2000*a*).

Some ASIC subunits are specifically expressed in sensory neurons, like ASIC1b (Chen *et al.* 1998) and ASIC3 (Waldmann *et al.* 1997*a*; Voilley *et al.* 2001), whereas ASIC1a (Bassilana *et al.* 1997; Olson *et al.* 1998; Voilley *et al.* 2001), ASIC2a (Price *et al.* 1996, 2000; Bassilana *et al.* 1997; Lingueglia *et al.* 1997; Garcia-Anoveros *et al.* 2001), ASIC2b (Lingueglia *et al.* 1997) and ASIC4 (Akopian *et al.* 2000; Grunder *et al.* 2000) are also found in central neurons.

In sensory neurons, ASIC currents are thought to play an important role in nociception during a tissue acidosis and inflammation (Olson *et al.* 1998; Waldmann & Lazdunski, 1998; Benson *et al.* 1999; Kress & Zeilhofer, 1999; Waldmann *et al.* 1999; Sutherland *et al.* 2000*a*,*b*; Voilley *et al.* 2001), and ASIC2a has been proposed to participate in touch sensation (Price *et al.* 2000; Garcia-Anoveros *et al.* 2001).

The role of ASIC1a, ASIC2a, ASIC2b and ASIC4 in central neurons (Price *et al.* 1996; Waldmann *et al.* 1996; Bassilana *et al.* 1997; Garcia-Anoveros *et al.* 1997) remains to be established. An acidosis accompanies brain ischaemia or epilepsy, and ASIC currents might contribute to the associated neuronal death. However, pH fluctuations also occur in normal brain function. Several studies with brain slices indicate that neuronal activity gives rise to significant and rapid changes in extracellular pH (Krishtal *et al.* 1987; Chesler & Kaila, 1992). Because of the limited spatial and temporal resolution of pH microelectrodes used in those

studies, the global pH variations that have been reported may underestimate the actual pH changes occurring within or in the vicinity of the synaptic cleft (Chesler & Kaila, 1992). The content of synaptic vesicles is acidic (Ozkan & Ueda, 1998) and synaptic release during neuronal activity is expected to create an extracellular acidification in the vicinity of the synaptic cleft. For hippocampal neurons, an intravesicular pH of 5.7 has been measured with a pH-sensitive fluorescent probe (Miesenbock *et al.* 1998). The same study showed a transient decrease in the extracellular pH to about 6.4 after secretion of synaptic vesicles.

Synaptic vesicles of hippocampal glutamatergic neurons also contain a high amount of Zn^{2+}, particularly in the dentate granule cells and their projections, the mossy fibres (Frederickson, 1989). Vesicular Zn^{2+} is co-released with the neurotransmitter (i.e. glutamate), resulting in a transient increase of the local synaptic Zn^{2+} concentration up to 100–300 μM from resting levels below 500 nM (Assaf & Chung, 1984; Howell *et al.* 1984; Smart *et al.* 1994; Budde *et al.* 1997; Weiss *et al.* 2000). Zn^{2+} is known to exert a variety of effects on ion channels, among which are AMPA and NMDA receptors, and was thus proposed to be a neuromodulator of the excitatory glutamatergic synapse (Harrison & Gibbons, 1994; Smart *et al.* 1994; Henze *et al.* 2000; Vogt *et al.* 2000).

In order to understand the function of the brain ASIC subunits, particularly in hippocampus which is involved in memory processes and in the physiopathology of ischaemia (Schmidt-Kastner & Freund, 1991; Henze *et al.* 2000), we recorded and characterized the molecular constitution of the ASIC-like current in hippocampal neurons. We previously showed that Zn^{2+} potentiates the activation of ASIC2a-containing ASIC channels (Baron *et al.* 2001). We demonstrate here that the hippocampal ASIC-like current is coactivated by Zn^{2+} resulting in an increase in neuronal excitability.

METHODS

Primary cultured hippocampal neurons

Primary cell cultures derived from rat embryonic hippocampi, containing mainly neurons over astrocytes, were established as described previously (Goslin & Banker, 1991; Lauritzen *et al.* 1997). In brief, 18- to 19-day-pregnant Wistar rats were stunned and killed by decapitation, according to national and institutional guidelines. Embryos were removed and hippocampi were dissected, incubated in 0.125% trypsin for 35 min at 37°C, and dissociated mechanically. Cells were plated in modified Eagle's medium (MEM) containing 10% dialysed inactivated horse serum (Sigma), 6 g l^{-1} glucose, 50 U ml^{-1} penicillin, and 50 μg ml^{-1} streptomycin. Cells were plated (day 0) at a density of ~750 000 cells per 35-mm poly-L-lysine-coated tissue culture plates (Falcon). After 48 h, the culture medium was replaced with serum-free MEM with 2% B27 supplement (Gibco) and 6 g l^{-1} glucose, and kept in 95% air–5% CO_2 at 37°C. Cells were used for electrophysiological recordings 7–20 days after plating. Neurons with triangular-shaped cell bodies, a typical feature of pyramidal neurons, were selected for recording.

Patch-clamp recordings of hippocampal ASIC-like currents

Ion currents were recorded using the whole-cell patch-clamp technique (Hamill *et al.* 1981). Data were sampled at 500 Hz and low-pass filtered at 3 kHz using pCLAMP 8 software (Axon Instruments, USA). The statistical significance of differences between sets of data was estimated by the single-sided Student test. The pipette solution contained (mM): KCl 140, NaCl 5, $MgCl_2$ 2, EGTA 5, K_2ATP 2, Hepes 10 (pH 7.35), and the bath solution contained (mM): NaCl 150, KCl 5, $MgCl_2$ 2, $CaCl_2$ 2, glucose 10 mM, Hepes 10 (pH 7.45). CNQX 20 μM, kynurenic acid 10 μM, $MgCl_2$ 7 mM and bicuculline 10 μM were added in order to inhibit glutamate- and GABA-induced currents. MES or acetate were used instead of Hepes to buffer bath solution pH ranging from 6 to 5, and from 4.5 to 3, respectively. $ZnCl_2$ was added to the bath solution at 300 μM (Baron *et al.* 2001). Changes in extracellular pH were induced by shifting one out of six outlets of a microperfusion system in front of the cell. Experiments were carried out at room temperature (20–24°C). Bovine serum albumin (0.1%) was added in extracellular solutions containing the spider toxin PcTX1 (Escoubas *et al.* 2000) to prevent its adsorption to tubing and containers. Amiloride, CNQX, bicuculline, capsaicin, capsazepine and kynurenic acid were all from Sigma.

RESULTS

ASIC-like current of primary cultured hippocampal neurons

The expression of ASIC1a and ASIC2a was previously studied in hippocampal neurons by *in situ* hybridization. A high level of overlapping expression of the two subunits was particularly found in the pyramidal neurons of CA1 and CA3 subfields of the hippocampus (Bassilana *et al.* 1997; Waldmann *et al.* 1997*a*,*b*). However, the presence of functional hippocampal ASIC channels was never assessed. When the neurons were held at −50 mV, acidification of the extracellular medium triggered a transient inward current that was frequently followed by a plateau phase (Fig. 1*A* and *C*). At −50 mV, a drop to pH 5 induced a mean peak current of 17.15 ± 1.86 pA pF^{-1} and a mean plateau current of 1.41 ± 0.33 pA pF^{-1} (cell capacitance: 39.8 ± 2.7 pF, n = 52). The *I–V* curve shows that the peak transient current (Fig. 1*A* and *B*, ○) is highly selective for Na^+ (E_{rev} (reversal potential) = +80 mV) whereas the plateau current was non-selective (E_{rev} = +15 mV; Fig. 1*A* and *B*, ●).

The hippocampal ASIC-like peak current showed a high sensitivity to pH, with an activation threshold around pH 6.9 (Fig. 1*C* and *D*). Between pH 7.4 and 5, the activation of the peak current could be fitted by a sigmoidal curve, with a half-maximal activation at pH 6.2 and a Hill slope factor (n_H) of 1.48 (Fig. 1*D*). These activation properties are intermediate between those of heterologously expressed homomeric ASIC1a and heteromeric ASIC1a+2a currents ($pH_{0.5}$ = 6.4 and n_H = 1.65 for ASIC1a, $pH_{0.5}$ = 5.5 and n_H = 1.10 for ASIC1a+2a (Baron *et al.* 2001; Fig. 1*D*). This suggests that the hippocampal ASIC-like current flows through a mixture of different channels. This view is

supported by the fact that the current is not fully activated at pH 5 and can be further increased at pH 4.

Pharmacological properties of hippocampal ASIC-like current

The peak current was fully inhibited by 500 μM amiloride, a known blocker of ASIC channels (Lingueglia *et al.* 1993; Waldmann *et al.* 1997b, 1999), whereas the plateau current was not fully suppressed (Fig. 2*A*). The hippocampal ASIC-like current was not inhibited by 10 μM capsazepine, and 100 μM capsaicin evoked only a small inward current in hippocampal neurons (0.7 ± 0.3 pA pF^{-1}, $n = 5$, not shown), showing that a contamination of the ASIC-like current by the pH-activated VR1 current (Tominaga *et al.* 1998; Szallasi & Di Marzo, 2000) can be ruled out. In the majority (80 %) of the recorded neurons, the hippocampal ASIC-like peak current induced at pH 6 was inhibited by 46 ± 8 % ($n = 12$) by the tarantula toxin PcTX1, a specific blocker of homomeric ASIC1a channels (Escoubas *et al.* 2000) (Fig. 2*B*), whereas the inhibition was complete in the remaining 20 % of cells. This result shows that the hippocampal ASIC-like current is due to a mixture of homomeric ASIC1a channels and at least one other PcTx1-resistant ASIC channel.

Effect of Zn^{2+} on hippocampal ASIC-like current

Previous work with recombinant channels has shown that Zn^{2+} co-applied with acidic pH increases the amplitude of ASIC2a-containing currents (Baron *et al.* 2001). We tested the effect of Zn^{2+} on the hippocampal ASIC-like current with two purposes in mind. The first was to use Zn^{2+} as a pharmacological tool to reveal the involvement of ASIC2a subunits in hippocampal ASIC assemblies. The second was to establish a possible physiological role for Zn^{2+} in the activation of these channels. In 80 % of the recorded cells, 300 μM Zn^{2+} increased the peak hippocampal ASIC-like current, with no effect on the sustained current (Fig. 3*A*). The PcTX1-resistant peak current was more sensitive to Zn^{2+} than the whole ASIC-like current (Fig. 3*B*), consistent with the fact that the homomeric ASIC1a current is insensitive to Zn^{2+} (Baron *et al.* 2001). In the presence of PcTX1, 300 μM Zn^{2+} increased the amplitude of the peak ASIC-like current by a factor of 4.74 ± 0.73 ($n = 4$) at pH 6.9, by a factor of 1.86 ± 0.19 ($n = 6$) at pH 6, and by a

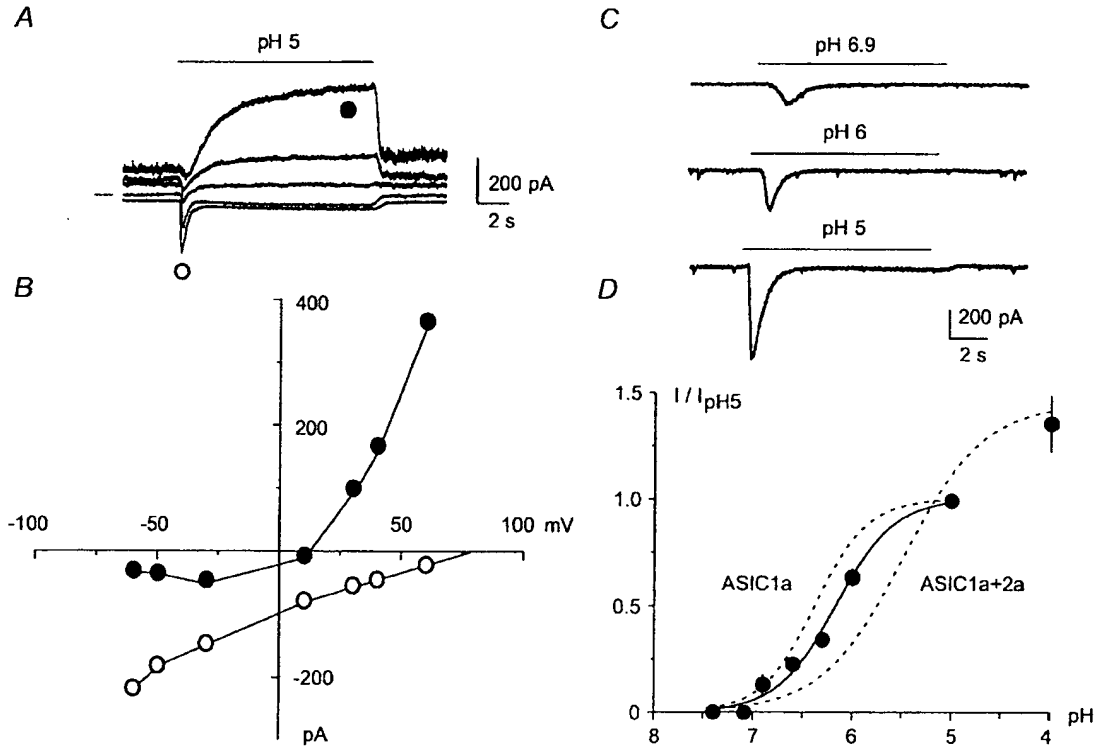

Figure 1. ASIC-like current in hippocampal neurons

A, hippocampal ASIC-like currents activated at pH 5 and recorded at −60, −30, +10, +30 and +60 mV. The 0 pA current level is indicated on the left. *B*, current–potential relationship of hippocampal ASIC-like current obtained from traces shown in *A*. ○, peak current; ●, plateau current. *C*, hippocampal ASIC-like currents induced by pH 6.9, 6 and 5. Currents were recorded at −50 mV. *D*, pH-dependent activation of the hippocampal ASIC-like current. Current amplitude was expressed as a fraction of the current induced by pH 5 ($I/I_{pH\,5}$), and plotted as mean ± S.E.M., n ranging from 8 to 18. Between pH 7.4 and 5, data could be fitted by a sigmoidal curve, showing a $pH_{0.5}$ of 6.2 and a Hill coefficient of 1.48. The dashed curves represent the pH-dependent activation of the homomeric ASIC1a and of the heteromeric ASIC1a+2a (1:1) currents expressed in *Xenopus* oocytes (Baron *et al.* 2001).

factor of 1.33 ± 0.11 ($n = 4$) at pH 5. These values are similar to those obtained for the ASIC1a+2a current expressed in *Xenopus* oocytes or in COS cells (Baron *et al.* 2001). The few Zn^{2+}-insensitive currents were highly (90–100 %) inhibited by PcTX1, and would thus correspond to homomeric ASIC1a currents.

To investigate the molecular association involved in hippocampal Zn^{2+}-sensitive ASIC-like current, we measured the pH sensitivity of the PcTX1-resistant Zn^{2+}-sensitive ASIC-like current (Fig. 3*C*, ○) and compared it with the pH sensitivity of the PcTx1-sensitive Zn^{2+}-insensitive ASIC-like current (Fig. 3*C*, ●). The PcTx1-sensitive Zn^{2+}-insensitive current showed a $pH_{0.5}$ of 6.3 with a maximal activation at pH 5, which would be expected from homomeric ASIC1a current. In contrast, the PcTX1-resistant Zn^{2+}-sensitive current was not maximal at pH 5 and greatly increased at pH 4. Between pH 7.4 and 5, a $pH_{0.5}$ of 6.0 was obtained, a value significatively lower than that for both the PcTX1-sensitive Zn^{2+}-insensitive current (ASIC1a-like) or the whole ASIC-like current. These results support the suggestion that ASIC2a-containing heteromers are involved between pH 7.4 and 5, whereas the further increase in current at pH 4 could be mainly due to homomeric ASIC2a channels.

The Zn^{2+} sensitivity of the peak hippocampal ASIC-like current thus appears to be conferred by a PcTX1-resistant current, probably flowing through ASIC1a+2a channels.

Effect of Zn^{2+} and ASIC-like current on the membrane potential of hippocampal neurons

Membrane potential variations have been recorded in the current-clamp mode. Hippocampal neurons had a resting potential of −49.8 ± 2.0 mV ($n = 29$) which usually prevented the triggering of spontaneous action potentials (APs) (Fig. 4*A* and *D*). Acidification of the extracellular medium induced a biphasic depolarization with a transient phase and a plateau (Fig. 4*Aa–c*), compatible with kinetics of the hippocampal ASIC-like current (Fig. 4*Ad*). The transient depolarizations induced by pH shifts from 7.4 to 6.6 or 5 triggered an initial AP (Fig. 4*Ab* and *c*, enlargements shown), whereas the threshold of the AP was not reached by the transient depolarization induced by a pH drop to 6.9 (Fig. 4*Aa*). However, spontaneous AP trains could often be recorded during the plateau of the depolarization induced by pH drops to 6.9 or to 6.6 (Fig. 4*Aa* and *b*), whereas lower pH values (pH 5 in Fig. 4*Ac*) induced a sustained depolarization to around −20 mV but did not produce any AP. This can be easily explained by an inactivation of the voltage-sensitive Na^+ channels by the sustained depolarization, and the prevention of any AP triggering.

The transient peak of the acid-induced depolarization at pH 5 (46.4 ± 2.3 mV; $n = 12$) corresponds to a membrane potential close to 0 mV, whereas the maximal depolarization induced by a pH drop from 7.4 to 6.9 (10.6 ± 4.0 mV; $n = 9$) would bring the membrane potential to around −40 mV (Fig. 4*B*). Figure 4*C*, showing the relationship between the ASIC current density and the membrane depolarization induced by the same pH drop on the same neuron, illustrates the fact that 25 % of the maximal ASIC current could induce 50 % of the maximal depolarization. Thus, a slight drop of the extracellular pH and a submaximal activation of ASIC channels may cause important changes in the excitability of hippocampal neurons.

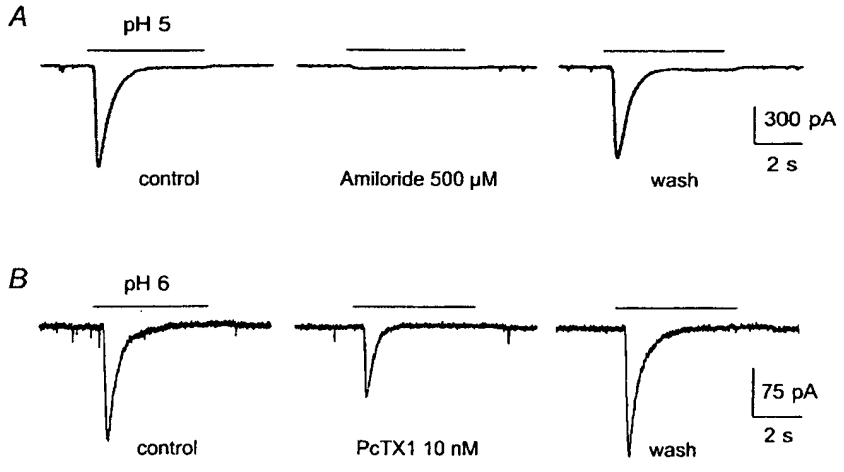

Figure 2. Pharmacological properties of the hippocampal ASIC-like current

A, reversible inhibition of hippocampal ASIC-like current by 500 μM amiloride. *B*, reversible inhibition of hippocampal ASIC-like current by 10 nM of the toxin PcTX1. Currents were recorded at −50 mV. Amiloride and PcTX1 were given before and during the pH drop.

Zn^{2+} potentiates the hippocampal ASIC-like current. It also increases the submaximal acid-induced transient depolarizations. Figure 4*D* shows the effect of 300 μM Zn^{2+} co-applied with pH 6.9. In the absence of Zn^{2+}, APs were only recorded during the plateau phase of the depolarization induced by pH 6.9 (Fig. 4*Da*), whereas, in the presence of 300 μM Zn^{2+}, APs were also triggered during the increased transient depolarization (Fig. 4*Db*). The depolarization induced by a pH drop to 5 was not significantly modified by Zn^{2+} (not shown). This was expected considering that a

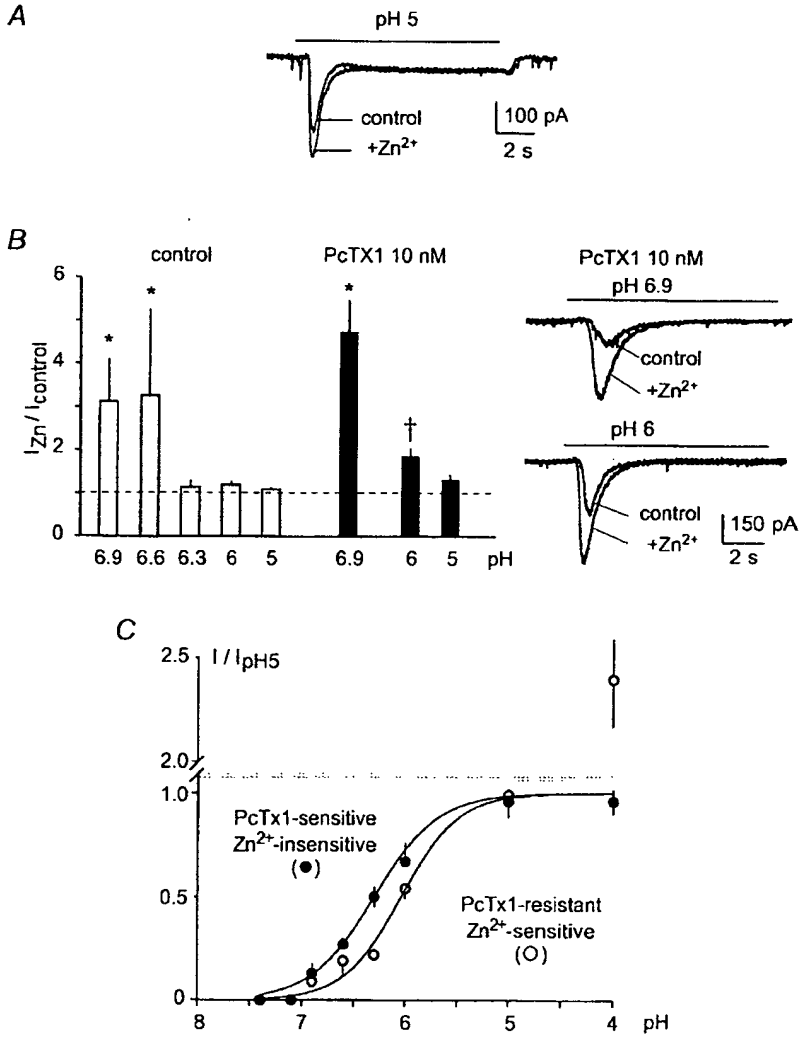

Figure 3. Effect of Zn^{2+} on the hippocampal ASIC-like current

A, 300 μM Zn^{2+} co-applied with acidic pH increases the amplitude of the peak hippocampal ASIC-like current without affecting the plateau phase. Currents were recorded at −50 mV. *B*, effect of 300 μM Zn^{2+} on hippocampal ASIC-like currents induced by pH ranging from 6.9 to 5. Current amplitude ratio ($I_{Zn}/I_{control}$) was measured for each pH value, in the absence (□) and in the presence of 10 nM PcTX1 (■), and plotted as mean ± S.E.M., *n* ranging from 4 to 22; * significantly different from corresponding pH 5 ratio ($P < 0.05$); † Significantly different from corresponding control (no PcTX1) pH ratio ($P < 0.005$). Currents were recorded at −50 mV. On the right side on the histogram, original current traces are shown to illustrate the effect of Zn^{2+} on hippocampal ASIC-like current induced by pH 6.9 (top) and pH 6 (bottom) in the presence of PcTX1 (holding potential: −50 mV). *C*, pH-dependent activation of the PcTX1-sensitive Zn^{2+}-insensitive ASIC-like current (●) and of the PcTX1-resistant Zn^{2+}-sensitive ASIC-like current (○). Data for PcTX1-resistant ASIC-like current were obtained from the same experiments as in *B*. Data for PcTX1-sensitive Zn^{2+}-insensitive ASIC-like current were obtained from neurons (20% of total recorded neurons) showing an ASIC-like current highly sensitive to PcTX1 (90–100% inhibited) and not potentiated by Zn^{2+}. Current amplitude was expressed as a fraction of the current induced by pH 5 (I/I_{pH5}), and plotted as mean ± S.E.M., *n* ranging from 4 to 18. Between pH 7.4 and 5, data could be fitted by sigmoidal curves, showing a $pH_{0.5}$ of 6.3 for the PcTX1-sensitive Zn^{2+}-insensitive ASIC-like current and a $pH_{0.5}$ of 6.0 for the PcTX1-resistant Zn^{2+}-sensitive ASIC-like current.

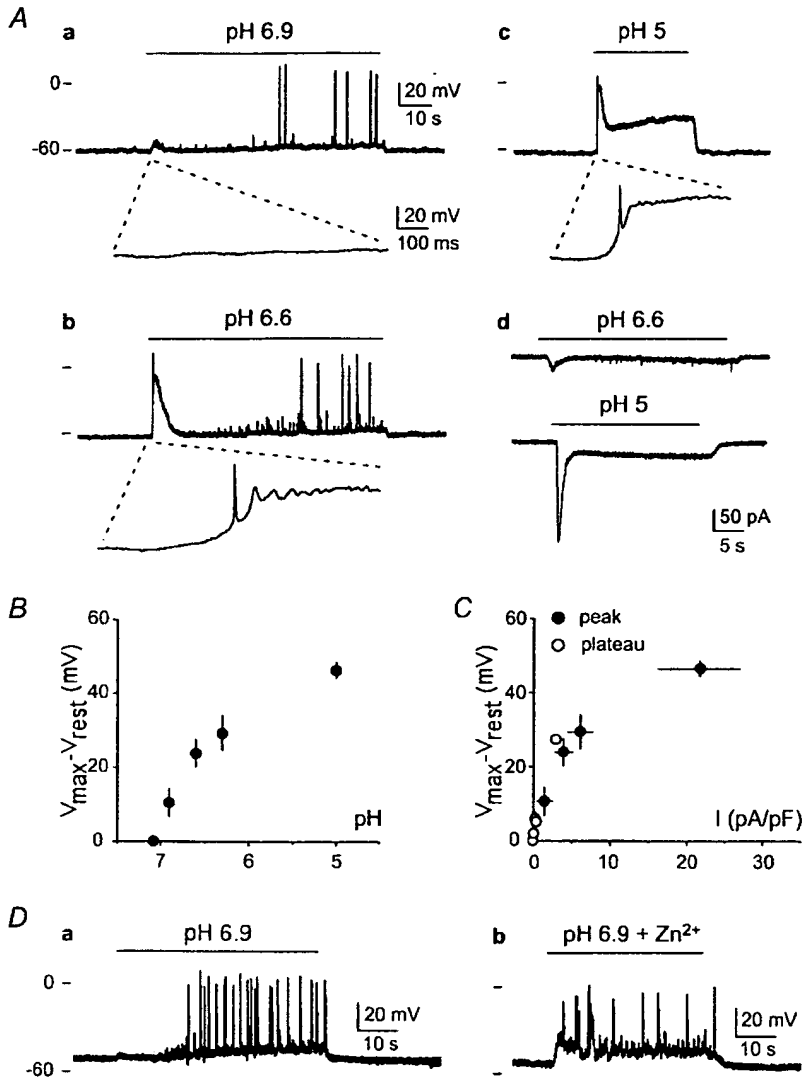

Figure 4. Effect of ASIC current activation on membrane potential of hippocampal neurons

A, membrane depolarization induced by pH 6.9 (*a*), pH 6.6 (*b*) and pH 5 (*c*) in a single neuron. The initial acid-induced depolarization and AP is shown on a higher scale (100-fold) under each recording. Membrane potential was recorded in current-clamp mode with 0 pA current. Resting potential was −63 mV. Ticks on the left side of recordings represent the 0 mV level (upper tick) and the −60 mV level (lower tick). On the same neuron, ASIC-like currents activated by pH 6.6 and 5 were subsequently recorded in voltage-clamp mode at −60 mV (*d*). *B*, mean maximal membrane depolarization induced by ASIC-like current activation ($V_{max} - V_{rest}$) as a function of extracellular pH. Recordings with a resting membrane potential (V_{rest}) between −45 and −55 mV were selected, and action potentials were excluded of measurements. Mean ± S.E.M. values are shown, *n* ranging from 3 to 12. *C*, mean maximal membrane depolarization induced by ASIC-like current activation ($V_{max} - V_{rest}$) as a function of current density. For membrane potential measurements, recordings with a resting membrane potential between −45 and −55 mV (V_{rest}) were selected, and action potentials were excluded of measurements. ASIC-like current density (pA pF^{-1}) was subsequently measured on the same neurons, at holding potential between −45 and −55 mV. Membrane potential and ASIC-like current amplitude were measured during the transient phase (●) and during the sustained plateau phase (○) for the same pH value. Mean ± S.E.M. values are shown, *n* ranging from 3 to 12. *D*, effect of 300 μM Zn^{2+} on membrane depolarization induced by ASIC-like current activation. Membrane depolarization induced by pH 6.9 (*a*) and pH 6.9 + 300 μM Zn^{2+} (*b*) on a single neuron. Membrane potential was recorded in current-clamp mode with 0 pA current. Resting membrane potential was −53 mV. Ticks on the left side of recordings represent the 0 mV level (upper tick) and the −60 mV level (lower tick).

pH change of this magnitude already induced a quasi-maximal depolarization (Fig. 4C).

DISCUSSION

ASIC-like currents in CNS neurons

Several ASIC-like currents have been recorded in different types of central neurons. However, the available data show an important diversity of ASIC-like currents depending on the neuronal type. In mouse cerebellar granule cells, the half-maximal activation of ASIC-like current was obtained at $pH_{0.5} = 6.4$, and the current was nearly completely inhibited by PcTX1 ($IC_{50} = 0.7$ nM). These two properties suggested that the ASIC-like current mainly flows through homomeric ASIC1a channels in cerebellar granule cells (Escoubas *et al.* 2000). With a half-maximal activation at pH 6.8 (Grantyn & Lux, 1988), ASIC-like currents in rat tectal neurons also seem to flow through homomeric ASIC1a channels, although a pharmacological analysis using PcTX1 would be needed to confirm this. In rat ventromedial hypothalamic neurons (Ueno *et al.* 1992), the properties of ASIC-like currents are quite different with a threshold at pH 6.5, a maximal activation at pH 4 and $pH_{0.5} = 4.9$. These properties seem closer to those of the heteromeric ASIC1a+2a current (Baron *et al.* 2001). In mouse cortical neurons, low $pH_{0.5}$ values also suggest the involvement of heteromeric ASIC1a+2a channels (Varming, 1999). However, here again, because no pharmacological tools or antibodies were available, it was impossible to elucidate the exact molecular nature of the ASIC channels.

We report here the first characterization of ASIC-like current in hippocampal neurons. Extracellular acidification induces a biphasic current, i.e. a transient Na^+ current followed by a sustained non-selective cation current. The partial block by the ASIC1a-specific toxin PcTX1 (Escoubas *et al.* 2000), the pH dependence and the Zn^{2+} co-activation of the hippocampal current suggest that the transient current flows through a mixture of PcTX1-sensitive Zn^{2+}-insensitive homomeric ASIC1a channels and of PcTX1-resistant Zn^{2+}-sensitive ASIC2a-containing channels. The biphasic pattern of the PcTX1-resistant current activation curve (Fig. 3C, ○) suggests that the PcTX1-resistant current involves as least two different channel types: putative heteromeric ASIC1a+2a with a $pH_{0.5}$ of 6.0, and putative homomeric ASIC2a channels mainly responsable for the increase in current amplitude at pH 4. The pH sensitivity of heteromeric ASIC1a+2a channels is highly dependent on the stoichiometry of the two subunits. Whereas homomeric ASIC1a current shows a $pH_{0.5}$ of 6.4 and the homomeric ASIC2a shows a $pH_{0.5}$ of 4.4, the heteromeric ASIC1a+2a (1:1) current shows a $pH_{0.5}$ of 5.5 and the heteromeric ASIC1a+2a (1:2) current shows a $pH_{0.5}$ of 5.1 (Baron *et al.* 2001; A. Baron, unpublished data). Thus, the $pH_{0.5}$ of 6.0 obtained for the PcTX1-resistant Zn^{2+}-sensitive hippocampal current activated between pH 7.4 and 5 suggests that the heteromeric ASIC1a+2a channels would contain a higher proportion of ASIC1a subunits than of ASIC2a subunits. This hypothesis is supported by semi-quantitative RT-PCR experiments performed on the same hippocampal neurons as those used in patch-clamp experiments, which showed a 10-fold lower level of ASIC2a mRNA compared to ASIC1a mRNA (N. Voilley, unpublished data). This suggests a higher probability of a heteromeric association between ASIC1a and ASIC2a subunits rather than a homomeric ASIC2a association, and that heterotetrameric ASIC1a+2a channels could involve more ASIC1a than ASIC2a subunits.

ASIC2b is known to induce a sustained outward-rectifying non-selective cationic current when associated with other ASIC subunits (Lingueglia *et al.* 1997). Since ASIC1a, ASIC2a and ASIC2b are expressed in hippocampal neurons (Price *et al.* 1996; Waldmann *et al.* 1996; Bassilana *et al.* 1997; Garcia-Anoveros *et al.* 1997), it is likely that heteromeric ASIC2b-containing channels are responsible for the sustained non-selective cation current recorded in hippocampal neurons. However, it is difficult to postulate the stoichiometry or the other subunits involved in these heteromeric channels (ASIC1a+2b, ASIC2a+2b or even ASIC1a+2a+2b). The participation of ASIC2b in the plateau phase is thus highly probable but the involvement of another channel type cannot be ruled out. Further biochemical evidence will be needed to confirm the presence and the molecular composition of functional heteromeric ASIC channels in hippocampal neurons.

Effects of extracellular pH variations on neuronal activity

There are situations in which acidic pH may lead to a decrease in neuronal excitability (Hsu *et al.* 2000). Protons inhibit NMDA currents and voltage-dependent Ca^{2+} currents, whereas $GABA_A$ currents are stimulated (Chesler & Kaila, 1992). In contrast, a rapid external acidification has been shown to excite a variety of neurons, due to the activation of ASIC-like currents (Gruol *et al.* 1980; Krishtal *et al.* 1987; Jarolimek *et al.* 1989; Walz, 1989; Chesler & Kaila, 1992; Varming, 1999). Neurons of rat ventral medulla oblongata have been shown to respond to small extracellular pH variations by a transient increase in AP frequency (Jarolimek *et al.* 1990). A rapid acid-triggered depolarization and the generation of spikes was also reported in mouse cortical spinal neurons (Gruol *et al.* 1980; Varming, 1999).

We show that ASIC-like current activation triggers a membrane depolarization and trains of APs in hippocampal neurons. Small pH changes, compatible with local transient acidifications reported in the CNS (Krishtal *et al.* 1987; Jarolimek *et al.* 1989; Chesler & Kaila, 1992; Miesenbock *et al.* 1998), can increase neuronal excitability by raising the

membrane potential to a level near the voltage-dependent Na^+ channel threshold.

Under certain pathological conditions, such as brain ischaemia, the local extracellular pH becomes quite acidic, reaching values around 6.5 (Ohno *et al.* 1989; Nedergaard *et al.* 1991). Activation of sustained ASIC currents is then expected to produce an intense firing of neurons which itself might contribute to neuronal death during an ischemic insult. Very recently, variations of expression of ASIC subunits has been related to physiopathological processes. Ischaemia induces the increase of ASIC2a expression in neurons of hippocampus and cortex (Johnson *et al.* 2001), whereas epilepsy induces a marked decrease in ASIC2b mRNA levels in all hippocampus areas and in ASIC1a mRNA levels in the CA1–2 fields (Biagini *et al.* 2001). Taken altogether, these results suggest an important role for ASIC subunits in both normal and pathological activity of hippocampus.

Effect of Zn^{2+} on ionic currents and neuronal excitability

Ever since the discovery that Zn^{2+} is present in large amounts in hippocampus, there has been intense speculation concerning a possible synaptic signalling role for this metal in brain function. In general, exogenous Zn^{2+} tends to lead to excitatory bursting (Harrison & Gibbons, 1994; Reece *et al.* 1994; Henze *et al.* 2000). Some of this excitatory effect is likely to be due to an inhibition of voltage-dependent K^+ channels as well as an inhibition of GABA channels and a potentiation of AMPA receptors. In contrast to its excitatory effects, Zn^{2+} blocks NMDA receptors (Harrison & Gibbons, 1994; Smart *et al.* 1994; Henze *et al.* 2000). Zn^{2+} was also reported to play a role in neurodegeneration associated with pathologies such as ischaemia and epilepsia (Harrison & Gibbons, 1994; Smart *et al.* 1994; Choi & Koh, 1998; Weiss *et al.* 2000).

We show that hippocampal ASIC-like current activation and the potentiation by Zn^{2+} modulates neuronal excitability by increasing the membrane depolarization induced by small pH changes. This effect was observed at Zn^{2+} concentrations compatible with the physiological range of synaptically released Zn^{2+} (100–300 μM) (Assaf & Chung, 1984; Howell *et al.* 1984; Smart *et al.* 1994; Budde *et al.* 1997; Weiss *et al.* 2000). ASIC channels might thus be important physiological targets of Zn^{2+} in the hippocampus.

REFERENCES

Akopian, A. N., Chen, C. C., Ding, Y., Cesare, P. & Wood, J. N. (2000). A new member of the acid-sensing ion channel family. *NeuroReport* **11**, 2217–2222.

Assaf, S. Y. & Chung, S. H. (1984). Release of endogenous Zn^{2+} from brain tissue during activity. *Nature* **308**, 734–736.

Babinski, K., Catarsi, S., Biagini, G. & Seguela, P. (2000). Mammalian ASIC2a and ASIC3 subunits co-assemble into heteromeric proton-gated channels sensitive to Gd^{3+}. *Journal of Biological Chemistry* **275**, 28519–28525.

Babinski, K., Le, K. T. & Seguela, P. (1999). Molecular cloning and regional distribution of a human proton receptor subunit with biphasic functional properties. *Journal of Neurochemistry* **72**, 51–57.

Baron, A., Schaefer, L., Lingueglia, E., Champigny, G. & Lazdunski, M. (2001). Zn^{2+} and H^+ are coactivators of acid sensing ion channels. *Journal of Biological Chemistry* **276**, 35361–35367.

Bassilana, F., Champigny, G., Waldmann, R., de Weille, J. R., Heurteaux, C. & Lazdunski, M. (1997). The acid-sensitive ionic channel subunit ASIC and the mammalian degenerin MDEG form a heteromultimeric H^+-gated Na^+ channel with novel properties. *Journal of Biological Chemistry* **272**, 28819–28822.

Benson, C. J., Eckert, S. P. & McCleskey, E. W. (1999). Acid-evoked currents in cardiac sensory neurons: A possible mediator of myocardial ischemic sensation. *Circulation Research* **84**, 921–928.

Biagini, G., Babinski, K., Avoli, M., Marcinkiewicz, M. & Seguela, P. (2001). Regional and subunit-specific downregulation of acid-sensing ion channels in the pilocarpine model of epilepsy. *Neurobiology Disease* **8**, 45–58.

Budde, T., Minta, A., White, J. A. & Kay, A. R. (1997). Imaging free zinc in synaptic terminals in live hippocampal slices. *Neuroscience* **79**, 347–358.

Chen, C. C., England, S., Akopian, A. N. & Wood, J. N. (1998). A sensory neuron-specific, proton-gated ion channel. *Proceeding of the National Academy of Science of the USA* **95**, 10240–10245.

Chesler, M. & Kaila, K. (1992). Modulation of pH by neuronal activity. *Trends in Neurosciences* **15**, 396–402.

Choi, D. W. & Koh, J. Y. (1998). Zinc and brain injury. *Annual Review of Neuroscience* **21**, 347–375.

Coscoy, S., Lingueglia, E., Lazdunski, M. & Barbry, P. (1998). The Phe-Met-Arg-Phe-amide-activated sodium channel is a tetramer. *Journal of Biological Chemistry* **273**, 8317–8322.

de Weille, J. R., Bassilana, F., Lazdunski, M. & Waldmann, R. (1998). Identification, functional expression and chromosomal localisation of a sustained human proton-gated cation channel. *FEBS Letters* **433**, 257–260.

Escoubas, P., De Weille, J. R., Lecoq, A., Diochot, S., Waldmann, R., Champigny, G., Moinier, D., Menez, A. & Lazdunski, M. (2000). Isolation of a tarantula toxin specific for a class of proton-gated Na^+ channels. *Journal of Biological Chemistry* **275**, 25116–25121.

Frederickson, C. J. (1989). Neurobiology of zinc and zinc-containing neurons. *International Review of Neurobiology* **31**, 145–238.

Garcia-Anoveros, J., Derfler, B., Neville-Golden, J., Hyman, B. T. & Corey, D. P. (1997). BNaC1 and BNaC2 constitute a new family of human neuronal sodium channels related to degenerins and epithelial sodium channels. *Proceedings of the National Academy of Sciences of the USA* **94**, 1459–1464.

Garcia-Anoveros, J., Samad, T. A., Woolf, C. J. & Corey, D. P. (2001). Transport and localization of the DEG/ENaC ion channel BNaC1alpha to peripheral mechanosensory terminals of dorsal root ganglia neurons. *Journal of Neuroscience* **21**, 2678–2686.

Goslin, K. & Banker, G. (1991). Rat hippocampal neurons in low-density culture. In *Culturing Nerve Cells*, ed. Banker, G. & Goslin, K. pp. 251–283. Massachussets Institute of Technology, Cambridge, MA, USA.

GRANTYN, R. & LUX, H. D. (1988). Similarity and mutual exclusion of NMDA- and proton-activated transient Na^+-currents in rat tectal neurons. *Neuroscience Letters* **89**, 198–203.

GRUNDER, S., GEISSLER, H. S., BASSLER, E. L. & RUPPERSBERG, J. P. (2000). A new member of acid-sensing ion channels from pituitary gland. *Neuroreport* **11**, 1607–1611.

GRUOL, D. L., BARKER, J. L., HUANG, L. Y., MACDONALD, J. F. & SMITH, T. G. JR (1980). Hydrogen ions have multiple effects on the excitability of cultured mammalian neurons. *Brain Research* **183**, 247–252.

HAMILL, O. P., MARTY, A., NEHER, E., SAKMANN, B. & SIGWORTH, F. J. (1981). Improved patch-clamp techniques for high-resolution current recording from cells and cell-free membrane patches. *Pflügers Archiv* **391**, 85–100.

HARRISON, N. L. & GIBBONS, S. J. (1994). Zn^{2+}: an endogenous modulator of ligand- and voltage-gated ion channels. *Neuropharmacology* **33**, 935–952.

HENZE, D. A., URBAN, N. N. & BARRIONUEVO, G. (2000). The multifarious hippocampal mossy fiber pathway: a review. *Neuroscience* **98**, 407–427.

HOWELL, G. A., WELCH, M. G. & FREDERICKSON, C. J. (1984). Stimulation-induced uptake and release of zinc in hippocampal slices. *Nature* **308**, 736–738.

HSU, K. S., LIANG, Y. C. & HUANG, C. C. (2000). Influence of an extracellular acidosis on excitatory synaptic transmission and long-term potentiation in the CA1 region of rat hippocampal slices. *Journal of Neuroscience Research* **62**, 403–415.

JAROLIMEK, W., MISGELD, U. & LUX, H. D. (1989). Activity dependent alkaline and acid transients in guinea pig hippocampal slices. *Brain Research* **505**, 225–232.

JAROLIMEK, W., MISGELD, U. & LUX, H. D. (1990). Neurons sensitive to pH in slices of the rat ventral medulla oblongata. *Pflügers Archiv* **416**, 247–253.

JOHNSON, M. B., JIN, K., MINAMI, M., CHEN, D. & SIMON, R. P. (2001). Global ischemia induces expression of acid-sensing ion channel 2a in rat brain. *Journal of Cerebral Blood Flow and Metabolism* **21**, 734–740.

KRESS, M. & ZEILHOFER, H. U. (1999). Capsaicin, protons and heat: new excitement about nociceptors. *Trends in Pharmacological Sciences* **20**, 112–118.

KRISHTAL, O. A., OSIPCHUK, Y. V., SHELEST, T. N. & SMIRNOFF, S. V. (1987). Rapid extracellular pH transients related to synaptic transmission in rat hippocampal slices. *Brain Research* **436**, 352–356.

LAURITZEN, I., DE WEILLE, J. R. & LAZDUNSKI, M. (1997). The potassium channel opener (−)-cromakalim prevents glutamate-induced cell death in hippocampal neurons. *Journal of Neurochemistry* **69**, 1570–1579.

LINGUEGLIA, E., DE WEILLE, J. R., BASSILANA, F., HEURTEAUX, C., SAKAI, H., WALDMANN, R. & LAZDUNSKI, M. (1997). A modulatory subunit of acid sensing ion channels in brain and dorsal root ganglion cells. *Journal of Biological Chemistry* **272**, 29778–29783.

LINGUEGLIA, E., VOILLEY, N., WALDMANN, R., LAZDUNSKI, M. & BARBRY, P. (1993). Expression cloning of an epithelial amiloride-sensitive Na^+ channel. A new channel type with homologies to *Caenorhabditis elegans* degenerins. *FEBS Letters* **318**, 95–99.

MIESENBOCK, G., DE ANGELIS, D. A. & ROTHMAN, J. E. (1998). Visualizing secretion and synaptic transmission with pH-sensitive green fluorescent proteins. *Nature* **394**, 192–195.

NEDERGAARD, M., KRAIG, R. P., TANABE, J. & PULSINELLI, W. A. (1991). Dynamics of interstitial and intracellular pH in evolving brain infarct. *American Journal of Physiology* **260**, R581–588.

OHNO, M., OBRENOVITCH, T. P., HARTELL, N., BARRATT, S., BACHELARD, H. S. & SYMON, L. (1989). Simultaneous recording of tissue PCO2, interstitial pH and potassium activity in the rat cerebral cortex during anoxia and the subsequent recovery period. *Neurology Research* **11**, 153–159.

OLSON, T. H., RIEDL, M. S., VULCHANOVA, L., ORTIZ-GONZALEZ, X. R. & ELDE, R. (1998). An acid sensing ion channel (ASIC). localizes to small primary afferent neurons in rats. *NeuroReport* **9**, 1109–1113.

OZKAN, E. D. & UEDA, T. (1998). Glutamate transport and storage in synaptic vesicles. *Japanese Journal of Pharmacology* **77**, 1–10.

PRICE, M. P., LEWIN, G. R., MCILWRATH, S. L., CHENG, C., XIE, J., HEPPENSTALL, P. A., STUCKY, C. L., MANNSFELDT, A. G., BRENNAN, T. J., DRUMMOND, H. A., QIAO, J., BENSON, C. J., TARR, D. E., HRSTKA, R. F., YANG, B., WILLIAMSON, R. A. & WELSH, M. J. (2000). The mammalian sodium channel BNC1 is required for normal touch sensation. *Nature* **407**, 1007–1011.

PRICE, M. P., SNYDER, P. M. & WELSH, M. J. (1996). Cloning and expression of a novel human brain Na^+ channel. *Journal of Biological Chemistry* **271**, 7879–7882.

REECE, L. J., DHANJAL, S. S. & CHUNG, S. H. (1994). Zinc induces hyperexcitability in the hippocampus. *NeuroReport* **5**, 2669–2672.

SCHMIDT-KASTNER, R. & FREUND, T. F. (1991). Selective vulnerability of the hippocampus in brain ischemia. *Neuroscience* **40**, 599–636.

SMART, T. G., XIE, X. & KRISHEK, B. J. (1994). Modulation of inhibitory and excitatory amino acid receptor ion channels by zinc. *Progress in Neurobiology* **42**, 393–341.

SUTHERLAND, S. P., BENSON, C. J., ADELMAN, J. P. & MCCLESKEY, E. W. (2000*a*). Acid-sensing ion channel 3 matches the acid-gated current in cardiac ischemia-sensing neurons. *Proceedings of the National Academy of Sciences of the USA* **98**, 711–716.

SUTHERLAND, S. P., COOK, S. P. & MCCLESKEY, E. W. (2000*b*). Chemical mediators of pain due to tissue damage and ischemia. *Progress in Brain Research* **129**, 21–38.

SZALLASI, A. & DI MARZO, V. (2000). New perspectives on enigmatic vanilloid receptors. *Trends in Neurosciences* **23**, 491–497.

TOMINAGA, M., CATERINA, M. J., MALMBERG, A. B., ROSEN, T. A., GILBERT, H., SKINNER, K., RAUMANN, B. E., BASBAUM, A. I. & JULIUS, D. (1998). The cloned capsaicin receptor integrates multiple pain-producing stimuli. *Neuron* **21**, 531–543.

UENO, S., NAKAYE, T. & AKAIKE, N. (1992). Proton-induced sodium current in freshly dissociated hypothalamic neurones of the rat. *Journal of Physiology* **447**, 309–327.

VARMING, T. (1999). Proton-gated ion channels in cultured mouse cortical neurons. *Neuropharmacology* **38**, 1875–1881.

VOGT, K., MELLOR, J., TONG, G. & NICOLL, R. (2000). The actions of synaptically released zinc at hippocampal mossy fiber synapses. *Neuron* **26**, 187–196.

VOILLEY, N., DE WEILLE, J., MAMET, J. & LAZDUNSKI, M. (2001). Nonsteroid anti-inflammatory drugs inhibit both the activity and the inflammation-induced expression of acid-sensing ion channels in nociceptors. *Journal of Neuroscience* **21**, 8026–8033.

WALDMANN, R., BASSILANA, F., DE WEILLE, J., CHAMPIGNY, G., HEURTEAUX, C. & LAZDUNSKI, M. (1997*a*). Molecular cloning of a non-inactivating proton-gated Na^+ channel specific for sensory neurons. *Journal of Biological Chemistry* **272**, 20975–20978.

Waldmann, R., Champigny, G., Bassilana, F., Heurteaux, C. & Lazdunski, M. (1997*b*). A proton-gated cation channel involved in acid-sensing. *Nature* **386**, 173–177.

Waldmann, R., Champigny, G., Lingueglia, E., De Weille, J. R., Heurteaux, C. & Lazdunski, M. (1999). H^+-gated cation channels. *Annals of the New York Academy of Sciences* **868**, 67–76.

Waldmann, R., Champigny, G., Voilley, N., Lauritzen, I. & Lazdunski, M. (1996). The mammalian degenerin MDEG, an amiloride-sensitive cation channel activated by mutations causing neurodegeneration in *Caenorhabditis elegans*. *Journal of Biological Chemistry* **271**, 10433–10436.

Waldmann, R. & Lazdunski, M. (1998). H^+-gated cation channels: neuronal acid sensors in the NaC/DEG family of ion channels. *Current Opinion in Neurobiology* **8**, 418–424.

Walz, W. (1989). pH shifts evoked by neuronal stimulation in slices of rat hippocampus. *Canadian Journal of Physiology and Pharmacology* **67**, 577–581.

Weiss, J. H., Sensi, S. L. & Koh, J. Y. (2000). Zn^{2+}: a novel ionic mediator of neural injury in brain disease. *Trends in Pharmacological Sciences* **21**, 395–401.

Acknowledgements

We thank V. Lopez for excellent technical assistance, M. Jodar for performing primary cultures, I. Lauritzen for helpful advice about hippocampal neurons, and N. Voilley and J. Mamet for helpful comments. This work was supported by the Centre National de la Recherche Scientifique (CNRS), the Institut National de la Santé et de la Recherche Médicale (INSERM), the Association Française contre les Myopathies (AFM), the Conseil Regional (PACA), The Ministère de la Recherche (ACI: Molécules et Cibles Thérapeutiques) and the Association pour la Recherche sur le Cancer (ARC).

Cellular/Molecular

Acid-Sensing Ion Channel 1 Is Localized in Brain Regions with High Synaptic Density and Contributes to Fear Conditioning

John A. Wemmie,[1,6,7,8] Candice C. Askwith,[3,7] Ejvis Lamani,[1] Martin D. Cassell,[4,6] John H. Freeman Jr,[5,6] and Michael J. Welsh[2,3,6,7]

Departments of [1]Psychiatry, [2]Physiology and Biophysics, [3]Internal Medicine, [4]Anatomy and Cell Biology, and [5]Psychology, and [6]Neuroscience Graduate Program and [7]Howard Hughes Medical Institute, University of Iowa, Iowa City, Iowa 52242 and [8]Department of Veterans Affairs Medical Center, Iowa City, Iowa 52242

The acid-sensing ion channel, ASIC1, contributes to synaptic plasticity in the hippocampus and to hippocampus-dependent spatial memory. To explore the role of ASIC1 in brain, we examined the distribution of ASIC1 protein. Surprisingly, although ASIC1 was present in the hippocampal circuit, it was much more abundant in several areas outside the hippocampus. ASIC1 was enriched in areas with strong excitatory synaptic input such as the glomerulus of the olfactory bulb, whisker barrel cortex, cingulate cortex, striatum, nucleus accumbens, amygdala, and cerebellar cortex. Because ASIC1 levels were particularly high in the amygdala, we focused further on this area. We found that extracellular acidosis elicited a greater current density in amygdala neurons than hippocampal neurons and that disrupting the ASIC1 gene eliminated H^+-evoked currents in the amygdala. We also tested the effect of ASIC1 on amygdala-dependent behavior; ASIC1-null mice displayed deficits in cue and context fear conditioning, yet baseline fear on the elevated plus maze was intact. These studies suggest that ASIC1 is distributed to regions supporting high levels of synaptic plasticity and contributes to the neural mechanisms of fear conditioning.

Key words: ASIC1; localization; CNS; fear conditioning; emotion; learning, memory

Introduction

Many years ago, it was recognized that rapid acidification of extracellular pH evokes a transient cation current in central neurons (Gruol et al., 1980; Krishtal and Pidoplichko, 1981). Because brain pH is tightly regulated *in vivo*, the physiological significance of this observation has been unclear. However, it was hypothesized that H^+-gated currents might be activated during synaptic transmission, because EPSPs acidified the extracellular fluid in hippocampal slices (Krishtal et al., 1987). The discovery of acid-sensing ion channels (ASICs), acid-sensing members of the DEG/ENaC family (Waldmann et al., 1997), suggested several candidate genes and offered an opportunity to explore the physiological role of neuronal H^+-evoked currents (Price et al., 2000, 2001; Immke and McCleskey, 2001; Wemmie et al., 2002).

Five ASICs (ASIC1a, 1b, 2a, 2b, and 3; a and b refer to splice variants) either are activated by acid or modulate acid-gated subunits in heterologous cells (for review, see Welsh et al., 2002; Bianchi and Driscoll, 2002). ASIC subunits assemble into homomultimeric and heteromultimeric channel complexes, and different subunit combinations generate currents with distinct kinetics and pH sensitivity (Lingueglia et al., 1997; Benson et al., 2002). The properties of H^+-gated currents in central neurons generally do not match those of the homomultimeric ASICs, suggesting that heteromultimeric subunit complexes generate the currents (Bolshakov et al., 2002). Because ASIC1a, 2a, and 2b are expressed in brain, combinations of these proteins could be responsible.

Disrupting ASIC1a in mice eliminated pH 5-evoked current in hippocampal neurons, identifying it as a key component of H^+-gated currents (Wemmie et al., 2002). Although ASIC1-null mice were viable, with no obvious anatomic or physiological abnormalities, they exhibited deficits in hippocampus-dependent spatial learning and cerebellum-dependent eyeblink conditioning. Moreover, ASIC1-null mice had impaired long-term potentiation (LTP) at Schaffer collateral–CA1 synapses. They also exhibited reduced excitatory postsynaptic potentials and NMDA receptor activation during high-frequency stimulation. These studies suggested a role for ASIC1 in processes that underlie learning and memory. Consistent with this possibility, in cultured neurons, ASIC1 protein distributed preferentially to dendrites and colocalized with the synaptic marker PSD-95, suggesting that ASIC1 is probably present in the postsynaptic membrane.

Received Feb. 11, 2003; revised April 23, 2003; accepted April 23, 2003.

This work was supported by the Howard Hughes Medical Institute (HHMI) (M.J.W., J.A.W.), a Veteran's Administration Research Career Development Award (J.A.W.), and National Institute of Neurological Disorders and Stroke Grant NS-38890 (J.H.F.). C.C.A. is an Associate and M.J.W. is an Investigator of the HHMI. We thank the University of Iowa DNA Core Facility (National Institutes of Health Grant DK-25295) for assistance. We thank Melissa Redeker for excellent assistance, Nicholas Pantazis for helpful discussion, Tom Moninger and the Central Microscopy Research Facility for assistance with microscopy and image analysis, and Christine Bromley and the University of Iowa Pathology Research Laboratory for assistance with tissue processing.

Correspondence should be addressed to Dr. John A. Wemmie, Department of Psychiatry, University of Iowa, Roy J. and Lucille A. Carver College of Medicine, 500 Eckstein Medical Research Building, Iowa City, IA 52242. E-mail: john-wemmie@uiowa.edu.

 0270-6474/03/235496-07$15.00/0

Understanding the physiologic contribution of ASIC1 to brain function requires knowledge of the protein localization. *In situ* hybridization suggested that ASIC1 mRNA was expressed throughout the CNS, with a greater abundance in hippocampus, cerebral cortex, olfactory bulb, and cerebellum (García-Añoveros et al., 1997; Waldmann et al., 1997). However, mRNA data and subsequent protein localization data (Olson et al., 1998; Alvarez de la Rosa et al., 2003) were limited. Therefore, we used immunohistochemistry to examine ASIC1 protein distribution further. ASIC1 levels differed between brain regions and were high in areas supporting rich synaptic connectivity. One location in which ASIC1 was particularly abundant was the amygdala. Because amygdala-dependent learning has been closely linked to LTP, the amygdala may serve as an especially useful model system for memory (McKernan and Shinnick-Gallagher, 1997) (Rogan et al., 1997). Therefore, we also explored the effect of ASIC1 disruption on H^+-evoked currents in amygdala neurons and amygdala-dependent behavior.

Materials and Methods

Antibody. Polyclonal antiserum (MTY19) was raised in rabbits against the 22 amino acid peptide from the C terminus of ASIC1, MTYAANILPHHPARGTFEDFTC, coupled to keyhole limpet hemocyanin (Poccono, Canadensis, PA). The IgG fraction was purified using the Econo-Pac serum IgG purification kit (Bio-Rad, Richmond, CA). Next, an Affi-gel 15 Gel (Bio-Rad) coupled to the nonspecific peptide GTCNAVTMDSDF was used to adsorb additional nonspecificity for 1 hr at 4°C (Labquake shaker; Labindustries, Berkeley, CA). To adsorb additional nonspecific components of the sera, we used protein extract obtained from ASIC1 knock-out brains coupled to Affi-gel 15 (Bio-Rad), although this step later proved unnecessary. The eluate from these columns was then bound for 4 hr at 4°C to the immunogenic peptide crosslinked to Affi-gel 15. The specific antibody was eluted with 50 mM glycine/HCl at a pH of 2.5, 150 mM NaCl, neutralized with 1 M Tris at a pH of 10.4, and adjusted to 1% BSA, 0.2% NaN_3 for storage at 4°C.

Immunohistochemistry. Coronal brain slices (7.5 μm) were cut on a cryostat (CM 1900; Leica Bannockburn, IL) from tissue that was fresh-frozen on dry ice and embedded in Tissue Freezing Medium (Electron Microscopy Sciences, Fort Washington, PA). The slices were dried overnight and hydrated with PBS. They were then fixed in PBS with 4% formaldehyde, 4% sucrose for 15 min, followed by 0.25% Triton X-100 in PBS for 5 min at room temperature. After two rinses with PBS, endogenous peroxidase activity was quenched with 3% H_2O_2 for 30 min. This was followed with three 5 min washes with PBS and blocking with Tris/NaCl/blocking reagent buffer (TNB) (TSA Fluorescence Systems, PerkinElmer Life Sciences, Boston, MA) for 30 min. Purified MTY19 (1:50 in TNB) or anti-calbindin D-28K (Chemicon International, Temecula, CA) was added and allowed to incubate for 2 hr. After three 5 min washes with PBS, α-rabbit IgG-horse radish peroxidase (HRP) (Amersham Biosciences, Piscataway, NJ) was used as a secondary antibody at 1:200 for 1 hr at 37°C. After another three 5 min washes with PBS, the signal was amplified by incubating in tyramide solution (TSA Fluorescence Systems, Perkin-Elmer Life Sciences, Boston, MA) for 10 min at room temperature. Finally, the slices were washed three more times for 5 min with PBS, mounted with Vectashield (Vector Laboratories, Burlingame, CA), and visualized by Bio-Rad MRC 1024 confocal microscope, or Olympus BX-51 epifluorescence microscope (Melville, NY) equipped with Spot RT Slater (Diagnostic Instruments, Sterling Heights, MI). The specific ASIC1 immunostaining was lost in paraffin-embedded tissue and when sections were prepared from brain perfused with formalin *in vivo* before sectioning.

Immunoblotting. From 500 μm Vibratome cut slices (Pelco, Redding, CA), the amygdala, CA1, CA3, posterior cingulate, posterior association cortex, habenula, and thalamus were dissected according to regions surrounded by a dashed line in Figure 1. Tissue homogenate was also obtained from the whole brain and cerebellum. The tissue was homogenized in PBS with protease inhibitors (aprotinin 40 μg/ml, leupeptin 40 μg/ml, pepstatin A 20 μg/ml, PMSF 40 μg/ml, and EDTA 2 mM) using a 1 ml Dounce homogenizer (Wheaton, Millville, NJ). The homogenate was cleared of large unground particles with a 10 min centrifugation at 3500 rpm (5415C; Eppendorf Hamburg, Germany). Membrane proteins were precipitated at 70,000 rpm for 30 min (TL-100; Beckman, Fullerton, CA). The pellet was resuspended in PBS with protease inhibitors. All steps in sample preparation were performed on ice or at 4°C. Protein concentration was determined (Lowry and Passanneau, 1972), and 100 μg was run on 8% acrylamide gel and Western blotted. The blot was first probed with MTY19 serum at 1:15,000, followed by α-rabbit IgG-HRP (Amersham Biosciences) at 1:10,000. The signal was detected by enhanced chemiluminescence (Pierce, Rockford, IL).

Whole-cell voltage-clamp experiments. Mouse hippocampal cultures were generated from postnatal day 1–2 pups as described previously (Wemmie et al., 2002). Amygdala cultures were generated by the same method except that the amygdala was dissected from 1 mm coronal sections using the external capsule as a landmark to define the borders of the lateral and basolateral amygdala. Culture medium contained insulin, transferrin, and sodium selenite (I-1884, Sigma, St. Louis, MO), resuspended in 50 ml H_2O, 2.5 μl/ml of medium. Whole-cell patch-clamp recordings were performed on neurons from at least two different preparations that were cultured for 1–2 weeks. Electrodes (3–5 MΩ) were filled with intracellular solutions containing (in mM): 120 KCl, 10 NaCl, 2 $MgCl_2$, 5 EGTA, 10 HEPES, and 2 ATP. The pH was adjusted to 7.2 with KOH. Extracellular solutions contained (in mM): 128 NaCl, 2 $CaCl_2$, 1 $MgCl_2$, 5.4 KCl, 5.55 glucose, 10 HEPES, and 10 MES. To inhibit spontaneous activity, 0.5 μM tetrodotoxin, 5 μM CNQX, 15 μM bicuculline methiodide, and 25 μM DL-2-amino-5-phosphonovaleric acid were added to the extracellular solutions. The pH was adjusted with tetramethylammonium hydroxide (TMA-OH) and the osmolarity adjusted with TMA-Cl. Neurons were held at −80 mV for recording, and extracellular pH was 7.4 unless otherwise indicated. All chemicals were obtained from Sigma.

Elevated-plus maze. A maze was constructed from stainless steel with a Plexiglas base (36 inches tall) and two pair of arms (2 × 11⅝ inches) intersecting at right angles. One pair of arms was closed and had six inch walls on three sides. The two open arms lacked walls. A 2 × 2 inch intersection connected the four arms. Naive mice (+/+, $n = 11$; −/−, $n = 11$) were placed onto the center of the maze and allowed 5 min to roam freely. Activity was recorded by a video camera suspended above the maze. A trained technician blinded to genotype recorded the time each animal spent in the closed arms, open arms, and stationary in the corner of the closed arms. The number of entries into the open central intersection was also determined. Statistical significance was tested with a two-sample *t* test.

Auditory fear conditioning. On day 1, naive mice (+/+, $n = 7$; −/−, $n = 9$) were placed in a conditioning chamber (Lafayette Instrument, Lafayette, IN). After 3 min, they were presented with a tone (80 dB, 20 sec) that coterminated with an electric foot-shock (1 mA, 1 sec). A total of seven pairings of the tone and shock were delivered, separated by 1 min intervals. Mice were then returned to their home cage. On day 2, to minimize freezing to context, the lights were dimmed, burgundy poster board was used to change the color of the back wall and ceiling, a wire mesh floor grate was inserted, white bench paper was placed under the floor grid, and the paper was dabbed with 1 drop of peppermint extract. The animals were placed in the conditioning chamber, observed for 3 min, and then presented with the same tone continuously for 6 min, minus the foot-shock. Freezing (defined as a crouched posture and an absence of movement) during 1 min intervals was quantified from videotapes by a trained observer blinded to genotype. Three −/− mice and one +/+ mouse were excluded from the training data because they climbed onto the wall of the chamber during at least one interval. Although this did not interfere with the conditioning protocol, it did interfere with scoring and disqualified them from the ANOVA with repeated measures. One +/+ mouse was excluded from the study because its tail was inadvertently pinched as it was being placed into the chamber. Another +/+ mouse was excluded because its freezing response was >3 SD from the mean. The context fear conditioning protocol was similar, except on day 1, the mice received three shocks and no tone was presented

(+/+, $n = 8$; −/−, $n = 7$). On day 2, the same chamber was used without changing the context.

Results and Discussion

ASIC1 immunolocalization in the brain

Previous *in situ* hybridization studies suggested that ASIC1 transcripts were abundant in layers CA1 through CA4 of the hippocampus (García-Añoveros et al., 1997; Waldmann et al., 1997). In addition, we have shown previously that disrupting ASIC1 impairs Schaffer collateral-CA1 LTP and adversely affects spatial learning (Wemmie et al., 2002). Therefore, we asked where in the hippocampal circuit ASIC1 protein was located. An affinity-purified rabbit polyclonal antibody against the C-terminal 22 amino acids of mouse ASIC1 was used to immunolabel coronal sections of mouse brain (Fig. 1*A*). As a control, we used ASIC1 −/− brains. In the hippocampus, the hilus (polymorphic layer) of the dentate gyrus showed the most prominent ASIC1 staining. This region is occupied by inhibitory and excitatory interneurons as well as mossy fibers and CA3 dendrites (Fig. 1*B*).

In contrast, ASIC1 immunostaining in CA1 and CA2 was relatively weak (Fig. 1*A*,*C*). Others have suggested that epitope masking may obscure ASIC1 detection in the brain (Olson et al., 1998). To address this possibility, we also immunoblotted protein obtained from the dentate gyrus and CA1. Although ASIC1 was detected, it was dramatically reduced in CA1 compared with the dentate gyrus (Fig. 1*D*). Thus, although ASIC1 may have important effects on CA1 function (Wemmie et al., 2002), the amount of protein in this region may be sparse relative to other areas.

Because ASIC1 distribution in the hippocampus was different than anticipated, we asked about its distribution elsewhere in the brain. Previous studies reported that ASIC1 mRNA was elevated in the cerebral cortex (García-Añoveros et al., 1997; Waldmann et al., 1997). Consistent with those reports, we found abundant ASIC1 protein in a number of specific cortical regions (Figs. 1*A*, 2, 3). ASIC1 staining was evident in the anterior and posterior cingulate cortex (Figs. 1*A*, 2*A*,*B*). The sensory and motor cortices were also immunopositive (Figs. 1*A*, 3). A subdomain of the sensory cortex in which ASIC1 staining was prominent was the whisker barrel field (Figs. 1*A*, 2*C*), an area that has served as a valuable model system for analyzing cortical plasticity (for review, see Fox, 2002). In contrast, ASIC1 immunostaining was low in the ectorhinal, perirhinal, and piriform cortex (Figs. 1*A*, 3).

ASIC1 immunostaining in sensorimotor and cingulate cortex tended to be elevated in layer III. For example, in the posterior cingulate, immunolabeling could be seen on pyramidal cell bodies in layer III (Fig. 2*A*,*B*, arrows) and also in layer I near the brain surface (Fig. 2*A*, asterisk). We also consistently observed stripes of staining perpendicular to the cortical layers and extending between layers I and III, possibly caused by apical dendrites extending from pyramidal neurons in the deeper layers (Fig. 2*A*,

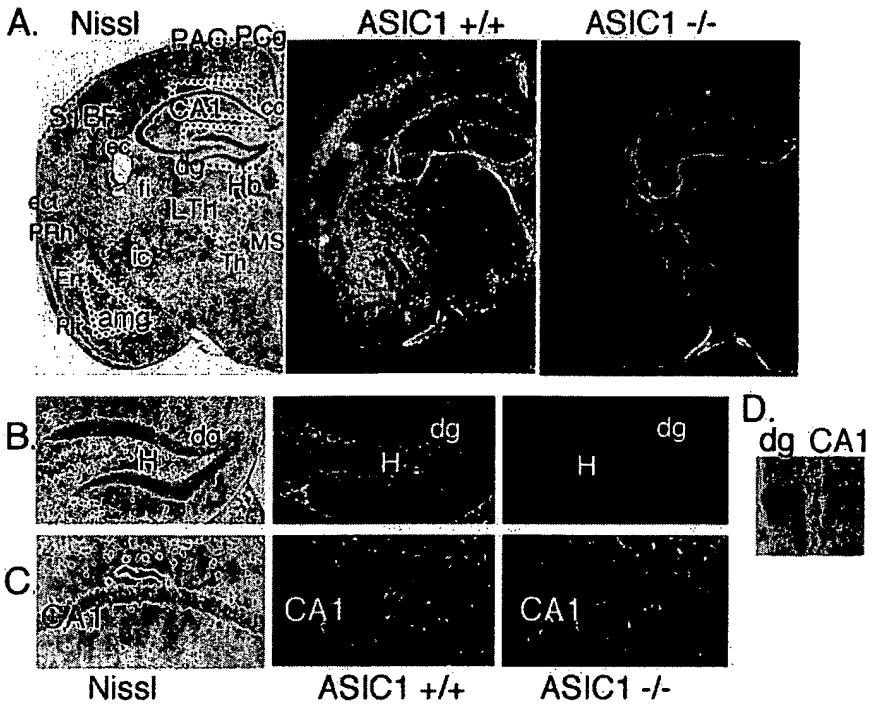

Figure 1. ASIC1 immunolocalization in forebrain. *A*, Coronal sections were stained for Nissl substance or immunolabeled for ASIC1 protein in +/+ and −/− mice. Areas marked by dashed lines in the Nissl-stained section are the areas dissected to prepare protein extracts for Western blotting in *D* and Figure 6*B*. Asterisks in ASIC1 +/+ hemisphere denote areas of nonspecific staining that did not occur bilaterally or in multiple sections. *B*, *C*, Enlarged images of dentate gyrus and CA1 respectively. *D*, Western blot of ASIC1 protein in 100 μg protein extract from dentate gyrus and CA1. amg, amygdala; cc, corpus callosum; dg, dentate gyrus; ec, external capsule; ect, ectorhinal cortex; En, endopiriform nuclei; fi, fimbria; Hb, habenula; H, hilus (polymorphic layer); ic, internal capsule; LTh, lateral thalamus; MS, medial septal nuclei; PAC, parietal association cortex; Pir, piriform cortex; PCg, posterior cingulate cortex; PRh, perirhinal cortex; S1BF, somatosensory barrel field; Th, thalamus.

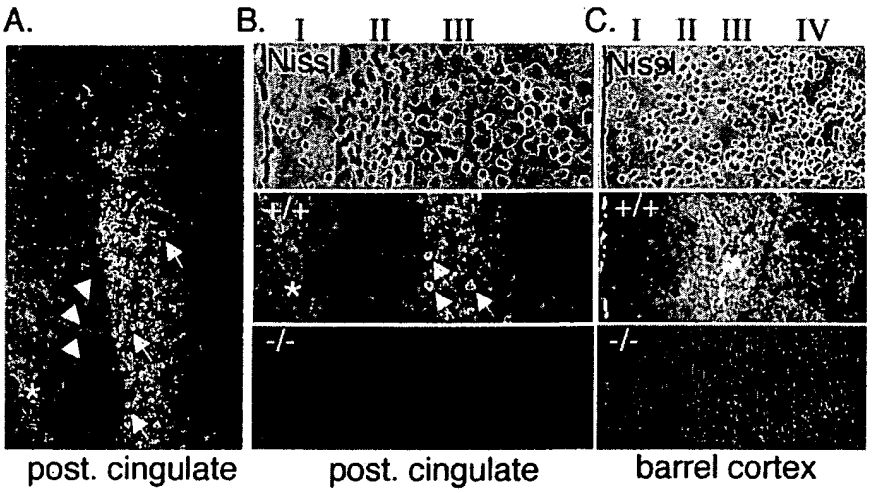

Figure 2. ASIC1 immunolocalization in cortex. *A*, *B*, Immunolabeling in the posterior (post.) cingulate cortex. Stripes extending through layer II are labeled with an arrowhead. Positive-staining pyramidal cells in layer III are labeled with arrows. *ASIC1-specific staining in layer I. *C*, ASIC1 immunostaining is also elevated in layer III of barrel cortex.

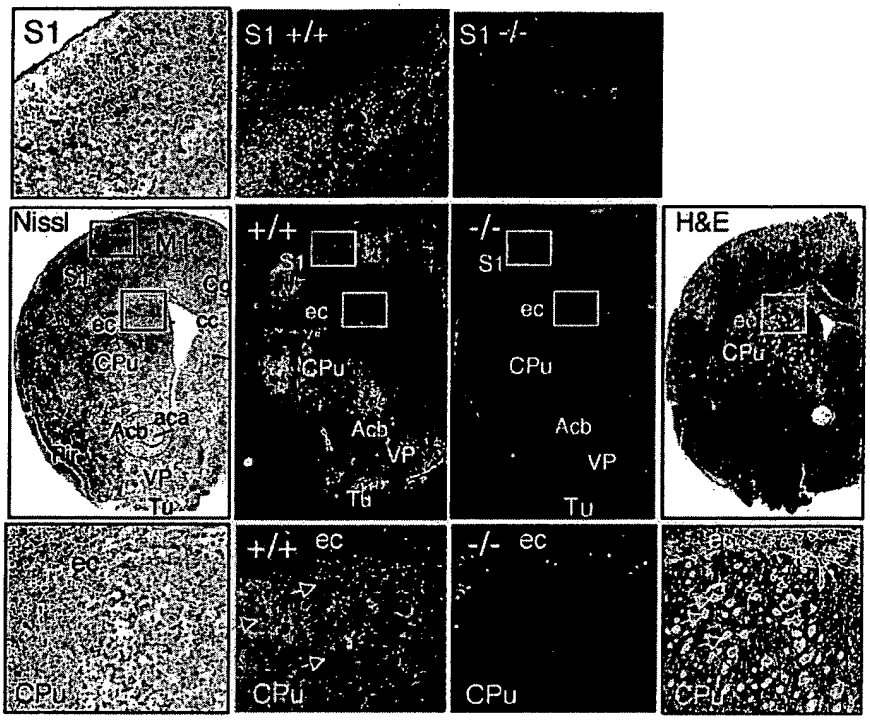

Figure 3. Immunolocalization of ASIC1 in the sensorimotor cortex and striatum. Coronal sections through the forebrain were stained for Nissl substance, hematoxylin and eosin (H&E), or ASIC1 protein in ASIC1 +/+ or −/− mice. Center row, staining of representative coronal slices. Top row, insets of somatosensory cortex at higher magnification. Bottom row, insets of external capsule/corpus callosum and striatum at higher magnification. White matter tracts are labeled with arrows. ASIC1 immunolabeling was noticeably reduced in the white matter tracts. Areas of staining that were not present bilaterally and not present in multiple slices, suggesting nonspecific staining, are marked with an asterisk. aca, anterior commissure; Acb, accumbens nucleus; cc, corpus callosum; Cg, cingulate cortex; CPu, caudate/putamen (striatum); ec, external capsule; M1, primary motor cortex; Pir, piriform cortex; S1, somatosensory cortex; VP, ventral pallidum; Tu, olfactory tubercle.

arrowhead). ASIC1 staining in barrel and motor cortex was also preferentially distributed to layer III (Figs. 1*A*, 2*C*). The significance of layer III specificity is not clear, although it is interesting to note that an NMDA receptor-dependent form of LTP in this layer has been implicated in barrel cortex function (Fox, 2002).

In addition to the cortex, we observed strong ASIC1 staining in certain subcortical structures, including the basal ganglia (Fig. 3). ASIC1 labeling was readily apparent in the striatum, in which it was distributed in gray matter, and was slightly more abundant dorsally and laterally (Fig. 3), regions that preferentially receive sensorimotor cortical input. The strong signal in gray matter of the striatum contrasted sharply with weak white matter staining, giving the ASIC1 distribution a dappled appearance (Fig. 3). We also observed strong ASIC1 in the ventral pallidum, olfactory tubercle, and nucleus accumbens (Fig. 3). The basal ganglia serve an important role in voluntary movement. The striatum and nucleus accumbens may also contribute to motivation and appetitive behavior and have been linked to addiction in humans (for review, see Cardinal et al., 2002; Hyman and Malenka, 2001). Yet, ASIC1 knock-out mice performed normally on the accelerating Rotarod (Wemmie et al., 2002) and displayed normal activity on the elevated plus maze (see below). Nevertheless, the high level of ASIC1 in the striatum suggests that given the appropriate challenge, ASIC1-null mice might exhibit abnormal striatum-dependent behavior.

In contrast to the basal ganglia, ASIC1 immunostaining in the thalamus was rather weak, with the exception of the habenula and the medial septal nuclei (Fig. 1*A*). The significance of the selective distribution between subcortical structures is not yet clear.

We also tested for ASIC1 protein in the olfactory bulb, because ASIC1 mRNA was reported to be elevated there (Waldmann et al., 1997). We found ASIC1 protein localized preferentially to the glomerular layer and most evident within glomeruli (Fig. 4, arrows). Immunolabeling of periglomerular cells was less intense, causing the striking glomerular pattern to stand out (Fig. 4). Glomeruli provide a site for synaptic contact between olfactory sensory neurons and intrinsic olfactory bulb neurons, including periglomerular cells, mitral cells, and tufted cells. Because olfactory sensory neurons are continuously replaced throughout life, synapses in the glomerulus undergo constant remodeling (for review, see Shepherd and Greer, 1998). This high degree of plasticity is unique in the mammalian brain. The strong ASIC1 signal in the glomeruli is consistent with the ability of ASIC1 to affect synaptic function (Wemmie et al., 2002).

The cerebellum contains abundant ASIC1 mRNA (García-Añoveros et al., 1997; Waldmann et al., 1997), and our eyeblink conditioning studies suggested that ASIC1 may have important effects on cerebellum-dependent learning (Wemmie et al., 2002). In the cerebellum, ASIC1 staining was particularly strong in the molecular layer, and in both the molecular and granule cell layers, it was distributed diffusely, suggesting that its source is rather widespread (Fig. 5). In these layers, the most prevalent cell types are granule and Purkinje cells. Because both produce H^+-evoked currents (Allen and Attwell, 2002; Escoubas et al., 2000; C. Askwith, unpublished observations), both probably contribute to the strong ASIC1 labeling.

The ASIC1 staining in the granule layer suggested that it may be distributed to granule cell dendrites, which are located there and receive afferent mossy fiber input. ASIC1 may also be present in granule cell axons, which project into the molecular layer where ASIC1 staining was strong (Fig. 5). However, because Purkinje cells are known to express large H^+-gated currents, Purkinje cell dendrites may account for much of the ASIC1 protein in the molecular layer. A Purkinje cell-specific antibody (anti-calbindin D-28K) produced a similar diffuse pattern in the molecular layer (Fig. 5*C*). Purkinje cell axons traverse the white matter to form presynaptic terminals in the deep nuclei; however, ASIC1 staining in these areas was not greater than that in the −/− controls. The absence of detectable ASIC1 protein in Purkinje cell axons suggests that in these cells, it may be preferentially localized to dendrites.

A general pattern that emerged in the study of ASIC1 localization in brain was a tendency for it to be enriched in areas receiving strong excitatory corticofugal input (cortical projections); examples include the cortex, striatum, nucleus accumbens, and dentate gyrus of the hippocampus. These structures are interconnected in a circuit referred to as the limbic corticostriatal loop (for review, see Cardinal et al., 2002). Components of this circuit are thought to contribute to the emotional importance of exter-

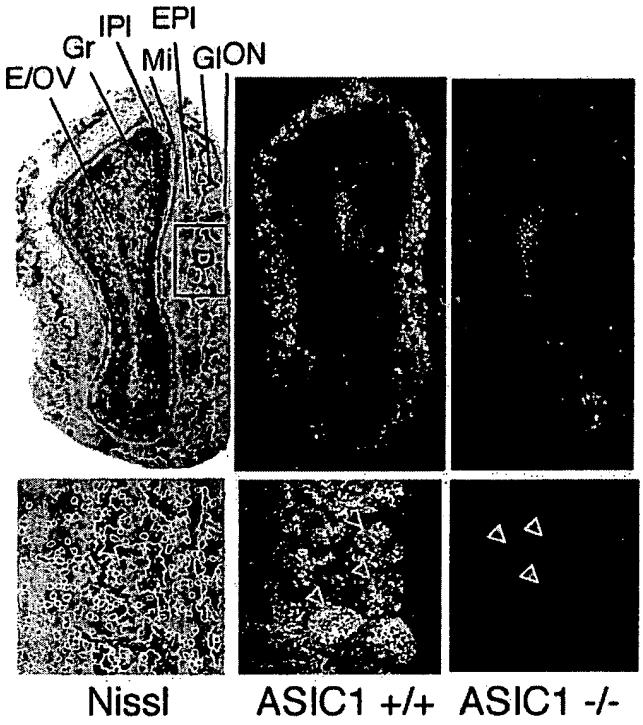

Figure 4. Immunolocalization of ASIC1 in the olfactory bulb. Coronal sections through the olfactory bulb were stained for Nissl substance or immunolabeled for ASIC1 protein in ASIC1 +/+ and −/− mice. Higher magnifications at bottom demonstrate ASIC1 immunostaining in glomeruli (arrowheads). E/OV, ependymal and subendymal layer/olfactory ventricle; EPl, external plexiform layer; Gl, glomerular layer; Gr, granule cell layer; IPl, internal plexiform layer; Mi, mitral cell layer; ON, olfactory nerve layer.

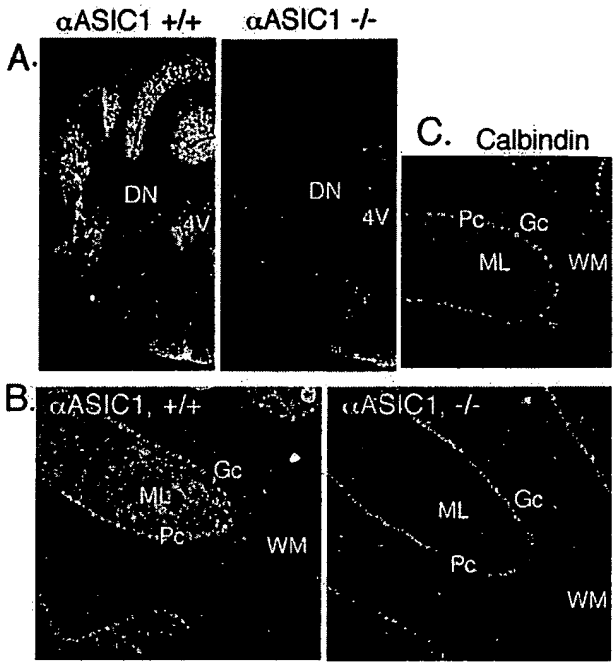

Figure 5. Immunolocalization of ASIC1 in the cerebellum. ASIC1 immunohistochemistry in coronal (*A*) and parasagittal (*B*) sections of the cerebellum. *C*, Immunostaining with anti-calbindin D-28K antibody in fresh-frozen tissue. 4V, fourth ventricle; DN, deep cerebellar nuclei; Gc, granule cell layer; ML, molecular layer; Pc, pyramidal cell layer; WM, white matter.

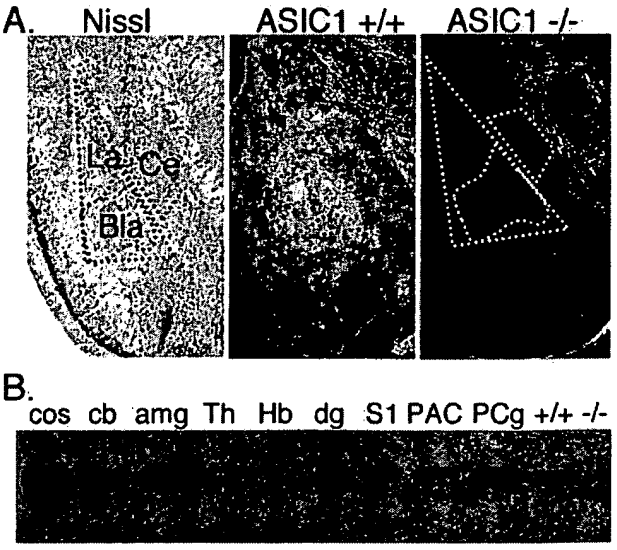

Figure 6. *A*, ASIC1 immunolocalization in the amygdala complex. Bla, basolateral nucleus; Ce, central nucleus; La, lateral nucleus. *B*, Western blotting of ASIC1 protein in 100 μg of protein extract per lane isolated from indicated brain region. Cos-7 cells transfected with mASIC1, cos. Because the entire cerebellum was used to generate the cb extract, the subcortical structures with little ASIC1 may have diluted out the high expression level seen by immunohistological staining in the cerebellar cortex (Fig. 5). +/+ and −/−, whole-brain extract from ASIC1 +/+ or −/− mouse; amg, amygdala; cb, cerebellum; dg, dentate gyrus; Hb, habenula; S1, somatosensory barrel field; Th, thalamus; PAC, parietal association cortex; PCg, posterior cingulate cortex.

nal stimuli and/or their expression. Another important component of this circuit is the amygdala complex, in which ASIC1 immunolabeling was intense, particularly in the lateral and basolateral nuclei (Figs. 1*A*, 6*A*). We obtained a similar result using Western blot to compare ASIC1 protein levels. ASIC1 was especially abundant in the amygdala and was present at higher levels than in the hippocampus or thalamus, for example (Fig. 6*B*).

These data are in contrast to those described recently by Alvarez de la Rosa et al. (2003), which suggested that ASIC1 protein was broadly distributed in neurons throughout the brain without a trend toward a particular brain region or cellular domain. One advantage of our experiments is that we used ASIC1 knock-out mice as a control for specificity. Moreover, multiple approaches, including immunohistochemistry, Western blotting, and measurement of H^+-gated current density (see below), all suggested that ASIC1 protein is preferentially distributed to specific domains. These studies are also consistent with our earlier experiments in cultured neurons transfected with ASIC1, which showed a dendritic and synaptic pattern of ASIC1 localization (Wemmie et al., 2002).

ASIC1 is a required component of H^+-activated channels in the amygdala

To explore the electrophysiological impact of ASIC1 expression in the amygdala, we measured H^+-gated currents in cultured amygdala neurons. Reducing extracellular pH to 5.0 evoked large transient currents in the majority of ASIC1 +/+ neurons (93%; $n = 27$) (Fig. 7). In contrast, none of the amygdala neurons from ASIC1 −/− mice generated transient currents in response to pH 5 ($n = 29$). These data indicate that ASIC1 makes a critical contribution to H^+-gated current in these cells. We also found that the mean current density of H^+-gated currents was more than threefold greater in amygdala than in hippocampal neurons (Fig. 7). Thus, compared with hippocampus, the amount of ASIC1

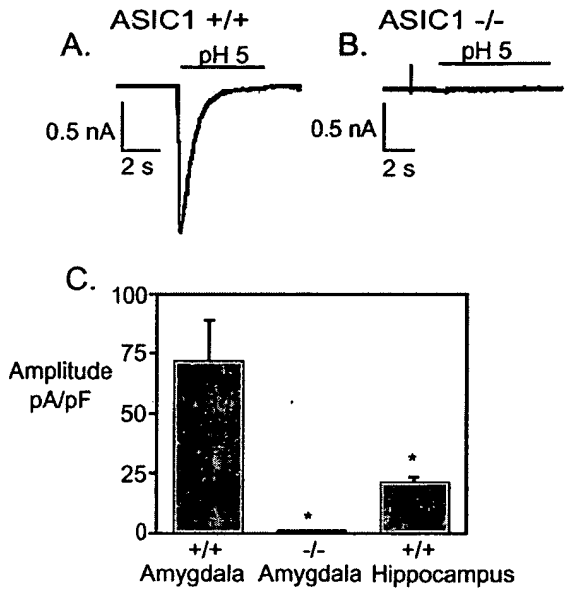

Figure 7. Proton-gated currents in amygdala neurons. *A*, *B*, Representative recordings of pH 5 evoked response in amygdala neurons from ASIC1 +/+ and −/− mice. *C*, Average current density of peak pH 5-evoked response in amygdala neurons from ASIC1 +/+ ($n = 14$) and −/− ($n = 18$) mice and hippocampal neurons from ASIC1 +/+ mice ($n = 67$; $^*p < 0.01$).

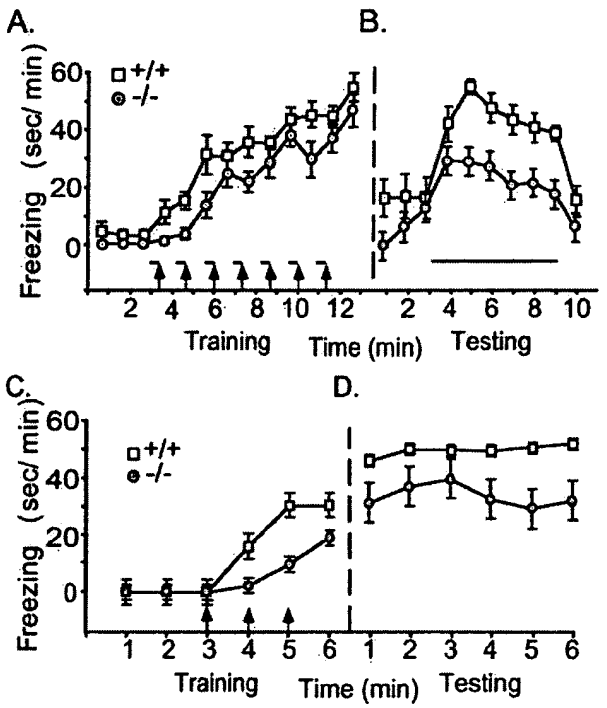

Figure 8. Behavioral analysis of learned fear. *A*, *B*, Cued fear conditioning. The amount of freezing in 1 min intervals was determined during training (*A*) and testing (*B*). During testing, the ASIC1 −/− mice froze significantly less than +/+ controls with the presentation of the conditioned stimulus (intervals 4–9) ($p = 0.02$) (+/+, $n = 5$; −/−, $n = 9$). *C*, *D*, Context fear conditioning. The difference in freezing between +/+ and −/− mice was significant during training (intervals 4–6; $p = 0.002$) and during testing ($p = 0.03$) (+/+, $n = 7$; −/−, $n = 8$). Foot shock, arrows; tone, bars. Statistical significance was tested by ANOVA with repeated measures.

protein and the average number of functional ASIC channels are much greater in the amygdala.

ASIC1 and amygdala-dependent behavior

Finding that ASIC1 protein was present in a number of structures in the limbic corticostriatal loop and that ASIC1 protein and H^+-gated currents were abundant in the amygdala suggested that ASIC1 might play an important role in behaviors controlled by these structures (Cardinal et al., 2002). To test this hypothesis, we examined the effect of ASIC1 disruption on performance in the elevated plus maze, a test of baseline fear. Both ASIC1 +/+ and −/− mice spent the majority of time in the closed arms (+/+ = 198 ± 4 sec; −/− = 217 ± 3 sec; mean ± SEM; $p = 0.21$), suggesting that the two groups found the open arms similarly aversive. In addition, the number of open arm entries (+/+ = 12 ± 1; −/− = 12 ± 1; mean ± SEM; $p = 0.96$), motor activity (time motionless in the corner of the closed arms, +/+ = 78 ± 5 sec; −/− = 75 ± 5 sec; mean ± SEM; $p = 0.88$), and risk assessment (time scanning edge, +/+ = 16 ± 0.5 sec; −/− = 14 ± 0.7 sec; mean ± SEM; $p = 0.56$) was similar for the two genotypes. Together, these data suggest that activity and baseline fear are normal in ASIC1 −/− mice.

The amygdala is a key component of the circuitry for learned fear (Faneslow and LeDoux, 1999). Our previous finding that ASIC1 disruption impaired synaptic plasticity and memory (Wemmie et al., 2002) raised the possibility that loss of ASIC1 might alter amygdala-dependent learning. We tested cued fear conditioning by repeatedly presenting a tone and foot shock and measuring the percentage of time spent freezing during 1-min intervals. With repeated stimuli, both the +/+ and −/− mice froze more, although the −/− mice lagged slightly behind. However, the robust freezing of −/− mice in the final minute of training (Fig. 8*A*) suggested that −/− animals were capable of expressing a strong fear response when trained extensively. The next day, we tested the ability of the tone to induce freezing in the absence of a shock. A continuous tone was presented for 6 min. Animals of both genotypes responded with an increase in freezing, indicating the occurrence of auditory fear conditioning (Fig. 8*B*). However, the ASIC1-null mice spent significantly less time freezing than their wild-type littermates.

The presence of ASIC1 in the primary sensory cortex and sensory neurons raised the possibility that the −/− mice performed poorly because of a sensory deficit. However, after each shock without exception, both −/− and +/+ mice responded by jumping, vocalizing, or running. The average duration of the response (+/+, 1.7 ± 0.2 sec; −/−, 1.5 ± 0.2 sec; mean ± SD; $p = 0.057$), and the percentage of shocks eliciting a vocalization (+/+, 80.7 ± 26.4%; −/−, 91.6 ± 23.7%; $p > 0.2$) was similar between the two groups. These results agree with our previous studies, which found that unconditioned responses to electrical shock during eyeblink conditioning were normal in ASIC1 −/− mice (Wemmie et al., 2002). In addition, at the behavioral level, we have found no differences in +/+ and −/− animals in mechanosensation, thermal sensation, or allodynia to skin or muscle stimulation (data not shown). Finally, both genotypes performed similarly on an accelerating Rotarod (Wemmie et al., 2002). Together, these data suggest that the observed differences in fear conditioning were not likely to have been the result of a sensory or motor deficit.

To test whether the fear conditioning deficit was restricted to cue, the mice were also conditioned to context. Again, the −/− mice acquired the freezing response more slowly on day 1 (Fig. 8*C*) and froze less on day 2, suggesting that the problem in fear conditioning is not restricted to auditory stimuli.

Conclusions

Consistent with the previously suggested role for ASIC1 in synaptic function (Wemmie et al., 2002), the ASIC1 protein was preferentially distributed to brain regions with strong excitatory synaptic input. Because ASIC1 was abundant in the lateral and basolateral nuclei of the amygdala, it is possible that the freezing deficit in the ASIC1-null mice is because of impaired learning, especially because baseline fear on the elevated plus maze was intact. However, ASIC1 was also expressed in other regions of the fear circuit, for example, the cingulate cortex, nucleus accumbens, and central nucleus of the amygdala, structures thought to contribute to the emotional importance of external stimuli and/or the expression of fear (Cardinal et al., 2002). Thus, ASIC1 might affect multiple brain regions underlying the acquisition and expression of the fear response. Additional studies will be necessary to delineate the multiple possible effects of ASIC1 on behavior. Understanding how ASIC1 contributes to brain function offers new possibilities for elucidating the molecular mechanisms of memory and emotion.

References

Allen NJ, Attwell D (2002) Modulation of ASIC channels in rat cerebellar Purkinje neurons by ischaemia-related signals. J Physiol (Lond) 543:521–529.

Alvarez de la Rosa D, Krueger SR, Kolar A, Shao D, Fitzsimonds RM, Canessa CM (2003) Distribution, subcellular localization and ontogeny of ASIC1 in the mammalian central nervous system. J Physiol (Lond) 546:77–87.

Benson CJ, Xie J, Wemmie JA, Price MP, Henss JM, Welsh MJ, Snyder PM (2002) Heteromultimerics of DEG/ENaC subunits form H^+-gated channels in mouse sensory neurons. Proc Natl Acad Sci USA 99:2338–2343.

Bianchi L, Driscoll M (2002) Protons at the gate: DEG/ENaC ion channels help us feel and remember. Neuron 34:337–340.

Bolshakov KV, Essin KV, Buldakova SL, Dorofeeva NA, Skatchkov SN, Eaton MJ, Tikhonov DB, Magazanik LG (2002) Characterization of acid-sensitive ion channels in freshly isolated rat brain neurons. Neuroscience 110:723–730.

Cardinal RN, Parkinson JA, Hall J, Everitt BJ (2002) Emotion and motivation: the role of the amygdala, ventral striatum, and prefrontal cortex. Neurosci Biobehav Rev 26:321–352.

Escoubas P, De Weille JR, Lecoq A, Diochot S, Waldmann R, Champigny G, Moinier D, Menez A, Lazdunski M (2000) Isolation of a tarantula toxin specific for a class of proton-gated Na^+ channels. J Biol Chem 275:25116–25121.

Faneslow MS, LeDoux JE (1999) Why we think plasticity underlying pavlovian fear conditioning occurs in the basolateral amygdala. Neuron 23:229–232.

Fox K (2002) Anatomical pathways and molecular mechanisms for plasticity in the barrel cortex. Neuroscience 111:799–814.

García-Añoveros J, Derfler B, Neville-Golden J, Hyman BT, Corey DP (1997) BNaC1 and BNaC2 constitute a new family of human neuronal sodium channels related to degenerins and epithelial sodium channels. Proc Natl Acad Sci USA 94:1459–1464.

Gruol DL, Barker JL, Huang LY, MacDonald JF, Smith Jr TG (1980) Hydrogen ions have multiple effects on the excitability of cultured mammalian neurons. Brain Res 183:247–252.

Hyman SE, Malenka RC (2001) Addiction and the brain: the neurobiology of compulsion and its persistence. Nat Rev Neurosci 2:695–703.

Immke DC, McCleskey EW (2001) Lactate enhances the acid-sensing Na^+ channel on ischemia-sensing neurons. Nat Neurosci 4:869–870.

Krishtal OA, Pidoplichko VI (1981) A "receptor" for protons in small neurons of trigeminal ganglia: possible role in nociception. Neurosci Lett 24:243–246.

Krishtal OA, Osipchuk YV, Shelest TN, Smirnoff SV (1987) Rapid extracellular pH transients related to synaptic transmission in rat hippocampal slices. Brain Res 436:352–356.

Lingueglia E, de Weille JR, Bassilana F, Heurteaux C, Sakai H, Waldmann R, Lazdunski M (1997) A modulatory subunit of acid sensing ion channels in brain and dorsal root ganglion cells. J Biol Chem 272:29778–29783.

Lowry OH, Passanneau JV (1972) A multistep metabolite assay (for inorganic phosphate). In: A flexible system of enzymatic analysis, Ed 3 (Lowry OH, Passonneau JV, eds), pp 86–92. New York: Academic.

McKernan MG, Shinnick-Gallagher P (1997) Fear conditioning induces a lasting potentiation of synaptic currents *in vitro*. Nature 390:607–611.

Olson TH, Riedl MS, Vulchanova L, Ortiz-Gonzalez XR, Elde R (1998) An acid sensing ion channel (ASIC) localizes to small primary afferent neurons in rats. Neuron 9:1109–1113.

Price MP, Lewin GB, McIlwrath SL, Cheng C, Xie J, Heppenstall PA, Stucky CL, Mannsfeldt AG, Brennan TJ, Drummond HA, Qiao J, Benson CJ, Tarr DE, Hrstka RF, Yang B, Williamson RA, Welsh MJ (2000) The mammalian sodium channel BNC1 is required for normal touch sensation. Nature 407:1007–1011.

Price MP, McIllwrath SL, Xie J, Cheng C, Qiao J, Tarr DE, Sluka KA, Brennan TJ, Lewin GR, Welsh MJ (2001) The DRASIC cation channel contributes to the detection of cutaneous touch and acid stimuli in mice. Neuron 32:1071–1083.

Rogan MT, Stäubli UV, LeDoux JE (1997) Fear conditioning induces associative long-term potentiation in the amygdala. Nature 390:604–607.

Shepherd GM, Greer CA (1998) Olfactory bulb. In: The synaptic organization of the brain, Ed 4 (Shepherd GM, ed), pp 159–204. New York: Oxford UP.

Waldmann R, Champigny G, Bassilana F, Heurteaux C, Lazdunski M (1997) A proton-gated cation channel involved in acid-sensing. Nature 386:173–177.

Welsh MJ, Price MP, Xie J (2002) Biochemical basis of touch perception: mechanosensory function of degenerin/epithelial Na^+ channels. J Biol Chem 277:2369–2372.

Wemmie JA, Chen J, Askwith CC, Hruska-Hageman AM, Price MP, Nolan BC, Yoder PG, Lamani E, Hoshi T, Freeman JHJ, Welsh MJ (2002) The acid-activated ion channel ASIC contributes to synaptic plasticity, learning, and memory. Neuron 34:463–477.

Journal of Physiology (2002), 543.2, pp. 521–529

DOI: 10.1113/jphysiol.2002.020297
www.jphysiol.org

Modulation of ASIC channels in rat cerebellar Purkinje neurons by ischaemia-related signals

Nicola J. Allen and David Attwell

Department of Physiology, University College London, Gower Street, London WC1E 6BT, UK

Acid-sensing ion channels (ASICs), activated by a decrease of extracellular pH, are found in neurons throughout the nervous system. They have an amino acid sequence similar to that of ion channels activated by membrane stretch, and have been implicated in touch sensation. Here we characterize the pH-dependent activation of ASICs in cerebellar Purkinje cells and investigate how they are modulated by factors released in ischaemia. Lowering the external pH from 7.4 activated an inward current at −66 mV, carried largely by Na^+ ions, which was half-maximal for a step to pH 6.4 and was blocked by amiloride and gadolinium. The H^+-gated current desensitized within a few seconds, but approximately 30 % of cells showed a sustained inward current (11 % of the peak current) in response to the maintained presence of pH 6 solution. The peak H^+-evoked current was potentiated by membrane stretch (which occurs in ischaemia when $[K^+]_o$ rises) and by arachidonic acid (which is released when $[Ca^{2+}]_i$ rises in ischaemia). Arachidonic acid increased to 77 % the fraction of cells showing a sustained current evoked by acid pH. The ASIC currents were also potentiated by lactate (which is released when metabolism becomes anaerobic in ischaemia) and by FMRFamide (which may mimic the action of related mammalian RFamide transmitters). These data reinforce suggestions of a mechanosensory aspect to ASIC channel function, and show that the activation of ASICs reflects the integration of multiple signals which are present during ischaemia.

(Received 22 March 2002; accepted after revision 13 June 2002)
Corresponding author D. Attwell: Department of Physiology, University College London, Gower Street, London WC1E 6BT, UK.
Email: D.Attwell@ucl.ac.uk

Acid-sensing ion channels (ASICs), which are activated by extracellular protons and blocked by amiloride, were first reported in rat trigeminal and dorsal root ganglion neurons (Krishtal & Pidoplichko, 1981), and have since been found in a range of central and peripheral neurons and glia (Akaike & Ueno, 1994; Bevan, 1998). The protein subunits making up these channels contain two membrane-spanning regions and exist in at least six different forms: ASIC1a (also known as BNaC2), ASIC1b, ASIC2a (also known as MDEG1 or BNaC1), ASIC2b (MDEG2), ASIC3 (DRASIC) and ASIC4. ASIC proteins are structurally related to epithelial sodium channels, and to channels activated by mechanical stimuli and by the snail neuropeptide FMRFamide (Lingueglia *et al.* 1995; Waldmann *et al.* 1997; Waldmann & Lazdunski, 1998; Mano & Driscoll, 1999). Mutations in *C. elegans* mechano-transduction channels lead to constitutive activation of these channels and thus to an excessive cation entry causing neuronal degeneration (Driscoll & Chalfie, 1991), so the channel superfamily which includes the ASICs is denoted DEG/ENaC, for *deg*enerin/*e*pithelial *Na* channel.

Knocking out ASIC2 or ASIC3 alters touch sensation, suggesting a mechanosensing role for these subunits (Price *et al.* 2000, 2001), although direct evidence of mechanosensing by ASICs is lacking. Furthermore, the pH-gating of ASIC1- and ASIC3-containing channels is potentiated by the neuropeptide FMRFamide (Askwith *et al.* 2000). This raises the possibility that the common evolutionary history of the DEG/ENaC channel superfamily has resulted in ASICs being able to integrate several different signals – acidity, mechanical stimulation and peptide transmitter binding.

The widespread expression of ASIC channels throughout the CNS, and the large membrane current that they can generate, suggests that they may have an important functional role. However, many ASIC channels require a large and rapid fall of pH to be activated and it is unclear when this might happen in the CNS (see Discussion). This suggests that a co-agonist or modulator may be needed, in addition to acid pH, to activate the channels under natural conditions, but little is known about the modulation of ASIC channels in central neurons. Here we characterize pH-gated currents in cerebellar Purkinje cells, which express ASIC subunits 1a, 2a and 2b (Garcia-Anoveros *et al.* 1997; Lingueglia *et al.* 1997), and determine how they are modulated by factors present during ischaemia. We focus on ischaemia for two reasons. First, the fall of extracellular pH by more than one pH unit during ischaemia (Kraig *et al.* 1983; Silver & Erecinska, 1992) might be expected to activate ASICs. Second, Purkinje cells

are prone to dying necrotically in ischaemia (Cervos-Navarro & Diemer, 1991), despite their lack of the NMDA subtype of glutamate receptor which promotes ischaemic death in other neurons, and an ASIC-mediated cation influx might contribute to this death.

METHODS

Cerebellar slices and acutely isolated Purkinje cells

Cerebellar slices (250 μm thick) were cut from the brains of 12- to 14-day-old rats (killed by cervical dislocation in accordance with the UK Animals (Scientific Procedures) Act, 1986), in a solution containing (mM): NaCl 120, KCl 2.5, $MgCl_2$ 2, $CaCl_2$ 2, NaH_2PO_4 1, $NaHCO_3$ 26, glucose 10, Na-kynurenate (to block glutamate receptors) 1, bubbled with 95% O_2–5% CO_2. Slices were dissociated by papain treatment followed by trituration with a fine glass pipette, as for isolated salamander Müller cells (Brew & Attwell, 1987) but with the tonicity of the solution raised to that for mammals by the addition of NaCl and with the solutions bubbled with 100% O_2. When the dissociated slice was plated into the experimental chamber, granule cells could be identified by their small spherical appearance (diameter < 8 μm), and Purkinje cells by their larger size (diameter > 20 μm) and the remains of axons and dendritic trees (Hockberger *et al.* 1994; Billups *et al.* 1998). Deep cerebellar nuclear cells also have a large diameter, but are present at only one tenth of the number of Purkinje cells (Caddy & Biscoe, 1979) and furthermore are rarely obtained by papain dissociation of cerebellum (Hockberger *et al.* 1994), suggesting that they did not significantly contaminate our sample of Purkinje cells.

Electrodes

Purkinje cells (isolated or in cerebellar slices) were whole-cell clamped using electrodes pulled from thin-walled borosilicate tube with a resistance in external solution of 2–4 MΩ. The series resistance in whole-cell clamp mode was ~5 MΩ, leading to voltage errors of < 5 mV for peak ASIC currents of < 1 nA at a holding potential of −60 to −70 mV.

Solutions

Experiments were carried out at room temperature (23–26 °C). External solution contained (mM): NaCl 140, KCl 2.5, $MgCl_2$ 2, $CaCl_2$ 2.5, NaH_2PO_4 1, Hepes or Mes 10, glucose 10, pH adjusted with NaOH. Solutions were bubbled with 100% O_2 for slice experiments; the properties of isolated cells were not affected whether or not O_2 was bubbled, presumably because sufficient O_2 diffuses from the surface of the shallow bath solution for the metabolism of cells plated at low density, so bubbling was omitted. Hepes was used as the pH buffer for pH values > 6.7, and Mes for pH < 6.7 (at pH 6.7 the ASIC current amplitude was independent of the buffer used). NaH_2PO_4 was omitted from all solutions for experiments on gadolinium, which is chelated by phosphate (Caldwell *et al.* 1998). Most drugs (FMRFamide, $GdCl_3$, lysophosphatidylinositol) were added to the external solution from a stock solution in water. Arachidonic acid was added from a stock solution of its sodium salt in water, or from a stock of the acid in ethanol – results with the two stocks were indistinguishable. Na-lactate was added as a replacement for NaCl. For experiments on cell swelling, 140 mM NaCl was replaced by 100 mM NaCl plus 40 mM choline-Cl, and the choline-Cl was omitted to produce 25% hypotonic solution. None of these agents or manipulations affected the resting current at pH 7.4, apart from gadolinium and arachidonic acid which appeared to increase the resistance of the seal between the electrode and the cell. External solutions in different reservoirs were connected through a valve and tubing to a syringe needle, aimed at the whole-cell clamped cell. Solution was superfused through the needle at a rate of 11 ml min^{-1} into a bath of volume 1 ml. This flow rate gave a 10–90% activation time of 77 ± 5 ms in 19 cells for ASIC currents activated by a switch (using manual valves) from pH 7.4 to pH 6. The pipette solution contained (mM): either CsF 110, CsCl 30, NaCl 4 and (*N*-methyl-D-glucamine)$_2$EGTA 5, or KCl 140 and Na_2EGTA 5, or NaCl 140 and Na_2EGTA 5 (see text), in addition to $CaCl_2$ 0.5 and Hepes 10; pH was set to 7.0 using CsOH, KOH or NaOH respectively. When blockers of arachidonic acid metabolism were included in the internal solution (20 μM indomethacin to block cyclooxygenase, 20 μM nordihydroguiaretic acid (NDGA) to block lipoxygenase, and 20 μM 5,8,11,14-eicosatetraynoic acid (ETYA) to block epoxygense and lipoxygenase), we allowed > 8 min for them to diffuse into the cell before testing the effect of arachidonic acid. Electrode junction potentials (−6, −3 and 0 mV for the Cs^+-, K^+- and Na^+-based internal solutions) were compensated for. ASIC currents were evoked by low pH solution at 1–1.5 min intervals to allow 96–99% recovery from desensitization. All chemicals were from Sigma except FMRFamide, which was from Calbiochem.

Data analysis

Data are presented as means ± S.E.M. *P* values are from Student's two-tailed *t* test. Unless otherwise stated, drugs (or hypotonic solution) were applied for 2–3 min. Amplitudes of ASIC currents in the presence of drugs (or hypotonic solution) were measured as the average of two responses to acid pH solution applied after ~1 and 2 min in the drug, and were normalized to the average of two control responses measured ~1 and 2 min before the drug was applied and two responses measured ~1 and 2 min after washing out the drug with control solution (to compensate for slow rundown of the ASIC currents). For the pH dose–response curve (Fig. 1*F*), responses to test pH solutions (applied in random order) were normalized to the average of bracketing responses to pH 5 solution; most cells were tested with five different pH solutions as well as pH 5.

RESULTS

Purkinje cells show an ASIC-mediated current

In isolated Purkinje cells voltage clamped at −66 mV, stepping the external pH from 7.4 to 6.0 always led to the activation of a large inward current (mean value 806 ± 71 pA in 79 cells) which then desensitized (Fig. 1*A*). The current was reduced reversibly by 93 ± 2% by 100 μM amiloride in five cells (Fig. 1*A*), consistent with it being mediated by ASIC channels (Waldmann *et al.* 1997). During maintained application of pH 6.0 solution, the current desensitized with a time constant of 1.63 ± 0.10 s (in 20 cells). From the response to a second pulse of acid solution, the time constant of the current recovery from desensitization (assumed to be exponential) was 18.0 ± 1.5 s in three cells (data not shown) similar to data from other cell types (Bevan, 1998). In many cells desensitization was complete, while in 72 of 230 cells (31%) with a healthy appearance and input resistance, to which pH 6 solution was applied, a small sustained inward current was present after the desensitization (Figs 1*B* and 4*C*). In cells showing

a sustained current at the start of recording, the ratio of the sustained to the peak current evoked by pH 6 solution was 0.11 ± 0.01 (n = 72). The sustained current was not blocked by amiloride (5 cells, Fig. 1*B*), as reported previously in other preparations (Benson *et al.* 1999). During recordings in which the cell condition deteriorated, as assessed by a fall of input resistance, the sustained current tended to increase with time (Fig. 1*B*), suggesting that a sustained cation influx is more likely to be evoked by acid pH in cells with compromised health; these cells were excluded from further analysis.

Acid solution evoked a similar current in Purkinje cells in cerebellar slices (Fig. 1*C*, 6 cells) showing that the pH-activated current was not an artefact produced by cell isolation. In the slice, the activation kinetics of the current were slower and its amplitude was smaller than in isolated cells, presumably because the pH of the solution just outside the cell in the slice is altered more slowly by the superfusion solution, allowing more desensitization to occur during the current onset. All subsequent experiments were performed on isolated cells.

Consistent with previous work on ASIC-mediated currents, with Na^+ as the main cation in the whole-cell pipette, the reversal potential of the peak acid-evoked current was at ~0 mV, while with K^+ or Cs^+ as the main cation, the extrapolated reversal potential was more positive than +40 mV or +50 mV, respectively (Fig. 1*D*). This implies that Na^+ is the main carrier of the peak ASIC current, but does not rule out a small Ca^{2+} component since, from the Goldman–Hodgkin–Katz equation, a permeability ratio of P_{Ca}/P_{Na} = 0.4 as reported for ASIC1a channels (Waldmann *et al.* 1997) would displace the reversal potential measured with Na^+ as the main intracellular cation from 0 mV to only 0.35 mV. The sustained current component, when present, was too small to determine its ionic selectivity reliably.

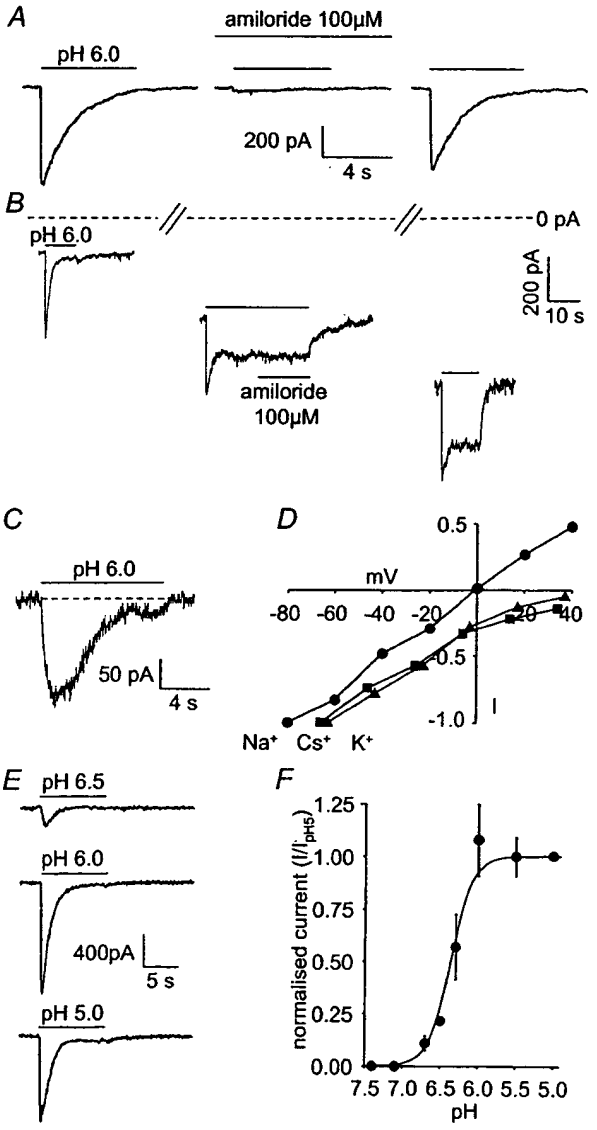

Figure 1. ASIC currents in cerebellar Purkinje neurons

Membrane potential was −66 mV and internal solution contained Cs^+ as the main cation, except where stated. *A*, response of an isolated Purkinje cell to pH 6.0 solution in control conditions, in the presence of 100 μM amiloride, and after washout of amiloride. *B*, increase of sustained component of response of an isolated Purkinje cell to pH 6.0 solution during deterioration of cell condition (shown by increase of holding current: distance below dashed line). Slashes on dashed line denote time intervals of ~2 min between the responses shown. Middle trace shows that amiloride does not block the sustained current. *C*, response of a Purkinje cell in a cerebellar slice to pH 6.0 solution (solutions contained 10 μM NBQX, 40 μM bicuculline and 1 μM TTX, to block AMPA and $GABA_A$ receptors and Na^+ action potentials). *D*, specimen *I–V* relations for the peak ASIC current evoked by pH 6.0 solution in three isolated cells whole-cell clamped with internal solutions in which the main cation was Na^+ (●), Cs^+ (■) or K^+ (▲); data were normalized to the inward current recorded at the most negative voltage tested. *E*, responses of an isolated cell to solutions of pH 6.5, 6.0 and 5.0. *F*, mean current–pH curve from 20 isolated cells. Smooth curve has the form $[H^+]_o^3/([H^+]_o^3 + H_{0.5}^3)$ with $pH_{0.5} = -\log_{10}H_{0.5}$ = 6.4.

The ASIC current was activated when the pH was lowered beyond 6.8, and larger acidifications produced a larger current, although in some cells the response to pH 5 solution was smaller than that to pH 6 (Fig. 1*E*). On average, the pH-dependence of the current could be fitted approximately by a Hill equation with a coefficient of 3 and a pH for half-maximal response of $pH_{0.5} = 6.4$ (Fig. 1*F*). This $pH_{0.5}$ is consistent with the transient current being generated mainly by homomers of ASIC1a (which have $pH_{0.5} = 6.2$–6.6) or possibly heteromers of ASIC1a and ASIC2b, and rules out a major contribution from channels made from ASIC2a alone ($pH_{0.5} = 4.1$), ASIC2b alone (which does not form functional channels), ASIC1a and ASIC2a ($pH_{0.5} = 4.8$), or ASIC2a and ASIC2b ($pH_{0.5} = 3.5$) (Bassillana *et al.* 1997; Lingueglia *et al.* 1997; Waldmann *et al.* 1997; Escoubas *et al.* 2000).

Potentiation by cell swelling

During brain ischaemia the extracellular pH becomes acid (due to a switch to anaerobic respiration) at the same time as a rise in extracellular $[K^+]$ (produced by Na^+–K^+ pump inhibition) leads to cell swelling (Hansen, 1985; Walz *et al.* 1993). Since structural relatives of ASIC channels can sense membrane stretch (see Introduction), we investigated whether the Purkinje cell ASIC current showed one of the signatures of mechanosensitive channels, a sensitivity to gadolinium (Hamill & McBride, 1996), or was modulated by membrane stretch.

Gadolinium (100 μM) completely abolished the ASIC current in all three cells tested (Fig. 2*A*), while 1 μM gadolinium gave a 51 ± 8 % block in two cells. In contrast,

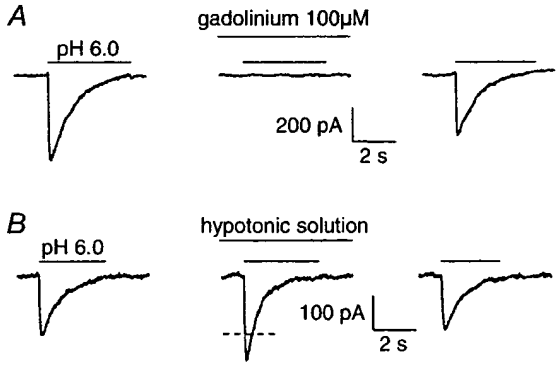

Figure 2. Modulation of ASIC currents by gadolinium and cell swelling

A, response of an isolated Purkinje cell to pH 6.0 solution in control conditions, after 1 min in the presence of 100 μM gadolinium, and 1 min after washout of the 2 min exposure to gadolinium. Solutions were phosphate-free (see Methods). *B*, response of an isolated Purkinje cell to pH 6.0 solution in normal external solution, after 1 min in 25 % hypotonic solution, and again in normal solution 1 min after the end of a 2 min exposure to hypotonic solution. Dashed line shows mean amplitude of control responses before and after hypotonic solution. Cells were clamped at −66 mV, with internal solution containing Cs^+.

100 μM gadolinium produced only a 65 %, 40 % or 20 % block of channels formed by expression of ASIC2a + ASIC3, ASIC3 or ASIC2a subunits, respectively, in oocytes (Babinski *et al.* 2000). The complete block by 100 μM gadolinium of the Purkinje cell ASICs presumably reflects the presence of ASIC1a and/or ASIC2b (see above). External solution that was made 25 % hypotonic (at constant sodium concentration, see Methods) had no effect on the resting Purkinje cell membrane current (15 cells, data not shown), but potentiated the ASIC response to pH 6 solution by 20 ± 2 % ($P = 2 \times 10^{-7}$; Fig. 2*B*). Thus, the Purkinje cell ASIC current is potentiated by cell swelling.

Potentiation by arachidonic acid

The rise of intracellular calcium concentration which occurs during brain ischaemia leads to an activation of phospholipase A_2 and a massive release of arachidonic acid (Rehncrona *et al.* 1982). Arachidonic acid is known to have effects on channels similar to those produced by membrane stretch, for example potentiating the opening of NMDA receptor channels (Miller *et al.* 1992; Paoletti & Ascher, 1994; Casado & Ascher, 1998). Because it has a so-called 'inverted cone' shape, with a head group narrower than its lipid tail, insertion of arachidonic acid into the membrane is expected to mimic membrane stretch at the outer interface of the lipid phase with the extracellular water (Casado & Ascher, 1998). In agreement with this idea and with the potentiation of ASIC currents by swelling described above, application of arachidonic acid consistently potentiated the peak ASIC response (Fig. 3*A*; $P = 3.4 \times 10^{-7}$ for 10 μM arachidonic acid). The potentiation took ~1 min to occur, and was roughly proportional to the concentration of arachidonic acid (Fig. 3*B*) as reported for the effect of arachidonic acid on mechanosensitive TREK-2 K^+ channels (Bang *et al.* 2000), implying that the potentiation mechanism was not saturated by the doses of arachidonic acid we used. The fractional potentiation by arachidonic acid was not significantly different for activation by solutions with pH between 6.7 and 6.0 (Fig. 3*C*), implying that arachidonic acid did not alter the pH-dependence of activation of the ASIC current. Blocking the breakdown of arachidonic acid, by including enzyme blockers in the whole-cell pipette (see Methods), did not affect the potentiation by arachidonic acid. With the blockers present, 5 μM arachidonic acid potentiated the ASIC current evoked by pH 6 solution by 45 ± 10 % in three cells, which is not significantly different ($P = 0.7$) to the 41 ± 5 % potentiation in the absence of blockers shown in Fig. 3*B*. Thus, the potentiation is produced directly by arachidonic acid and not by its derivatives.

In addition to potentiating the peak of the transient ASIC current, arachidonic acid either reversibly enhanced an existing sustained current component produced by acid

solution, or reversibly induced a sustained component where one did not occur in control conditions (Fig. 3*D*). Of 44 cells showing no sustained component in control solution, arachidonic acid (1–10 μM) induced a sustained component in 31 (70%), while in 13 cells showing a sustained component in control solution, arachidonic acid enhanced it in all 13 (100%; Fig. 3*E*). In total, 77% of cells had a sustained component induced or enhanced by arachidonic acid (Fig. 3*E*), and the fraction of cells showing a sustained component was thus increased from 23% in control solution (13/57, not significantly different ($P = 0.27$) from the 72/230 quoted above) to 77% with arachidonic acid present. For application of pH 6 solution, 1, 4, 5, 7 and 10 μM arachidonic acid produced an additional sustained current of 28.5 ± 7.8 pA ($P = 0.035$) in 4 of 5 cells (one cell showed no extra sustained current), 22.0 ± 2.5 pA ($P = 0.003$, in 4 of 4 cells), 27.6 ± 4.9 pA ($P = 0.005$, in 5 of 5 cells), 38.3 ± 3.9 pA ($P = 0.0002$, in 6 of 6 cells), and 34 pA (in 1 of 5 cells), respectively.

In the continuous presence of 10 μM arachidonic acid, 25% hypotonic solution increased the peak ASIC current evoked by pH 6 solution by 17 ± 7% in 6 cells, which is not significantly different ($P = 0.58$) from the 20 ± 2% potentiation produced by hypotonic solution in the absence of arachidonic acid (Fig. 2*B*). The lack of occlusion by arachidonic acid of the potentiation produced by cell swelling is consistent with the potentiation induced by arachidonic acid being far from saturated (Fig. 3*B*), or with arachidonic acid and swelling acting via different mechanisms.

In contrast to arachidonic acid, the head group of lysophosphatidylinositol (LPI) is broader than its lipid tail, and when it inserts into the membrane it is expected to mimic membrane compression at the outer membrane–water interface (Casado & Ascher, 1998). However, whereas for NMDA receptor channels LPI had the opposite effect to arachidonic acid and membrane stretch, decreasing channel opening (Casado & Ascher, 1998), we found no effect of LPI (2 μM) on ASIC responses to pH 6 solution (Fig. 3*F*; in 7 cells the peak current was 93 ± 6% of the control value, $P = 0.26$).

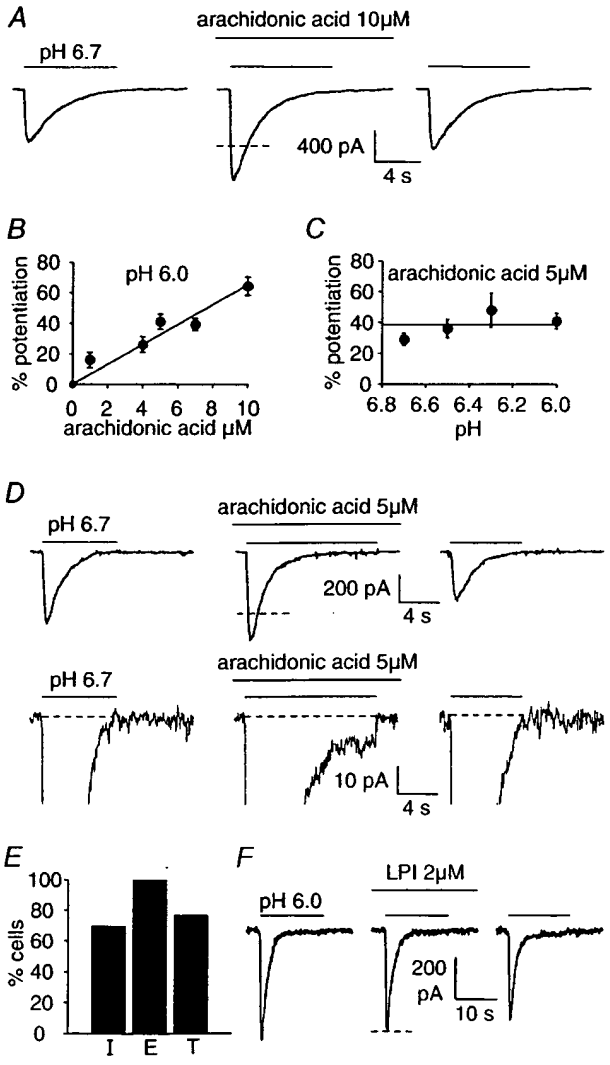

Figure 3. Modulation of ASIC currents in isolated Purkinje cells by arachidonic acid

A, response of a Purkinje cell to pH 6.7 solution in the absence of arachidonic acid, in the presence of 10 μM arachidonic acid, and after washout of the arachidonic acid. *B*, potentiation of the peak current response to pH 6.0 solution as a function of arachidonic acid concentration (data from 6, 4, 4, 5 and 20 cells for 1, 4, 5, 7 and 10 μM arachidonic acid). *C*, potentiation by 5 μM arachidonic acid of the peak response to solutions of different pH (5, 3, 2 and 4 cells for pH 6.7, 6.5, 6.3 and 6.0). *D*, induction by 5 μM arachidonic acid of a sustained component to the ASIC response to pH 6.7 solution. Top traces show entire responses; bottom traces are at higher amplification to show the sustained component. *E*, percentage of 44 cells lacking a sustained component in control solution in which arachidonic acid induced (I) a sustained component, percentage of 13 cells showing a sustained component in control solution which arachidonic acid enhanced (E), and percentage of all 57 cells in which arachidonic acid induced or enhanced a sustained component (total, T). *F*, lysophosphatidylinositol (LPI, 2 μM) does not alter the Purkinje cell response to pH 6.0 solution (data typical of 7 cells). Cells were clamped at −66 mV, with internal solution containing Cs^+. Dashed lines show mean amplitude of control responses bracketing responses in arachidonic acid and LPI.

Potentiation by lactate

During brain ischaemia, the switch to anaerobic respiration leads to the production of lactate, which can rise from a resting value of 1–2 mM to reach a concentration of 12–20 mM in the extracellular space (Schurr & Rigor, 1997). As for cardiac ASICs (Immke & McCleskey, 2001), 15 mM lactate potentiated the current through Purkinje cell ASICs activated by pH 6.7 solution by 25 ± 2% ($P = 0.0002$) in 6 cells (Fig. 4*A*). Analysis of the mechanism of this effect in cardiac ASICs has shown that lactate chelates Ca^{2+} and thereby increases the sensitivity to protons (Immke & McCleskey, 2001).

Modulation by neurotransmitters

The depolarization which occurs in ischaemia as a result of Na^+–K^+ pump inhibition leads to a rise in the extracellular concentration of most neurotransmitters (Phillis *et al.* 1991). We investigated whether the Purkinje cell ASIC current was modulated by the fast transmitters glutamate (100 μM, in the presence of 10 μM 2,3-dihydroxy-6-nitro-7-sulphamoyl-benzo(*f*)quinoxaline (NBQX) to block AMPA receptor currents, the pH-dependence of which could otherwise confound the results, 5 cells), GABA (100 μM, in the presence of 40 μM bicuculline to block pH-dependent $GABA_A$ receptor currents, 5 cells) and ATP (100 μM, 5 cells), or by adenosine (100 μM, 3 cells) which is also released in brain ischaemia (Phillis *et al.* 1991). None of these agents altered by more than 10% the amplitude of the current evoked by a switch to pH 6 solution (Fig. 4*B*).

As reported (Askwith *et al.* 2000) for heterologously expressed and dorsal root ganglion ASIC currents, both the initial peak, and the sustained component of the pH-gated current were potentiated by the neuropeptide FMRFamide (100 μM, Fig. 4*C*). In five cells the peak current evoked by pH 5 solution was potentiated by 51 ± 13% ($P = 0.007$), while in three cells showing a sustained response to pH 5 solution the sustained current was potentiated by 181 ± 67% ($P = 0.05$; Fig. 4*D*). However the structurally-related endogenous opioid peptide met-enkephalin-arginine-phenylalanine, which lacks an amide group (Fig. 4*E*), did not affect the ASIC current (reduced

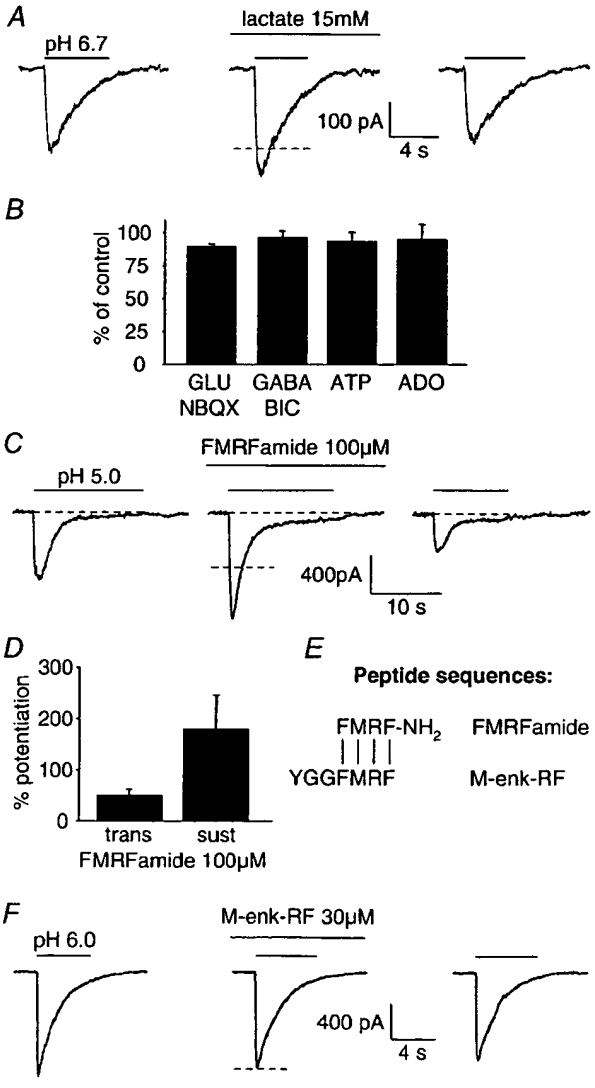

Figure 4. Modulation by lactate and neurotransmitters of ASIC currents in isolated Purkinje cells

A, response of an isolated cell to pH 6.7 solution in control conditions, in 15 mM lactate, and after washing out the lactate. *B*, mean peak ASIC current (evoked by pH 6.0 solution) in the presence of 100 μM glutamate (GLU) + 10 μM NBQX ($n = 5$ cells), 100 μM GABA + 40 μM bicuculline (BIC, $n = 5$), 100 μM ATP ($n = 5$), and 100 μM adenosine (ADO, $n = 3$). *C*, response of a Purkinje cell to pH 5.0 solution in control conditions, in the presence of 100 μM FMRFamide, and after washout of the neuropeptide. *D*, mean potentiation by FMRFamide of the peak and sustained components of the ASIC current evoked by pH 5.0 solution, in 5 and 3 cells respectively. *E*, alignment of sequences of FMRFamide and met-enkephalin-arginine-phenylalanine (M-enk-RF); vertical lines show identical amino acids. *F*, M-enk-RF (30 μM) did not potentiate the ASIC current evoked by pH 6.0 solution. Cells were clamped at −66 mV with internal solution containing Cs^+. Dashed lines show mean amplitude of control responses bracketing responses in lactate, FMRFamide and M-enk-RF.

by 3 ± 3 % in four cells, $P = 0.34$; Fig. 4*F*) suggesting that the amide group is obligatory for this potentiation. Although FMRFamide is not found in mammalian cerebellum, other RFamide peptides are, making them candidates for endogenous modulators of these channels (see Discussion).

DISCUSSION

Cerebellar Purkinje neurons exhibit a transient inward cation current in response to a solution of acid pH (Fig. 1). The amiloride sensitivity of this current indicates that it is generated by ASIC channels (Waldmann *et al.* 1997). Purkinje cells express ASIC subunits 1a, 2a and 2b, but the dependence of their ASIC currents on pH suggests that the properties of their ASICs are dominated by the presence of ASIC1a subunits, possibly in combination with ASIC2b. Notably, we have shown that Purkinje cell ASIC currents are not just controlled by the extracellular pH, but are modulated by a number of factors which are produced during brain ischaemia.

Membrane stretch is produced when the extracellular fluid becomes hypotonic, or during ischaemia when the extracellular [K^+] rises to 60 mM a few minutes after the start of a stroke (Hansen, 1985; Walz *et al.* 1993). Membrane stretch potentiated ASIC currents (Fig. 2), as did arachidonic acid (Fig. 3), which is released when the intracellular calcium concentration rises during brain ischaemia (Rehncrona *et al.* 1982). Arachidonic acid has been shown to mimic the effect of membrane stretch on NMDA receptor channels by distorting the membrane lipid bilayer (Casado & Ascher, 1998), and so may potentiate ASIC currents by the same mechanism as membrane stretch, but we cannot rule out an alternative mechanism of action. We found that 5–10 μM arachidonic acid produced a larger potentiation of the ASIC current than did 25 % hypotonicity. However, water movement to the whole-cell pipette will have reduced the membrane stretching effect of hypotonicity in our experiments, so membrane stretch may have a much larger effect *in vivo*. Arachidonic acid also induced or potentiated a sustained component to the response to acid solution (Fig. 3*D* and *E*), which will lead to a sustained cation influx in conditions of ischaemia. This current is small in our experiments on cells lacking most of their dendritic tree, but since ASICs are expressed in the dendrites of Purkinje cells (Duggan *et al.* 2002) the sustained current may be much larger in intact cells.

Our data are consistent with a mechanosensory aspect to ASIC channel function. Membrane stretch or arachidonic acid alone did not activate the Purkinje cell ASICs, but touch sensation is affected by knocking out ASIC2 or ASIC3 (Price *et al.* 2000, 2001). This suggests that ASICs which have a different subunit composition to those in Purkinje cells, or are linked to other interacting proteins, may show direct activation by membrane deformation. Interestingly, in *C. elegans*, the mechanosensitivity of channels composed of MEC-4 or MEC-10 subunits is conferred by interaction with MEC-2 (Goodman *et al.* 2002), which is homologous to stomatin – a scaffolding protein expressed strongly in Purkinje cells (Mannsfeldt *et al.* 1999). Thus, the swelling sensitivity of the Purkinje cell ASICs may be mediated by an interaction with stomatin.

Lactate also potentiated Purkinje cell ASIC currents (Fig. 4*A*), probably as a result of lactate chelating extracellular Ca^{2+} (Immke & McCleskey, 2001). This makes lactate a potential modulator of ASIC channels during ischaemia when the extracellular lactate concentration can rise from 1–2 mM to 12–20 mM as a result of the switch to anaerobic respiration (Schurr & Rigor, 1997).

Of the neurotransmitters which we tested, only FMRFamide potentiated Purkinje cell ASIC currents (Fig. 4*C* and *D*), as reported previously (Askwith *et al.* 2000) for currents mediated by ASIC1 and ASIC3 and for ASIC currents in dorsal root ganglion cells. The endogenous opioid peptide met-enkephalin-arginine-phenylalanine, which contains a C-terminal FMRF sequence but lacks the amide group, did not potentiate the Purkinje cell ASIC current, suggesting that the peptide binding site on ASICs recognizes in part the amide group. FMRFamide is not found in the vertebrate CNS, and its vertebrate analogue neuropeptide FF (which also potentiates ASIC currents (Askwith *et al.* 2000)) is only found at low levels in the cerebellum (Majane *et al.* 1989), but other RFamides have recently been discovered which are present in the cerebellum (Hinuma *et al.* 2000; Ukena & Tsutsui, 2001) and which may therefore be endogenous modulators of the Purkinje cell ASIC currents.

Activation of the Purkinje cell ASIC channels by a fall of pH *in vivo* may occur during synaptic transmission, as a result of the acid pH in presynaptic vesicles (about 5.5). When the vesicular contents are released during synaptic transmission a rapid acidification of the extracellular space may occur, and activation of ASIC channels (which are located in clusters in Purkinje cell dendrites (Duggan *et al.* 2002)) could contribute to postsynaptic currents. A rapid (though small) acidification during exocytosis has been detected both directly with a pH-sensitive dye (Krishtal *et al.* 1987) and indirectly from a modulatory effect on presynaptic calcium channels (DeVries, 2001). However, the idea that postsynaptic ASIC currents contribute significantly to excitatory or inhibitory synaptic transmission is apparently ruled out by the fact that glutamate or GABA receptor blockers, which we found to have little effect on the Purkinje cell ASIC current (Figs 4*B* and 1*C*), can essentially abolish postsynaptic currents in Purkinje cells (NBQX reduces AMPA receptor-mediated EPSCs by 97 % (Tempia *et al.* 1998); bicuculline reduces $GABA_A$ receptor mediated IPSCs by 96 % (Konnerth *et al.* 1990)).

During ischaemia, although the pH falls by up to one unit as a result of metabolism becoming anaerobic (Kraig *et al.* 1983; Silver & Erecinska, 1992), it takes several minutes to do so, which is too slow to evoke the large transient component of ASIC currents – channel desensitization occurring as the pH falls prevents a large current developing. Nevertheless some ASIC subunit combinations show a sustained current in low pH solution, and in Purkinje cells this was seen in ~30% of cells. Of the modulators that we tested, both arachidonic acid and FMRFamide significantly enhanced the sustained current component, and arachidonic acid increased to 77% the fraction of cells exhibiting a sustained component. Thus, when arachidonic acid is released in ischaemia, at a time when the extracellular space has become acid, it will co-activate (with the pH change) a tonic inward cation current in most Purkinje cells. This may contribute to neuronal death in two ways. First, Na^+ entry will tend to be followed by Cl^- entry and an osmotic entry of water, which will produce cell swelling and possibly membrane rupture. Second, since ASIC1a subunits (possibly in combination with ASIC2b) appear to dominate the Purkinje cell ASIC current and ASIC1a homomeric channels are calcium-permeable (Waldmann *et al.* 1997), there may be an increased Ca^{2+} entry which can cause cell death by activating Ca^{2+}-dependent proteases, lipases and nucleases. Testing the involvement of ASICs in ischaemic neuronal death is hindered at present by the fact that neither amiloride (Fig. 1*B*) nor toxin blockers of the channels block the sustained current component (Benson *et al.* 1999; Escoubas *et al.* 2000).

In summary, we have demonstrated that the activity of Purkinje cell ASIC channels reflects the integration of several signals which these channels sense: pH, membrane stretch, arachidonic acid, lactate, and peptide transmitters. Thus, the magnitude of ASIC currents and their contribution to neuronal depolarization or degeneration will reflect not just the pH of the extracellular solution but also the levels of the other signals sensed by these channels.

REFERENCES

Akaike, N. & Ueno, S. (1994). Proton-induced current in neuronal cells. *Progress in Neurobiology* **43**, 73–83.

Askwith, C. C., Cheng, C., Ikuma, M., Benson, C., Price, M. P. & Welsh, M. J. (2000). Neuropeptide FF and FMRFamide potentiate acid-evoked currents from sensory neurons and proton-gated channels. *Neuron* **26**, 133–141.

Babinski, K., Catarsi, S., Biagini, G. & Seguela, P. (2000). Mammalian ASIC2a and ASIC3 subunits co-assemble into heteromeric proton-gated channels sensitive to Gd^{3+}. *Journal of Biological Chemistry* **275**, 28519–28525.

Bang, H., Kim, Y. & Kim, D. (2000). TREK-2, a new member of the mechanosensitive tandem-pore K^+ channel family. *Journal of Biological Chemistry* **275**, 17412–17419.

Bassillana, F., Champigny, G., Waldmann, R., De Weille, J. R., Heurteaux, C. & Lazdunski, M. (1997). The acid-sensitive ionic channel subunit ASIC and the mammalian degenerin MDEG form a heteromultimeric H^+-gated Na^+ channel with novel properties. *Journal of Biological Chemistry* **272**, 28819–28822.

Benson, C. J., Eckert, S. P. & McCleskey, E. W. (1999). Acid-evoked currents in cardiac sensory neurons. *Circulation Research* **84**, 921–928.

Bevan, S. (1998). Proton-gated ion channels in neurons. In *pH and Brain Function*, ed. Kaila, K & Ransom, B. R., pp. 447–475. Wiley-Liss, New York.

Billups, B., Rossi, D., Oshima, T., Warr, O., Takahashi, M., Sarantis, M., Szatkowski, M. & Attwell, D. (1998). Physiological and pathological operation of glutamate transporters. *Progress in Brain Research* **116**, 45–58.

Brew, H. & Attwell, D. (1987). Electrogenic glutamate uptake is a major current carrier in the membrane of axolotl retinal glial cells. *Nature* **327**, 707–709.

Caddy, K. W. & Biscoe, T. J. (1979). Structural and quantitative studies on the normal C3H and Lurcher mutant mouse. *Philosophical Transactions of the Royal Society* B **287**, 167–201.

Caldwell, R. A., Clemo, H. F. & Baumgarten, C. M. (1998). Using gadolinium to identify stretch-activated channels: technical considerations. *American Journal of Physiology* **275**, C619–621.

Casado, M. & Ascher, P. (1998). Opposite modulation of NMDA receptors by lysophospholipids and arachidonic acid: common features with mechanosensitivity. *Journal of Physiology* **513**, 317–330.

Cervos-Navarro, J. & Diemer, N. H. (1991). Selective vulnerability in brain hypoxia. *Critical Reviews in Neurobiology* **6**, 149–182.

Devries, S. H. (2001). Exocytosed protons feedback to suppress the Ca^{2+} current in mammalian cone photoreceptors. *Neuron* **32**, 1107–1117.

Driscoll, M. & Chalfie, M. (1991). The Mec-4 gene is a member of a family of *Caenorhabditis elegans* genes that can mutate to induce neuronal degeneration. *Nature* **349**, 588–593.

Duggan, A., Garcia-Anoveros, J. & Corey, D. P. (2002). The PDZ domain protein PICK1 and the sodium channel BNaC1 interact and localize at mechanosensory terminals of DRG neurons and dendrites of central neurons. *Journal of Biological Chemistry* **277**, 5203–5208.

Escoubas, P., De Weille, J. R., Lecoq, A., Diochot, S., Waldmann, R., Champigny, G., Moinier, D., Menez, A. & Lazdunski, M. (2000). Isolation of a tarantula toxin specific for a class of proton-gated Na^+ channels. *Journal of Biological Chemistry* **275**, 25116–25121.

Garcia-Anoveros, J., Derfler, B., Neville-Golden, J., Hyman, B. T. & Corey, D. P. (1997). BNaC1 and BNaC2 constitute a new family of human neuronal sodium channels related to degenerins and epithelial sodium channels. *Proceedings of the National Academy of Sciences of the USA* **94**, 1459–1464.

Goodman, M. B., Ernstrom, G. G., Chelur, D. S., O'Hagan, R., Yao, C. A. & Chalfie M. (2002). MEC-2 regulates *C. elegans* DEG/ENaC channels needed for mechanosensation. *Nature* **415**, 1039–1042.

Hamill, O. P. & McBride, D. W. Jr (1996). The pharmacology of mechanogated membrane ion channels. *Pharmacological Reviews* **48**, 231–252.

Hansen, A. J. (1985). Effect of anoxia on ion distribution in the brain. *Physiological Reviews* **65**, 101–148.

HINUMA, S., SHINTANI, Y., FUKUSUMI, S., IIJIMA, N., MATSUMOTO, Y., HOSOYA, M., FUJII, R., WATANABE, T., KIKUCHI, K., TERAO, Y., YANO, T., YAMAMOTO, T., KAWAMATA, Y., HABATA, Y., ASADA, M., KITADA, C., KUROKAWA, T., ONDA, H., NISHIMURA, O., TANAKA, M., IBATA, Y. & FUJINO, M. (2000). New neuropeptides containing carboxy-terminal RFamide and their receptor in mammals. *Nature Cell Biology* **2**, 703–708.

HOCKBERGER, P. E., YOUSIF, L. & NAM, S. C. (1994). Identification of acutely isolated cells from developing rat cerebellum. *Neuroimage* **1**, 276–287.

IMMKE, D. C. & MCCLESKEY, E. W. (2001). Lactate enhances the acid-sensing Na^+ channel on ischemia-sensing neurons. *Nature Neuroscience* **9**, 869–870.

KONNERTH, A., LLANO, I. & ARMSTRONG, C. M. (1990). Synaptic currents in cerebellar Purkinje cells. *Proceedings of the National Academy of Sciences of the USA* **87**, 2662–2665.

KRAIG, R. P., FERREIRA-FILHO, C. R. & NICHOLSON, C. (1983). Alkaline and acid transients in cerebellar microenvironment. *Journal of Neurophysiology* **49**, 831–850.

KRISHTAL, O. A., OSIPCHUK, Y. V., SHELEST, T. N. & SMIRNOFF, S. V. (1987). Rapid extracellular pH transients related to synaptic transmission in rat hippocampal slices. *Brain Research* **436**, 352–356.

KRISHTAL, O. A. & PIDOPLICHKO, V. I. (1981). Receptors for protons in the membrane of sensory neurons. *Brain Research* **214**, 150–154.

LINGUEGLIA, E., CHAMPIGNY, G., LAZDUNSKI, M. & BARBRY, P. (1995). Cloning of the amiloride-sensitive FMRFamide peptide-gated sodium channel. *Nature* **378**, 730–733.

LINGUEGLIA, E., DE WEILLE, J. R., BASSILANA, F., HEURTEAUX, C., SAKAI, H., WALDMANN, R. & LAZDUNSKI, M. (1997). A modulatory subunit of acid-sensing ion channels in brain and dorsal root ganglion cells. *Journal of Biological Chemistry* **272**, 29778–29783.

MAJANE, E. A., PANULA, P. & YANG, H.-Y. T. (1989). Rat brain regional distribution and spinal cord neuronal pathway of FLFQPQRF-NH_2, a mammalian FMRF-NH_2-like peptide. *Brain Research* **494**, 1–12.

MANNSFELDT, A. G., CARROLL, P., STUCKY, C. L. & LEWIN, G. R. (1999). Stomatin, a MEC-2 like protein, is expressed by mammalian sensory neurons. *Molecular and Cellular Neuroscience* **13**, 391–404.

MANO, I. & DRISCOLL, M. (1999). DEG/ENaC channels: a touchy superfamily that watches its salt. *Bioessays* **21**, 568–578.

MILLER, B., SARANTIS, M., TRAYNELIS, S. F. & ATTWELL, D. (1992). Potentiation of NMDA receptor currents by arachidonic acid. *Nature* **355**, 722–725.

PAOLETTI, P. & ASCHER, P. (1994). Mechanosensitivity of NMDA receptors in cultured mouse central neurons. *Neuron* **13**, 645–655.

PHILLIS, J. W., WALTER, J. A. & SIMPSON, R. E. (1991). Brain adenosine and transmitter amino acid release from the ischemic rat cerebral cortex: effects of the adenosine deaminase inhibitor deoxycoformin. *Journal of Neurochemistry* **56**, 644–650.

PRICE, M. P., LEWIN, G. R., MCILWRATH, S. L., CHENG, C., XIE, J., HEPPENSTALL, P. A., STUCKY, C. L., MANNSFELDT, A. G., BRENNAN, T. J., DRUMMOND, H. A., QIAO, J., BENSON, C. J., TARR, D. E., HRSTKA, R. F., YANG, B., WILLIAMSON, R. A. & WELSH, M. J. (2000). The mammalian sodium channel BNC1 is required for normal touch sensation. *Nature* **407**, 1007–1011.

PRICE, M. P., MCILWRATH, S. L., XIE, J., CHENG, C., QIAO, J., TARR, D. E., SLUKA, K. A., BRENNAN, T. J., LEWIN, G. R. & WELSH, M. J. (2001). The DRASIC cation channel contributes to the detection of cutaneous touch and acid stimuli in mice. *Neuron* **32**, 1071–1083.

REHNCRONA, S., WESTERBERG, E., AKESSON, B. & SIESJO, B. K. (1982). Brain cortical fatty acids and phospholipids during and following complete and severe incomplete ischemia. *Journal of Neurochemistry* **38**, 84–93.

SCHURR, A. & RIGOR, B. M. (1997). Brain anaerobic lactate production: a suicide note or a survival kit? *Developmental Neuroscience* **20**, 348–357.

SILVER, I. A. & ERECINSKA, M. (1992). Ion homeostasis in rat brain *in vivo*: intra- and extracellular [Ca^{2+}] and [H^+] in the hippocampus during recovery from short-term, transient ischemia. *Journal of Cerebral Blood Flow and Metabolism* **12**, 759–772.

TEMPIA, F., MINIACI, M. C., ANCHISI, D. & STRATA, P. (1998). Postsynaptic current mediated by metabotropic receptors in cerebellar Purkinje cells. *Journal of Neurophysiology* **80**, 520–528.

UKENA, K. & TSUTSUI, K. (2001). Distribution of novel RFamide-related peptide-like immunoreactivity in the mouse central nervous system. *Neuroscience Letters* **300**, 153–156.

WALDMANN, R., CHAMPIGNY, G., BASSILANA, F., HEURTEAUX, C. & LAZDUNSKI, M. (1997). A proton-gated channel involved in acid-sensing. *Nature* **386**, 173–177.

WALDMANN, R. & LAZDUNSKI, M. (1998). H^+-gated cation channels: neuronal acid sensors in the ENaC/DEG family of ion channels. *Current Opinion in Neurobiology* **8**, 418–424.

WALZ, W., KLIMASZEWSKI, A. & PATERSON, I. A. (1993). Glial swelling in ischemia: a hypothesis. *Developmental Neuroscience* **15**, 216–225.

Acknowledgements

We thank Céline Auger, Liam Drew, Alasdair Gibb, Martine Hamann, Paikan Marcaggi, Paola Pedarzani, David Rossi and Angus Silver for comments on the manuscript. Supported by the Wellcome Trust and a Wolfson–Royal Society award to D.A. Nicola Allen is in the four year PhD Programme in Neuroscience at University College London.

Proc. Natl. Acad. Sci. USA
Vol. 95, pp. 10240–10245, August 1998
Neurobiology

A sensory neuron-specific, proton-gated ion channel

CHIH-CHENG CHEN*, STEVEN ENGLAND*, ARMEN N. AKOPIAN*, AND JOHN N. WOOD†

Molecular Nociception Group, Department of Biology, Medawar Building, University College, Gower Street, London WC1E 6BN, United Kingdom

Edited by Richard Axel, Columbia University, New York, NY, and approved June 18, 1998 (received for review March 2, 1998)

ABSTRACT **Proton-gated channels expressed by sensory neurons are of particular interest because low pH causes pain. Two proton-gated channels, acid-sensing ionic channel (ASIC) and dorsal root ASIC (DRASIC), that are members of the amiloride-sensitive ENaC/Degenerin family are known to be expressed by sensory neurons. Here, we describe the cloning and characterization of an ASIC splice variant, ASIC-β, which contains a unique N-terminal 172 aa, as well as unique 5′ and 3′ untranslated sequences. ASIC-β, unlike ASIC and DRASIC, is found only in a subset of small and large diameter sensory neurons and is absent from sympathetic neurons or the central nervous system. The patterns of expression of ASIC and ASIC-β transcripts in rat dorsal root ganglion neurons are distinct. When expressed in COS-7 cells, ASIC-β forms a functional channel with electrophysiological properties distinct from ASIC and DRASIC. The pH dependency and sensitivity to amiloride of ASIC-β is similar to that described for ASIC, but unlike ASIC, the channel is not permeable to calcium, nor are ASIC-β-mediated currents inhibited by extracellular calcium. The unique distribution of ASIC-β suggests that it may play a specialized role in sensory neuron function.**

Tissue acidosis is a naturally occurring phenomenon that occurs in ischemic, damaged, or inflamed tissue. The reduction in pH in response to such events can be dramatic. In patients with intermittent claudication, the intramuscular pH can drop to 6.0 during exercise, whereas in an experimental model of cardiac infarction, the pH of the cardiac circulation was reduced to pH 5.7 (1). Associated with these conditions is a feeling of pain. This can be reproduced experimentally by infusion of low pH solutions into skin (2, 3) or muscle (4).

In vitro studies have shown that low extracellular pH can evoke inward currents in both central nervous system and peripheral sensory neurons. Krishtal and Pidoplichko (5) demonstrated that low pH evoked inward currents in rat trigeminal ganglion neurons, and similar observations have been made in rat dorsal root ganglion (DRG) neurons (6–8) Low pH responses from DRG are characteristically multiphasic in nature, suggesting the existence of distinct types of channel (see, e.g., ref. 7). The molecular cloning of a number of proton-gated channels supports this conclusion.

Three mammalian proton-gated channels have been cloned recently: acid-sensing ionic channel (ASIC) (9), dorsal root ASIC (DRASIC) (10), and a mammalian degenerin homologue (MDEG-1) (11, 12). A modulatory subunit, MDEG-2, also has been found (12). All of these channels belong to the degenerin/ENaC channel superfamily, and are composed of two hydrophobic segments, intracellular N and C terminals, and a large extracellular loop (13). ASIC, DRASIC, and MDEG1 each form functional channels when expressed in COS-7 cells. Evidence for heteromultimer formation between ASIC and MDEG also has been obtained (14). The electrophysiological properties of these channels are diverse, as is their cellular localization. ASIC and MDEG-1 are widely expressed in nervous tissue (9, 12) whereas DRASIC is found not only in sensory neurons (10) but also in the brain and spinal cord. The role of proton-gated channels in the central nervous system is unknown.

We report here the cloning of a new functional splice variant of ASIC, named ASIC-β, which has electrophysiological properties distinct from other proton-gated channels and is expressed exclusively in a subset of small and large diameter DRG sensory neurons. This distribution is unique among proton-gated channels so far discovered and suggests that ASIC-β has a specialized role in sensory neuron function.

MATERIALS AND METHODS

Molecular Cloning of ASIC-Related Genes. Sequences from the C-terminal region of rat ASIC and mouse BNaC2 (brain sodium channel) were chosen as templates to design PCR primers: 5′-ACTGTACTCCGGAGCAGTACAAGG-3′ 5′-GAGTTCCAGCACTGTGAGGATGCT-3′ that are able to amplify a 350-bp DNA fragment from DRG cDNA (9, 11). The PCR-amplified DNA fragments were labeled with ^{32}P (GIBCO Rad-prime kit) and used as probes to screen a DRG cDNA library. Clones (200,000) from a size-fractionated (2–4 kb) oligo(dT)-primed cDNA library from neonatal rat DRG were screened by hybridization with the PCR probes (25 ng, specific activity 2×10^9 cpm/μg) in 4× SSC containing 0.5% SDS, 5× Denhardt's solution, 100 μg/ml boiled salmon sperm DNA, 10 μg/ml poly(U), and 10 μg/ml poly(C) at 65°C for 4 h. The DRG cDNA filters were given a final wash in 0.2× SSC/0.5% SDS at 65°C. In total, 32 positive clones were picked and analyzed by sequencing.

Northern Blot Analysis. Specific N-terminal sequences of different ASIC clones were chosen as templates to synthesized cRNA probes. ASIC (nucleotide positions 750–1,068 corresponding to amino acids 74–179) was subcloned into pGEM-3Z by using *Eco*RI and *Pst*I sites; ASIC-β (320–700 corresponding to amino acids 18–163) was subcloned into pGEM-11Zf by *Apa*I sites. For DRASIC, a 380-bp DNA fragment was amplified by PCR by using primers 5′-GTGC-GCCACTACACGCTATGCCAAGGAGC-3′ 5′-GGGGAA-CATGTGTTCGATGCCCATTCAAC-3′ and was subcloned into T-vector (Promega); for cyclophilin, a 300-bp DNA fragment was amplified by PCR by using primers 5′ ACCC-CACCGTGTTCTTCGAC-3′ 5′ CATTTGCCATGGACAA-GATG-3 and was subcloned into T-vector. Antisense labeled cRNA was synthesized from these templates by using SP6 RNA polymerase and [^{32}P]-UTP. Such cRNAs were used to

The publication costs of this article were defrayed in part by page charge payment. This article must therefore be hereby marked "*advertisement*" in accordance with 18 U.S.C. §1734 solely to indicate this fact.

This paper was submitted directly (Track II) to the *Proceedings* office.
Abbreviations: DRG, dorsal root ganglion; ASIC, acid-sensing ionic channel; DRASIC, dorsal root ASIC; MDEG-1, a mammalian degenerin homologue; UTR, untranslated region.
Data deposition: The sequence reported in this paper (ASIC-β) has been deposited in the GenBank database (accession no. AJ006519).
*The first three authors contributed equally to this paper.
†To whom reprint requests should be addressed. e-mail: j.wood@ucl.ac.uk.

probe Northern blots with 20–50 μg of total RNA in each lane. Hybridization was carried out in 50% formaldehyde, 5× SSC containing 0.5% SDS, 5× Denhardt's solution, 100 μg/ml boiled salmon sperm DNA, 10 μg/ml poly(U), and 10 μg/ml poly(C) at 68°C for 24 h, with a final wash in 0.1× SSC with 0.5% SDS at 75°C.

***In Situ* Hybridization.** The same templates used for probing Northern blots were labeled with digoxygenin-UTP (15). After *in situ* hybridization, sections were double-labeled with neuronal sub-population markers. mAb against peripherin or N-52 (Chemicon and Sigma) were used at a 1:500 dilution in blocking solution (1× PBS containing 10% sheep serum/0.5% Triton X-100). Fluorescein isothiocyanate-conjugated secondary antibodies (Boehringer Mannheim) were used at a 1:200 dilution in blocking solution. For IB4 staining, the IB4-fluorescein isothiocyanate (4 μg/ml, Sigma) was diluted in 1:300 PBS containing 0.1 mM CaCl2, MgCl2, MnCl2, and 0.2% Triton X-100 (16).

Expression of ASIC-β in COS Cells. To express functional channels in COS-7 cells, ASIC-β was subcloned into the Invitrogen pTracer-CMV vector that expresses green fluorescent protein using *Eco*RI restriction sites. The resulting plasmids were transfected into COS-7 cells by electroporation. For electroporation, COS-7 cells cultured on 100-mm Petri dishes (80–90% confluence) were trypsinized and resuspended in 350 μl of ice-cold HEBS buffer. Plasmid (20–30 μg) then was mixed with the cells in an electroporation cuvette for a total of 5 min. After transfection, the cells were seeded at low density on 30-mm Petri dishes and cultured in 2 ml of DMEM with 10% fetal calf serum at 37°C, for 2–3 days.

Electrophysiology. Whole-cell voltage-clamp recordings (17) were made 2–3 days after transfection. Membrane currents were recorded by using an Axopatch 200B amplifier. Currents were low pass filtered at 5 kHz (4-pole Bessel filter) and digitized by using a Digidata 1200 interface. Acquisition and analysis of currents was achieved by using PCLAMP6 software. Pipettes were pulled from borosilicate glass (Clark Electromedical, Reading, UK) and had DC resistances of ≈3 mΩ when filled with the pipette solution. All recordings were made at room temperature (18–22°C).

The extracellular recording solution was comprised of (in mM): NaCl 146; KCl 5; Glucose 10; $MgCl_2$ 1; $CaCl_2$ 0.01. For extracellular solutions with pH values of 7.4–6.5, 10 mM Hepes was used as the buffer, whereas for solutions of pH 6.5–4.0, 10 mM Mes was used to provide optimal buffering capacity over the wide pH range (3.5 units) required. The normal pH of the extracellular solution was 7.4. In some ion substitution experiments, extracellular sodium chloride was replaced with an equal amount of choline chloride. The effect of extracellular calcium concentration on low pH-evoked currents was investigated by substitution of choline chloride with an equal concentration of calcium chloride, in the absence of extracellular sodium ions.

Low pH solutions were applied via a U-tube (18) placed close (<1 mm) to the cell of interest. The use of the U-tube ensured that the cell was bathed completely in the test solution ensuring that no buffering by the bulk extracellular medium occurred. Low pH solutions usually were applied for 10–20 s, with at least 2 min between applications. The intracellular solution contained (in mM): KCl 120; NaCl 8; $MgCl_2$ 3; Hepes (free acid) 40; 1,2-bis(2-aminophenoxy)ethane-*N*,*N*,*N*′,*N*′-tetraacetate (free acid) 10, at pH 7.35.

RESULTS

Molecular Cloning of Splice Variants of ASIC. An ASIC-related clone with distinct 5′ and 3′ untranslated regions (UTRs) named ASIC-α and a splice variant with a unique 5′ region and the same C-terminal and 3′ UTR as ASIC-α named ASIC-β were identified in a rat DRG cDNA library by homology cloning (Fig. 1*A*). The proposed ORFs of these clones show that they have a similar molecular structure with two putative transmembrane domains, intracellular N and C terminals, and a large extracellular loop (Fig. 1*B*).

The ASIC-α transcript encodes the 526-aa protein named ASIC (9) but has distinct 5′ and 3′ UTRs from the previously reported sequence. There are two types of 5′ UTR in the DRG ASIC-α clones (Fig. 1*A*). The major population of ASIC-α (90%) has a 5′ UTR of up to 530 bp that is GC-rich (73%). A small percentage (10%) of ASIC-α clones have a short 5′ UTR (≈100 bp) that corresponds to the sequence reported for ASIC 5′ UTRs found in brain (Fig. 1*A*). All of the ASIC-related clones in DRG have an identical 3′ UTR that is different from the ASIC UTR reported in brain. An L1-like repetitive sequence reported in ASIC (9) is not found in DRG ASIC-α or β transcripts.

The longest ORF of ASIC-β is 513 aa in length, sharing the same 341 aa with the C terminus of ASIC-α. The N-terminal 172 amino acids of ASIC-β are unique, with highest homology to DRASIC (43.8%), 39.7% identity to both ASIC-α and MDEG1, and 22.6% identity to the FMRFamide-gated sodium channel (FaNaC) (19) (Fig. 1*C*). These five proteins share three conserved cysteines within the N-terminal region of the extracellular loop. There are two additional cysteine residues in ASIC-β when compared with DRASIC, ASIC-α

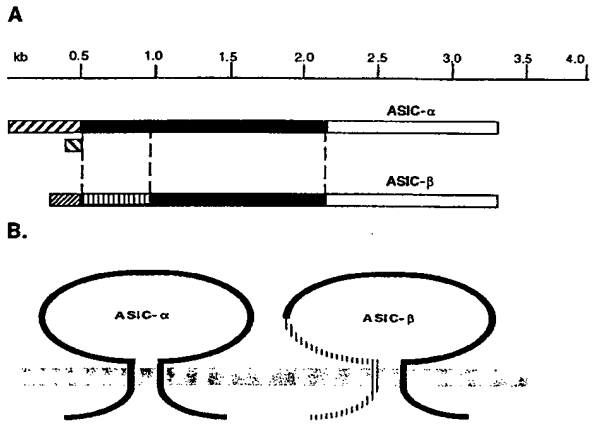

C.

```
                                                                  ____
ASIC-alpha  MELKTEEEEV GGVQPVSIQA PASSSTLHGL AHIPSVERLS LKRALWALCF   50
ASIC-beta   --AGS-LD-G DDS.-RDLV- --N------A S-V-VEGGPG PRQ-------   49
DRASIC      -KPRSDL--A QRR-ASD-RV ----C-M--- G---GPGG-T -R-G---T-V   50
MDEG1       -D--ESPS-. -SL--S---I --NT-----I RHIFVYGP-T IR-V---VA-   49

              ___TM1_______
ASIC-alpha  LGSLAVLLCV CTERVQYYFC YHHVTKLDEV AASQLTFPAV TLCNLNEFRF  100
ASIC-beta   VIA-GAF--Q VGD--A--LS -P---I---- -T-E-V---- -F--T-AV-L   99
DRASIC      -L---AF-YQ VA---R--GE F--K-T---R ESH----F-- ----I-PL-R  100
MDEG1       V---GL--VE SS---S---S -Q-------- V-QS-V---- ------G---   99

ASIC-alpha  SQVSKNDLYH AGELLALLNN RYEIPDTQMA DEKQLEILQD KANFRSFKPK  150
ASIC-beta   --L-YP--LY LA.PMLG-D. ....ESDDP. ...GVPLAPP GPEA..-SGE  137
DRASIC      -RLTP---HW --TALLG-D. ....-AEHA- YLRA-GQPPA PPGF..MPSP  143
MDEG1       -RLTT----- --------DV NLQ---PHL- -PTV--A-RQ ----KHY---  149

ASIC-alpha  PFNMREFYDR AGHDIRDMLL SCHFRGEACS AEDFK  185
ASIC-beta   ---LHR--N- SC-RLE---- Y-SYC-GP-G PHN-S  172
DRASIC      T-D-AQL-A- ---SLE---- D-RY--QP-G P-N-T  178
MDEG1       Q-S-L--LH- V---LK--M- Y-K-K-QE-G HQ--T  184
```

FIG. 1. Structure of ASIC splice variants and primary sequence alignment of ASIC-β with four other known members of the family. (*A*) The gene structure of ASIC splice variants. Three different transcripts are distinguished by their 5′UTRs (hatched) but share the same 3′UTR (white). The coding regions are black apart from the unique N terminus of ASIC-β (striped). (*B*) The proposed molecular structures of ASIC-α and ASIC-β shows that both proteins have the same two transmembrane domain structure, with intracellular N and C terminals. The striped region of AIC-β shows its unique N-terminal region including the first transmembrane domain. (*C*) The N-terminal sequence alignment of four ASIC-related proteins. Block letters present the cysteine resides that are conserved amongst the four proteins, implying a similar secondary structure.

MDEG1, and FaNaC, suggesting that the secondary structure of ASIC-β might have some unique features. N-terminal splicing at a similar position also is found in the related MDEG2 transcript, which differs in 236 aa from MDEG1 (12), but this N-terminal sequence has no homology to the N terminus of ASIC-α. Additional homology cloning with different probes derived from ASIC-related clones showed that the major transcripts represented in our DRG library are ASIC-α, ASIC-β, and DRASIC but not MDEG1.

Tissue Distribution of Sensory Neuron-Associated, Proton-Gated Channels. We examined the tissue distribution of ASIC-β and compared it with that of the other proton-gated channels expressed in sensory neurons. We used Northern blotting and examined the respective distributions in a variety of neuronal and nonneuronal tissues and also some cell lines.

ASIC-α was found in many neuronal tissues, including DRG, spinal cord, trigeminal ganglia, and the trigeminal mesencephalic nucleus. The cell lines PC12, ND7/23, and N-tera2 also expressed ASIC-α (Fig. 2). In contrast, ASIC-β, seen as a 3.2-kb transcript, was found only in the DRG and not in other tissues or cell lines. DRASIC has been reported to be a sensory neuron-specific, proton-gated channel (10). However, in addition to the DRG, we found low level transcripts of DRASIC in superior cervical ganglia, spinal cord, and also the brain stem. These data suggest that ASIC-β is the only proton-gated channel that is expressed exclusively in sensory neurons.

We next examined the cell-type distribution of different ASIC splice variants in DRG. We used peripherin to label small diameter sensory neurons and IB4 to label the neurotrophin-independent cells that also comprise a large proportion of nociceptors (16). We used an anti-neurofilament antibody N-52 to define the large diameter neurons that are mainly mechanoreceptors and proprioreceptors (19). By using 5′ coding region probes of ASIC-α and ASIC-β for *in situ* hybridization, we found that both ASIC-α and ASIC-β are expressed in 20–25% of L4 DRG neurons (Fig. 3). The ASIC-α-positive neurons are mainly small diameter cells (>90%) that coexpress peripherin but not IB4 (Fig. 3). In contrast, ASIC-β-positive neurones are comprised of both small diameter and large diameter neurones, of which 70% express neurofilaments and only 30% coexpress peripherin (Fig. 3*A*). These data demonstrate that ASIC-β exhibits both a tissue- and cell-specific distribution of expression that is clearly different to that shown by ASIC-α.

Expression of ASIC-β in COS-7 Cells. Transfected cells were identified by the presence of green fluorescent protein. Application of low pH to ASIC-β expressing COS cells at a holding potential of −60 mV evoked rapidly activating inward currents (Fig. 4*A*). The threshold for activation of the current was approximately pH 6.5, and the current was maximal at approximately pH 4.0. Fig. 4*B* shows the mean pH response curve recorded from six ASIC-β transfected COS cells. The half-point for activation of the current in this series of experiments was pH 5.9. The inward currents evoked in response to pH 4.0 were variable in magnitude (range was 0.272 ± 8.41 nA), and the mean response was 2.39 ± 0.33 nA in 27 cells). In 83% (34 of 41) of fluorescent cells, a response was observed to the application of pH 4.0–4.5, whereas in 17 of 17 untransfected COS-7 cells, application of pH 4.0–4.5 evoked no change in membrane current.

The pH-activated currents normally reached peak amplitude in ≈1 s in response to the lower pH solutions and rapidly inactivated (or desensitized) in the continued presence of low pH. The time taken to peak was related to the applied pH, with the quickest activation times occurring in response to the lowest pH. The effect of pH on the time taken for inactivation of the current showed a similar pH dependency but was much more marked (Fig. 4*C*).

Ionic Basis of ASIC-β-Mediated Inward Current. The reversal potential for the rapid phase of the low pH activated current was established by using either a linear ramp voltage–clamp protocol or by sequentially stepping the command

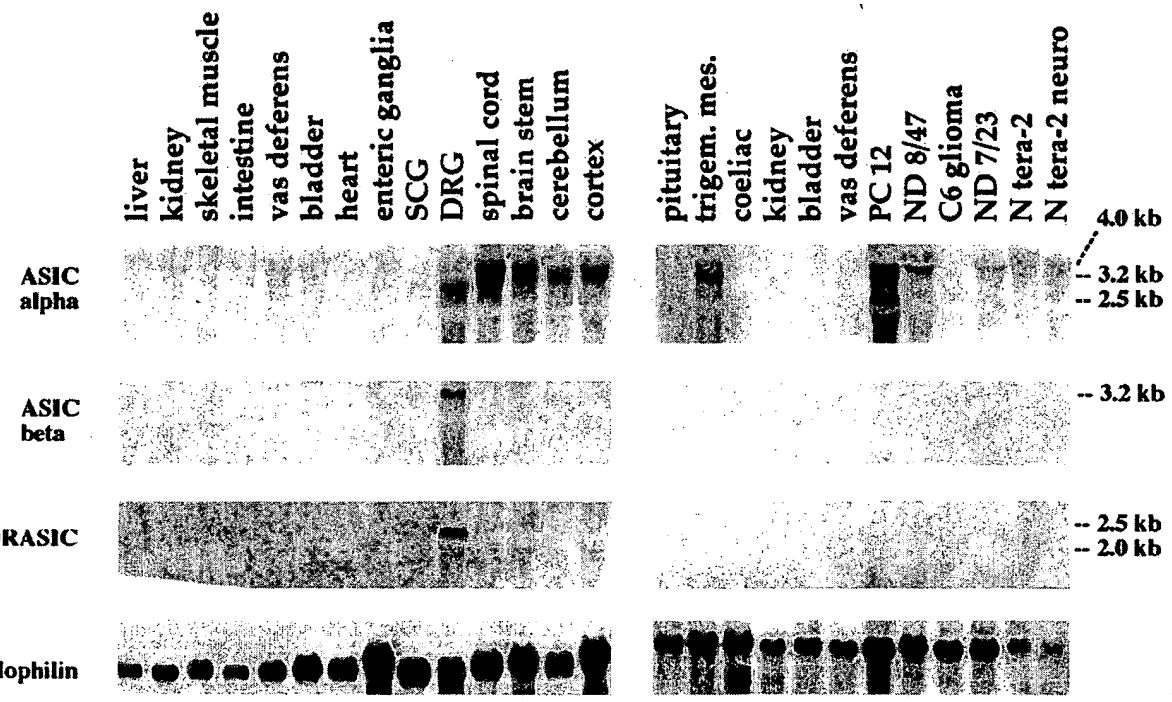

FIG. 2. Northern blots of ASIC-β distribution. The Northern blots were probed by N-terminal unique sequences of ASIC-α, ASIC-β, and DRASIC. All three proton-gated channels are expressed in sensory neurons. ASIC-α is distributed in many neural tissues and cell lines. There are three different sizes of ASIC-α transcripts in PC12 cells that are 2.5, 3.2, and 4.0 kb, but there is only one major transcript of 3.2 kb in sensory neurons. ASIC-β is only expressed in DRG as a 3.2-kb transcript. DRASIC is predominantly in DRG with two sizes of transcripts, 2.0 and 2.5 kb, but also is expressed in superior cervical ganglion, spinal cord, and brain stem. The relative amount of RNA loading is indicated by cyclophilin probe.

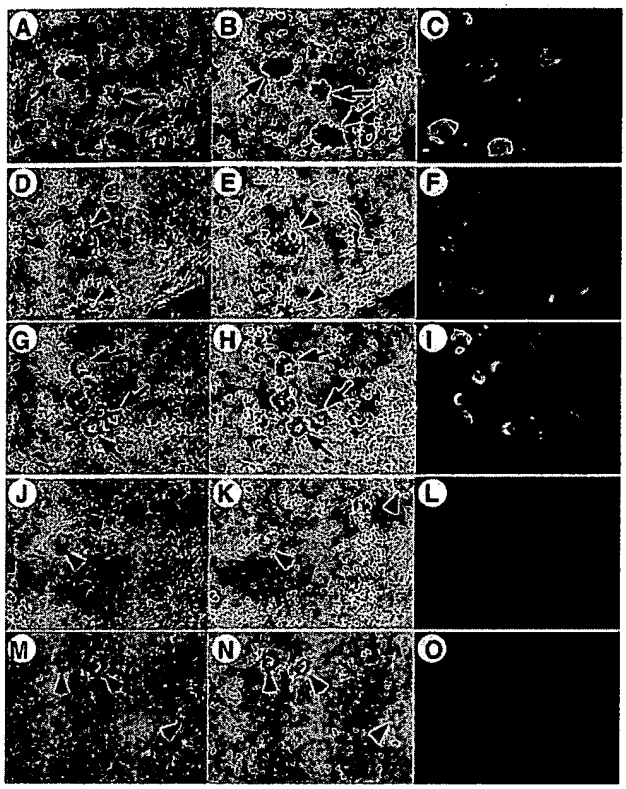

FIG. 3. Cell specificity of ASIC-α and ASIC-β in DRG. *In situ* hybridization of ASIC-α and ASIC-β, double-labeled with anti-peripherin (*A–I*) or isolectin B4 (*J–O*). The left column is overlayed images of *in situ* (middle column) and immunocytochemistry (right column) results. The expression of ASIC-α transcript is most (>90%) colocalized with peripherin (*A–C*, indicated by arrows). However, ASIC-β transcript is distributed in either peripherin-positive (30%) or peripherin-negative (70%) neurons (*D–I*). The colocalization of ASIC-β and peripherin is indicated by arrows (*G* and *H*). The expression of ASIC-β in peripherin-negative large diameter neurones is shown by arrowheads (*D* and *E*). Neither ASIC-α (*M–O*, indicated by arrowheads) nor ASIC-β (*J–L*, indicated by arrowheads) have colocalized staining with isolectin B4, which corresponds to GDNF-dependent small diameter neurons.

potential to a range of values while evoking the inward current (Fig. 4*D*). The command potential was ramped over a period of 240 ms between potentials of −80 and +60 mV. The speed of the ramp allowed us to make accurate recordings despite the rapidly activating and inactivating nature of the response. The reversal potential was found to be 26.1 ± 2.3 mV (n = 8). If the channel were only sodium permeable, the reversal potential would be expected to be approximately +73 mV, given the composition of the intra- and extracellular solutions used. It thus seemed likely that the channel was also permeable to other cations, most notably K+, because of its presence in such high concentration. Ion substitution studies confirmed that the channel was also permeable to K+. Replacement of extracellular sodium with choline abolished inward currents, but on some occasions, small outward currents were seen, confirming that the channel was permeable to potassium ions (data not shown). These currents were small because most recordings were made at a holding potential of −60 mV, close to the reversal potential of potassium ions with the solutions used.

Previous studies have demonstrated that increasing the extracellular calcium concentration reduced the magnitude of proton-activated inward currents passing through the ASIC channel (9). This was not the case for ASIC-β. Fig. 5*A* shows that, in the presence of 146 mM NaCl, increasing the extracellular calcium concentration had no effect on the magnitude

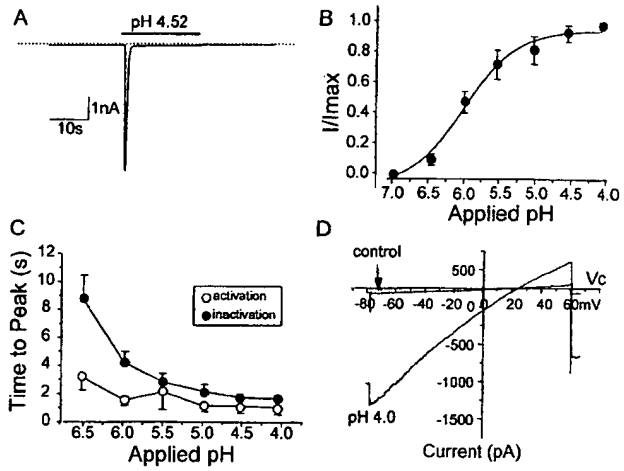

FIG. 4. Characteristics of the pH response in COS-7 cells expressing ASIC-β. Typical response to low pH in ASIC-β transfected COS cells. The cell was voltage-clamped at −60 mV and low pH applied at the bar. Dotted line indicates zero current level. (*B*) pH response relationship obtained from experiments similar to that in *A*. Responses were normalized against the maximal response and plotted against the pH. The half-point for activation of the current was pH 5.9. (*C*) Time taken for the current to activate and inactivate plotted against pH. (*D*) Recordings made during a change in command potential by using a linear ramp protocol (duration of ramp 240 ms). Current was recorded under control conditions and during application of low pH. The current reverses at approximately +25 mV.

of the inward currents evoked by the application of pH 4.0 buffer. In addition, ASIC-β was found not to be permeable to calcium ions. In the experiment shown in Fig. 5*B*, a response to pH 4.0 was obtained under control conditions (Fig. 5*B*, *Left*), and then extracellular NaCl was replaced by choline chloride and the cell was exposed to pH 4.0 buffer in the presence of a range of extracellular calcium concentrations. On removing extracellular sodium, no inward current was detected in response to low pH, and even when the calcium concentration was increased to 50 mM, no inward current was detected. Fig. 5 *A* and *B* are representative of experiments on four cells. Sodium ions were not a cofactor for calcium permeability. We recorded reversal potentials for ASIC-β-mediated currents with 140 mM Na^+ in the external medium, with or without 20 mM Ca^{2+}. The mean reversal potentials were 25.2 ± 2.3 mV (n = 4) in the absence and 24.8 ± 2.8 mV (n = 4) in the presence of Ca^{2+}, demonstrating that the channel is impermeant to calcium, even if Na^+ ions are present.

Pharmacology of ASIC-β-Mediated Currents. We investigated the effect of amiloride, a known inhibitor of other proton-gated channels, on ASIC-β-mediated currents (20). Cells were voltage-clamped at −60 mV and given a 20-s exposure to pH 4.5 solution, first in the absence and then the presence of increasing concentrations of amiloride. The threshold concentration for inhibition of low pH-evoked currents was between 1 and 10 μM. Fig. 5*C* shows an inhibition response curve for amiloride constructed from experiments on six cells. The data points were fitted with a single Boltzman function, giving an IC_{50} of 21 μM.

Capsaicin is known to have an excitatory action on small diameter sensory neurons. Moreover, it has been suggested that capsaicin and protons activate a similar ion channel (21). To investigate whether capsaicin could activate the ASIC-β channel, we exposed ASIC-β-transfected COS cells to 500 nM capsaicin. In four of four cells, capsaicin evoked no change in membrane current, whereas a subsequent application of low pH to the same cells produced characteristically large inward currents (Fig. 5*D*).

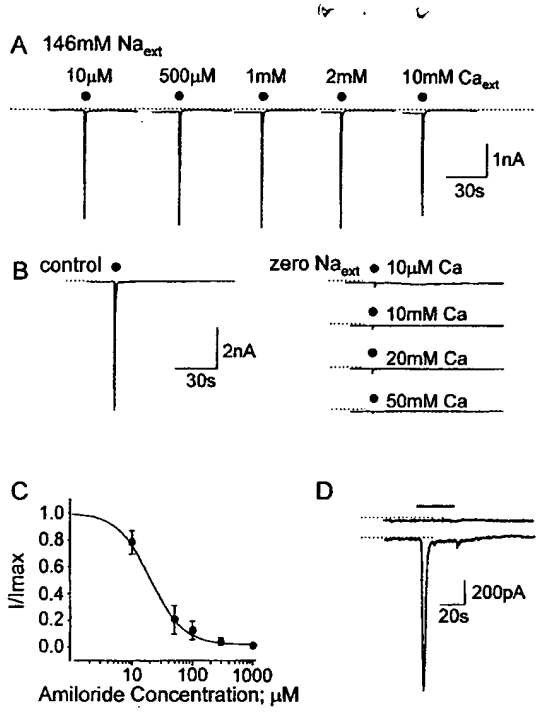

FIG. 5. Calcium dependency and pharmacology of ASIC-β-mediated currents in COS cells. (*A*) Responses obtained to pH 5.1 (at the closed circles) in the presence of increased extracellular calcium concentration. Recordings were made from the same cell at intervals of 3 min. (*B, Left*) Control response to pH 5.1 and (*Right*) responses to low pH in the absence of extracellular sodium and increased calcium concentration are shown. Current flowing via ASIC-β is not inhibited by extracellular calcium, nor is the channel permeable to calcium. Dotted line indicates zero current level. (*C*) Amiloride inhibits ASIC-β mediated current. The IC_{50} derived from this plot was 21 μM. (*D*) Capsaicin does not activate ASIC-β. Recordings made from the same cell; holding potential was −60 mV. Upper trace shows that application of capsaicin (500 nM) at the bar failed to evoke an inward current. pH 4.1, at the bar 3 min later (lower trace), evoked a robust inward current. Traces have been separated for clarity, and the dotted line indicates zero current for each recording.

DISCUSSION

Protons evoke a sensation of pain, and a variety of hyperalgesic mediators potentiate the pain-inducing actions of low pH, suggesting that proton-gated channels play a central role in nociception (4). In this study, we provide detailed information on the expression of proton-gated channel transcripts in sensory neurons. The alternative splicing of ASIC results not only in two different gene products, ASIC-α and ASIC-β, but also in two different ASIC-α transcripts, each of which has a distinct 5′ UTR. The coding region of both ASIC-α transcripts corresponds to that of ASIC (9). The 5′ heterogeneity of ASIC-α and ASIC-β may be generated initially by transcription from different promoters, which may be tissue-specific (see, e.g., ref. 22). In addition, we found two other splice variants of ASIC. One has a 29-aa deletion between codons 74 and 102 of ASIC-α. The other has a 600-bp insertion between codons 236 and 237 of ASIC-α. This insert causes a premature stop in translation and results in a new ASIC-like protein that has a shorter and unique C terminus. We named this channel ASIC-γ and have shown that it forms a functional proton-gated channel when expressed in COS cells (data not shown). However, the level of expression of the ASIC-γ transcript is low, and we were not able to detect it on Northern blots.

As well as ASIC splice variants, two other proton-gated channels DRASIC and MDEG2 also are found in sensory neurons (10, 12). Such heterogeneous expression of proton-gated channels may imply a complex response of sensory neuron subpopulations to tissue acidosis. All ASIC splice variants and DRASIC alone can form functional channels when expressed in COS cells so that they may be able to function individually or combine with others to form heteromeric channels. Although the heteromultimerization of these proton-gated channels has not been demonstrated, a recently isolated modulatory subunit MDEG2 has been shown to form heteromultimers with DRASIC that result in altered channel properties (14). It is possible that this kind of modulatory subunit may interact with other proton-gated channels in sensory neurons.

At present, ASIC-β is the only proton-gated channel that has been shown to be exclusively expressed in sensory neurons. DRASIC and ASIC-α also show high levels of expression in DRG but also are found outside the spinal ganglia (refs. 9 and 10 and this study). The DRG-specific expression of ASIC-β suggests that this transcript may arise from alternative splicing of a pre-mRNA generated by a DRG-specific promoter. Similar alternative splicing also is found in MDEG1 and MDEG2, which have the same splicing site as ASIC-α and ASIC-β, but neither MDEG1 nor MDEG2 is sensory neuron-specific. It thus will be interesting to analyze the ASIC-β promoter and compare it with other DRG-specific promoters. The specific splicing of ASIC-β mainly occurs in large diameter neurons that are different from the neurons expressing ASIC-α in DRG. The unique expression pattern of ASIC-β is also different from that of other known DRG-specific genes (see, e.g., refs. 23–25).

The expression of ASIC in brain and DRG previously has been examined by using nonisotopic *in situ* hybridization with a probe containing an L1 repeat (9). By using the L1-containing probe to screen a DRG random-primed cDNA library, we found ≈2,500 positives from a pool of 200,000 clones, compared with nine positive clones when using an ASIC-specific probe under identical conditions. This suggests that the L1 repetitive sequence exists in both ASIC and many other transcripts. We therefore used unique N-terminal coding regions to construct specific probes to investigate the expression of different ASIC splice variants in sensory neurons. Our *in situ* hybridization studies reveal that 90% of ASIC-α-positive cells are small diameter peripherin-positive neurons, most of which are nociceptors. The results also show that ASIC-β is expressed in ≈20% of the total number of neurons and is found in both small and large diameter neurons.

The functional properties of the proton-gated channels so far described can be grouped broadly into two categories. First, there are those channels that show a rapid time course for activation and inactivation in response to low pH, and second, there are those that activate and inactivate much more slowly. ASIC-α (9) is typical of the former group, whereas DRASIC falls into the latter (10). We found that the kinetic properties of ASIC-β are very similar to those of ASIC-α. The currents were quick to reach a maximum and desensitized in the continued presence of low pH. The pH dependency of currents passing through the two channels was also similar (EC_{50} for ASIC-α was ≈pH 6 (9) vs. pH 5.9 for ASIC-β. Both channels also show a preference for Na^+. In addition, reversal potential studies showed that the ASIC-β channel was also permeable to K+ ions, although much less so than to Na^+.

The major difference between the electrophysiological properties of ASIC-α and ASIC-β is related to the calcium permeability of the respective channels. ASIC-α discriminates poorly between cations, and the channel will pass Ca^{2+} ions, although the channel is 2.5 times more permeable to Na^+. However, low pH-evoked currents passing through the ASIC-α channel are inhibited at high extracellular calcium concentrations >100 μM (9). In our study, we found that the ASIC-β channel was not permeable to calcium ions, nor did raising the extracellular calcium concentration become inhibitory (Fig. 5). ASIC-β-mediated currents thus exhibit similar properties to

the native fast pH-evoked current recorded from voltage-clamped DRG neurons in response to low pH (26). It seems possible that ASIC-β mediates currents that contribute to the fast proton-activated current in sensory neurons. DRASIC-mediated currents are slow and sustained (10), similar to the sustained pH-mediated currents recorded from DRG neurons (7, 26). However, we found that, in addition to DRG, transcripts for DRASIC were also present, albeit at lower levels, in superior cervical ganglia, spinal cord, and brain stem, where sustained proton-evoked currents have not been described. ASIC-β is thus the only identified proton-gated channel expressed exclusively in sensory neurons.

Amiloride inhibited ASIC-β-mediated currents in the COS cells with a similar efficiency to that seen with ASIC-α-mediated current. This may indicate that the binding site for amiloride in the respective channels is in a conserved region. This region is presumably not present in the DRASIC channel because amiloride produces potentiation of currents passing through this channel (10). It has been suggested that the selective neurotoxin capsaicin and protons may activate the same channel in sensory neurons (26). The recent molecular cloning of the capsaicin-gated channel VR1 suggests that this is not the case because VR1-mediated currents were reported not to be activated by low pH (27). We found that capsaicin was not able to activate ASIC-β when expressed in the COS cells. These findings, taken together with other studies of cloned proton-gated channels, suggest that proton-gated and capsaicin-gated channels are different molecular entities.

Almost all (80–100%) DRG neurons have been shown to respond to low pH stimulation, but only half of them appear to be nociceptors (21, 28). It thus seems likely that, in addition to sensing tissue acidosis, proton-gated channels have other roles. ASIC-β is the first cloned proton-gated channel to be found in a subset of large diameter sensory neurons, in addition to the smaller, putative nociceptors. Drawing on models derived from studies of *Caenorhabditis elegans* mechanosensitive mutants, it is possible that ASIC-β could be a component of mechanosensitive channels that need to be tethered to the cytoskeleton to function (13). Proton-gated channel transcripts are also present throughout the central nervous system, and it is difficult to identify a role for these channels in this region simply in terms of acid sensing. It is possible that these channels play a role as autoreceptors, given the acidic content of synaptic vesicles (29). It is also possible that the channels may be activated by other endogenous ligands or by mechanosensory stimuli. Heteromultimerization of proton-gated channel subunits may produce channels with novel properties. It is also possible that proton-gated channel subunits may combine with ligand-gated ion channels [e.g., P2X receptors that also have two-transmembrane domains (30)] yielding a completely different repertoire of channel and receptor properties.

ASIC-β can be added to the growing family of proton-gated channels (9–13). The exclusive expression of the channel in DRG neurons is consistent with a role in sensory transduction, although not necessarily in nociception. The presence of ASIC-β in large diameter sensory neurons, as well as the widespread distribution of other proton-gated channels in the central nervous system, suggests an important, as yet unknown physiological role for these channels.

We thank the Wellcome Trust for support and Samantha Ravenall for expert technical assistance.

1. Jacobus, W. E., Taylor, G. J., Hollis, D. P. & Nunnally, R. L. (1977) *Nature (London)* **265,** 756–758.
2. Steen, K. H. & Reeh, P. W. (1993) *Neurosci. Lett.* **154,** 113–116.
3. Steen, K. H., Reeh, P. W., Anton, F. & Handwerker, H. O. (1992) *J. Neurosci.* **12,** 86–95.
4. Steen, K. H., Steen, A. E., Kreysel, H.-W. & Reeh, P. W. (1996) *Pain* **66,** 163–170.
5. Krishtal, O. A. & Pidoplichko, V. I. (1980) *Neuroscience* **5,** 2325–2327.
6. Kovalchuk, Y. N., Krishtal, O. A. & Nowycky, M. C. (1990) *Neurosci. Lett.* **31,** 237–242.
7. Bevan, S. & Yeats, J. (1991) *J. Physiol. (Lond)* **433,** 145–161.
8. Zeilhofer, H. U., Kress M. & Swandulla, D. (1997) *J. Physiol. (Lond)* **503,** 67–78.
9. Waldmann, R., Champigny, G., Bassilana, F., Heurteaux, C. & Lazdunski, M. (1997) *Nature (London)* **386,** 173–177.
10. Waldmann, R., Bassilana, F., de Weille, J., Champigny, G., Heurteaux, C., Lazdunski, M. (1997) *J. Biol. Chem.* **272,** 20975–20978.
11. Garcia-Anoveros, J., Derfler, B., Neville-Golden, J., Hyman, B. T. & Corey, D. P. (1997) *Proc. Natl. Acad. Sci. USA* **94,** 1459–1464.
12. Lingueglia, E., de Weille, J. R., Bassilana, F., Heurteaux, C., Sakai, H., Waldmann, R. & Lazdunski, M. (1997) *J. Biol. Chem.* **272,** 29778–29783.
13. Garcia-Anoveros, J. & Corey, D. P. (1997) *Annu. Rev. Neurosci.* **20,** 567–594.
14. Bassilana, F., Champigny, G., Waldmann, R., de Weille, J. R., Heurteaux, C. & Lazdunski, M. (1997) *J. Biol. Chem.* **272,** 28819–28822.
15. Schaeren-Wimers, N. & Gerfin-Moser, A. (1993) *Histochemistry* **100,** 431–440.
16. Molliver, D. C., Wright, D. E., Leitner, M. L., Parsadanian, A. S., Doster, K., Wen, D., Yan, Q. & Snider, W. D. (1977) *Neuron* **19,** 849–861.
17. Hammill, O. P., Marty, A., Neher, E., Sakmann, B. & Sigworth, F. J. (1981) *Pflugers Arch.* **391,** 1108–1112.
18. Bormann, J. (1992) in *Practical Electrophysiological Methods*, eds. Kettenman, H. & Grantyn, R. (Wiley-Liss, New York), pp. 136–140.
19. Guidato, S., Bajaj, N. P. & Miller, C. C. (1996) *Neurosci. Lett.* **217,** 157–160.
20. Palmer, L. G. (1984) *Membr. Biol.* **80,** 153–165.
21. Bevan, S. & Geppetti, P. (1994) *Trends Neurosci.* **17,** 509–512.
22. Elliott, C. E., Becker, B., Oehler, S., Castanon, M. J., Hauptmann, R. & Wiche, G. (1997) *Genomics* **42,** 115–125.
23. Akopian, A. N. & Wood, J. N. (1995) *J. Biol. Chem.* **270,** 21264–21270.
24. Chen, Chih-Cheng, Akopian, A., Sivilotti, L., Colquhoun, D., Burnstock, G. & Wood, J. N. (1995) *Nature (London)* **377,** 428–432.
25. Akopian, A. N., Sivilotti, L. & Wood, J. N. (1996) *Nature (London)* **379,** 257–262.
26. Bevan, S. (1996) *Prog. Brain Res.* **113,** 201–213.
27. Caterina, M. J., Schumacher, M. A., Tominaga, M., Rosen, T. A., Levine, J. D. & Julius, D. (1997) *Nature (London)* **389** 816–824.
28. Akaike, N. & Ueno, S. (1994) *Prog. Neurobiol.* **43,** 73–83.
29. Shen, H., Chan, J., Kass, I. S. & Bergold, P. J. (1995) *Neurosci. Lett.* **158,** 115–118.
30. Wood, J. N. & Docherty, R. J. (1997) *Ann. Rev. Physiol.* **59,** 457–482.